Using zebrafish as a model for investigating the neuropathophysiology of iron overload during development

Ayaat Hassan

A thesis submitted to
the faculty of graduate studies
in partial fulfillment of the requirements
for the degree of
Master of Science

Graduate Program in Biology
York University
Toronto, Ontario

August 2019

Abstract

In this research, we used larval zebrafish (*Danio rerio*) to examine the effects of iron (Fe) exposure on neurophysiological performance and oxidative-stress responses during development. Our findings demonstrated that exposure to elevated Fe levels from 0 to 5 days post-fertilization (dpf) increased iron levels in the larvae. These Fe-exposed fish exhibited delays in touch-evoked escape response and decreased swimming activity, indicating impairments in sensory-motor function. Results from the reactive oxygen species (ROS) assay suggested that the impairment was likely associated with the increased ROS generation after iron exposure. mRNA expression levels of major iron transport genes (e.g., DMT1, IREG1) were not decreased by iron exposure until 5 dpf. Interestingly, the expression levels of various oxidative stress-responsive genes (e.g., SOD2, CAT, GST) were differentially modulated by iron exposure. Overall, our research suggested that exposure to elevated iron resulted in oxidative stress, which led to neurophysiological dysfunction in developing zebrafish.

Acknowledgements

First, I would like to thank Dr. Kwong for taking me on as a master's student and providing me with this great opportunity to conduct research in his lab and learn a wide variety of both technical and laboratory skills that made me the researcher I am today. You allowed me to work independently, while also assisting me whenever I needed it, especially when it came to improving my understanding of statistics. Your constant and prompt feedback was really appreciated. A big thanks to Dr. Tsushima, for his valuable research advice and support throughout both my undergraduate years and as my advisor for my master's thesis. Also, thanks to my other committee members, Dr. Paluzzi and Dr. Perry, for their thorough feedback on my thesis and the thought-provoking questions during my defence which helped me gain a better understanding of my research topic. I would also like to acknowledge Janet, our Zebrafish Technician, for showing me the ins and outs of zebrafish husbandry and breeding.

Thanks to all my family and friends who supported me throughout this whole long and challenging process. Special thanks to my parents for the constant support and encouragement, and their patience in listening to me incessantly discuss my research project, and my brother for the late-night pickups from the lab when my experiments ran longer than anticipated.

Table of Contents

List of Tables

List of Figures

List of Abbreviations

AF	Artificial Freshwater
AV	Atrioventricular
AO	Acridine Orange
AP-1	Activator Protein 1
ARE	Antioxidant Response Element
BBB	Blood Brain Barrier
Ca^{2+}	Calcium ion
CAT	Catalase
Cd	Cadmium
CM-H_2-DCFDA	chloromethyl -2',7'-dichlorodihydrofluorescein diacetate (fluorescent ROS indicator)
CNS	Central Nervous System
Co	Cobalt
CoPA	Commissural Primary Ascending Interneuron
CREB1	cAMP Responsive Element Binding Protein 1
Cu	Copper
Cr	Chromium
Dcytb	Duodenal Cytochrome B
ddPCR	Droplet Digital PCR
DMT1	Divalent Metal Transporter 1
Dpf	days post fertilization
DRG	Dorsal Root Ganglion
FAC	Ferric Ammonium Citrate
Fe^{2+}	Ferrous Iron
Fe^{3+}	Ferric Iron
Fe-S	Iron-Sulfur Cluster
FTH	Ferritin Heavy Chain
GPX	Glutathione Peroxidase
GSH	Reduced Glutathione
GST	Glutathione S Transferase
GSTP	Glutathione S Transferase Pi Class
HIF-1	Hypoxia Inducible Factor 1
Hpf	hours post fertilization
ICP-MS	Inductively Coupled Plasma Mass Spectrometry

IRE	Iron Responsive Element
IREG1	Iron-Regulated Transporter 1 (or ferroportin)
IRP	Iron Regulatory Protein
LC50	Lethal Concentration 50; concentration of compound lethal to 50% of exposed population
LIP	Labile Iron Pool
MDA	Malondialdehyde
Mn	Manganese
Mg^{2+}	Magnesium ion
MS-222	Tricaine mesylate (powder used for anaesthesia and euthanasia of fish)
Na^{+}	Sodium ion
NF-κB	Nuclear Factor kappa-light-chain-enhancer of activated B cells
Nrf2	Nuclear Factor Erythroid 2-related factor 2
NTBI	Non-Transferrin Bound Iron
Pb	Lead
PI3K-Akt	Phosphoinositide 3-Kinase- Protein Kinase B
PMCA	Plasma membrane Ca^{2+} ATPases
PNS	Peripheral Nervous System
RB	Rohon Beard neuron
ROS	Reactive Oxygen Species
Se	Selenium
SERCA	Sarcoplasmic-endoplasmic reticulum Ca^{2+} ATPase
-SH	Sulfhydryl/thiol group
SOD1	Superoxide Dismutase (Cu/Zn)
SOD2	Superoxide Dismutase (Mn)
SP1	Specificity Protein1
STEAP	Six-transmembrane epithelial antigen of prostate
Tf	Transferrin
TfR1/2	Transferrin Receptor 1, 2
UTR	Untranslated Region
VGCC	Voltage Gated Calcium Channel
VMR	Visual Motor Response
Zip14	Zinc Transporter 14
Zn	Zinc

1 Introduction

1.1 Biological Role of Iron

Iron is an essential transition metal for living organisms and is crucial for many physiological processes in vertebrates, including fish[1]. These include DNA synthesis, mitosis, oxygen transport, oxidative metabolism, and cellular respiration[2]. In the brain, where it is highly abundant, iron plays a key role in neuron myelination, neurotransmitter synthesis (e.g., serotonin, dopamine, norepinephrine), and neurotransmission[3,4]. Iron is also involved in host immunity against pathogen invasion[5].

All these functions can be carried out as a result of iron's chemical properties. Iron exists in multiple oxidation states and is thus redox-active, mediating the transfer of single electrons through oxidation/reduction reactions between ferrous (Fe^{2+}) and ferric (Fe^{3+}) iron, and can be employed in biological processes involving such reactions[2,6]. Its properties also allow it to form ligands with biomolecules via oxygen, nitrogen or sulfur atoms, and is thus utilized as a co-factor in numerous enzymes. The reactivity of iron is determined by the ligand to which it is bound to. That, in addition to its redox state (Fe^{2+} or Fe^{3+}) decides its biological role (e.g., O_2 transport, redox reactions, iron storage, electron transfer, hydrolysis)[2]. The major classes of iron containing proteins are: (1) Fe-S cluster containing proteins (e.g., respiratory complexes I, II, III of the electron transport chain, or enzymes involved in catalyzing chemical reactions), (2) heme-containing proteins involved in the transport and metabolism of O_2 (e.g., hemoglobin, myoglobin), and (3) other iron-containing enzymes involved in numerous reactions, including redox reactions[3,7–12].

Due to its importance in numerous physiological properties (especially its close link with O_2 metabolism), iron levels must be maintained at homeostatic levels to fuel these reactions. In mammals, for instance, low iron levels result in iron deficiency anemia, characterized by fatigue and decreased immune function. A constant supply of iron is required; however, iron's redox-activity, which is crucial for numerous cellular processes, can also render iron toxic if found at elevated levels in the body (i.e., iron overload). Iron in free form can redox-cycle with O_2 and cause oxidative damage to cells and tissues of the organism[2,6,13–15]. Therefore, free iron exists only in trace amounts in the body and is mainly in that state during transmembrane crossing, as Fe^{2+}. At normal physiological O_2 levels, most iron is complexed to biological compounds in a nonreactive form, as Fe^{3+} - protein complexes[7,9,10].

Although organisms have evolved to have complex regulatory systems to maintain iron at homeostatic levels, changes in physiological condition (e.g., dysregulation of iron transport proteins) or external environments (e.g., exposure to elevated level of iron due to pollution) may affect the organisms' capacities in regulating iron balance.

1.2 Iron Contamination of Freshwater Ecosystems

1.2.1 Anthropogenic Sources of Iron

Iron is highly abundant in the earth's crust (5.6 % by weight) and can be found in all freshwater ecosystems, where it can reach levels higher than other metals[11,16]. However, iron can also be introduced into freshwater ecosystems via anthropogenic sources. These include iron ore mining effluents[17], acid and coal mine drainage[18,19], wastewater runoff from industrial and municipal effluents[20], and acidic runoff from forestry

and peat production[21]. For example, drainage from coal mines – where iron pyrite oxidation of sulphuric acid occurs – results in the release of soluble iron, whereas acid mine drainage is produced by mining activities that lead to exposure of sulfidic minerals to air or water, causing the release of iron and sulfuric acid[19,22]. In addition to mining activities, runoff from contaminated soils (e.g., sulphate soils)[11], draining of peatlands, forests, arable lands[11], storm water runoff resulting to soil erosion and leaching of ferric iron into freshwater systems[23], and dredging of iron-rich river sediments[11] can also introduce iron into freshwater systems.

These anthropogenic activities can lead to an increase in iron levels that are 10 to 200 times higher than what is considered physiologically safe. In fact, iron levels in contaminated freshwater systems worldwide can range from 1-200 mg/L (Table 1)[10,11,16,18,20,22–29]. To compare, optimal levels for the health of most aquatic life are ≤ 0.3 mg/L[30]. Such high levels of iron can be toxic to aquatic organisms including fish, but despite this fact, iron contamination of freshwater ecosystems remains a pressing environmental concern that is often neglected and understudied[16]. For example, while active attempts have been made in decreasing metal contamination [e.g., cadmium (Cd) and lead (Pb)] in metal-impacted aquatic ecosystems over the past decade, many studies still recorded high levels of iron in those regions (Table 1).

Table 1: Iron Contamination of Freshwater Systems

Country	Freshwater System	Contamination Source	Total Iron[a] [mg/L]
Brazil	Monjolinho River	Domestic and industrial effluents	Autumn: 11.48; Summer: 109.36[31]
Brazil	Sinos River	Domestic and industrial sewage, eutrophication, erosion	Water: 0.12; (sediment; 7.18-24.868 ug/g dry weight)[25]
China	Fuyang River	Industrial wastewater from leather factories, steel plants, cement plants, and municipal wastewater	87.39 (highest reported)[20]
Canada	Wabush Lake, Newfoundland	Iron-ore mining effluents	0.279 (highest reported)[32]
Belgium	Scheppelijke Nete and Kneutersloop rivers	Metal effluents	0.267-10.44[28]
Japan	Mukawa River (freshwater aquaculture)	Unspecified	0.54-2.04[29]
USA	Walnut Creek	Ferric hydroxide from acid mine drainage; wells and natural springs	3.3[22]
USA	Tar Creek	Mine waste pile runoff and mine drainage	1.33-40[33]
UK	River Gaunless	Coal mine effluents	7.0 (highest reported)[34]
UK	Afon Goch Stream	Acid mine drainage	5.27-194.7[35]
Turkey	Streams in Alasehir	Mercury mine drainage	1.496-29.891[36]
Finland	Tributaries of Isojoki	Drainage from forest treatment and peat production	0.509-3.95[37]

[a] Dissolved and colloidal iron

Underestimation of the effect of iron was also seen when considering its risk assessment rating. Legislations worldwide attempt to maintain freshwater total iron concentrations (dissolved and undissolved) at 1 mg/L (e.g., UK and US)[30]. However, Canada is more stringent, with acceptable levels being capped at 0.3 mg/L (though some provinces set their own standards, which can be 1 mg/L or higher)[23]. Canada's lowering of the water quality criteria for iron is supported by a recent study examining the

consequences of long-term exposure to ferric iron at circumneutral pH water in the US. They demonstrated that the chronic iron criteria of 1 mg/L does not protect sensitive aquatic life, and the chronic iron value as measured by them should be lowered to 0.449 mg/L[19]. This is reinforced by other studies which also suggest the criteria of 1 mg/L is under protective of sensitive fish and other aquatic organisms[20,38,39]. For example, Malaysia has suggested lowering the criteria from 1 mg/L to a criterion maximum concentration (CMC) of 0.0372 mg/L (37.2 μg/L) to protect even the most vulnerable aquatic species[40].

1.2.2 Chemistry of Iron in Contaminated Freshwater Systems

The toxic effects of iron on fish in freshwater systems can vary as a result of iron's complex chemical speciation in water. Iron in contaminated waters exists in two forms: reduced ferrous iron (Fe^{2+}) and oxidized ferric iron (Fe^{3+}). Many factors, both biotic and abiotic, can affect its speciation (i.e., oxidation state). These include its redox-activity, pH, dissolved O_2, light, levels of binding agents such as Cl^-, OH^-, SO_4^{2-}, and organic ligands such as humic and tannic acids (dissolved organic matter; DOM)[10,11,21,39]. A brief overview can be found in Figure 1.

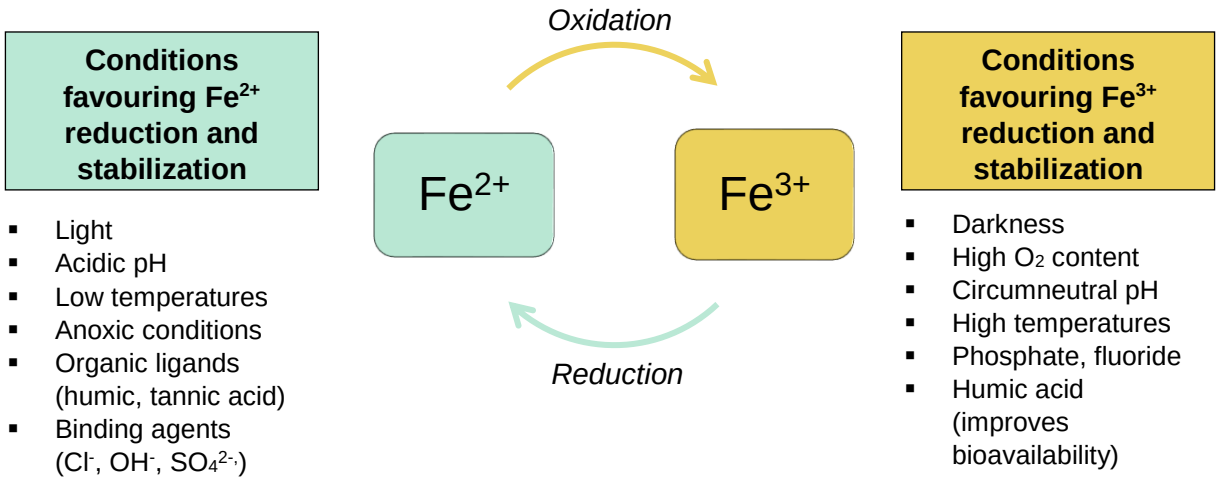

Figure 1. Speciation of Iron in Freshwater Systems.
High temperatures favour the oxidation of iron to its ferric form (i.e., by increasing the oxidation rate), while low temperatures can extend the half life of ferrous iron. The presence of any binding agents and organic ligands decreases the oxidation rate by stabilizing ferrous iron (while also decreasing its toxicity), while light can result in photoreduction of ferric iron when complexed to organic matter. Presence of phosphate and fluoride can increase the rate of ferrous iron oxidation, while sulfides and organic compounds induce the reduction of ferric iron[82,11,41]. Ferrous iron's toxicity is increased with increased acidity. Additionally, humic acid can decrease toxicity of ferrous iron, while improving the bioavailability of ferric iron[21,142].

Thus, depending on the surrounding water conditions, either ferrous or ferric iron will dominate, with differential effects on aquatic organisms. For example, ferrous iron is most stable, and thus predominantly found, in anoxic and acidic freshwaters (pH 4-5) where it is dissolved and highly bioavailable (and consequently very toxic) to fish[41,42] In well-oxygenated circumneutral pH waters (pH > 6.5), ferric iron is more thermodynamically stable and consists of at least 99.3-99.8% of iron found in these waters[10,11]. The half-life of ferrous iron in such waters, on the other hand, ranges in the area of seconds, with an increase in pH from 6 to 7 in well oxygenated waters reducing its half-life from hours to minutes[41]. It should be noted that most ferric iron in such waters is not in aqueous form; rather, it reacts with OH^- in the presence of O_2, forming insoluble ferric hydroxides, oxyhydroxides, and ferric oxides (i.e., colloidal iron), which can

precipitate out of solution, aggregating to form either low or high molecular weight ferric hydroxides[22,41]. Furthermore, it is comparatively less bioavailable, suggesting that it may not be lethal to fish[23]. Other species of iron contaminants (e.g., iron oxide nanoparticles; Fe_2O_3) have been revealed to also be toxic to fish[43].

The reason behind the differences in acidity and O_2 content of contaminated freshwaters (and thus the oxidation state of iron) is quite simple. Undiluted effluents are mainly acidic in nature and thus are composed of ferrous iron. As the effluent reaches the body of water, it becomes diluted, which increases its pH. This, in conjunction with the more oxidized environment, favours the production and consequent precipitation of ferric hydroxides[42,44]. Freshwater systems with buffering capacities can deal with low pH effluents, maintaining pH levels around neutral. However bodies of water with low buffering capacities like groundwater and ponds cannot, resulting in an overall decrease in pH, favouring the presence of ferrous iron[10,38,41,42,45]. However, such acidic and anoxic iron contaminated waters are not prevalent. In fact, ferric precipitates are the predominant form of iron found in freshwater systems that can sustain life (i.e., well oxygenated and non-acidic waters) and are more typically encountered by aquatic animals[19].

1.2.3 Toxic Effects of Iron on Fish and other Aquatic Organisms

Fish can absorb waterborne iron (both Fe^{2+} and Fe^{3+}) through their gills, skin, or via the gut by ingesting iron contaminated water and food (e.g., iron contaminated organisms and organic matter). Similar to other metals, if the exposure to iron is waterborne, the gill is the primary site of iron absorption[46]. Freshwater fish, unlike their marine counterparts, do not need to ingest water to maintain osmotic balance, therefore uptake of waterborne iron from the gut is likely minimal. On the other hand, developing

freshwater fish before exogenous feeding have been shown to exhibit water-drinking behaviour, and can thus potentially take up waterborne iron from the gut[47,48]. Interestingly, one study examining tissue-specific iron accumulation in adult whitefish (*Coregonus lavaretus*, freshwater species) following exposure to waterborne humic and non-humic bound ferric hydroxides demonstrated increased iron accumulation in the gut[21]. While it is unclear how this was able to occur, this suggests that waterborne iron uptake from the gut of freshwater fish may still be possible. Studies have revealed that iron accumulation in fish is localized in specific organs, such as the gills, fins, gut, gonads and liver, with decreasing bioaccumulation in the heart, brain, skin, and muscles following exposure to elevated iron levels[16,18,21,25,26,49,50]. Increased whole body iron levels in developing fish have also been recorded[50,51]. Metals that possess a high uptake rate and low elimination rate have a tendency to remain in the organism and accumulate over time, like iron[18]. Furthermore, organ specific accumulation of iron differs depending on whether exposure was chronic or acute, with increased incidences of accumulation in the heart and brain of tilapia following a 4-week exposure to iron, when compared to 72 hours[23].

For fish, like all other organisms, Fe^{2+} is the predominant ionic form for absorption. Due to its higher bioavailability, Fe^{2+} is thought to be more toxic to fish (e.g., 96-h LC50 of 3.7 mg/L for fathead minnows)[11,41,52–54]. However, the combined effects of the low pH of surrounding waters and the iron could likely result in increased toxicity[11,23,55–57]. In fact, a study examining the reason behind the high numbers of fish kill in natural ponds within Czech Republic demonstrated that the pH of these waters can range as low as 5.8, due to quarry waters of pH 3.17 and high ferrous iron content leaching into the ponds. This consequently caused lethal physical and internal damage to the inhabiting fish[10]. Another

laboratory-based study also exhibited high fish mortality following exposure to 2 mg/L Fe at pH 5.0 (when compared to pH 7.4) with the remaining surviving fish displaying severe physiological impairments, such as increased blood viscosity[57]. While LC50 studies demonstrate that ferric iron is not as lethal as ferrous iron, it can have negative effects on fish function[23].

Studies examining the effects of insoluble ferric hydroxides on freshwater fish have noticed a tendency for iron to accumulate on the gills of fish. This has shown to limit their respiratory capacity by physically clogging the gills, essentially suffocating them, or by damaging the branchial/lamellar epithelium, leading to hypertrophy and necrosis. Reduced oxygen uptake and disruption in ionic regulation have also been demonstrated. This was reported in numerous fish species including brown trout (*Salmo trutta*), perch (*Perca flavescens*), salmon, and tilapia[11,18,41,44,57–59]. Additionally, tilapia exposed to iron showed increased incidences of coughing, with overall decreased activity, while the common carp collected from ferrous contaminated freshwaters showed gill swelling and haemorrhaging[10,60].

There has also been a link of long-term exposure to ferric hydroxide precipitates to impairments in development, survival, growth, and reproduction (decreased egg release) of fish as a result of the ferric hydroxide precipitates[22,23,41,61,62]. These were assumed to be a result of iron precipitates reducing water visibility for developing fish thus impairing feeding success and stunting growth, or the precipitates settling on the freshwater bottom, which can cover food sources and spawning grounds. There have been suggestions that disturbances in fish metabolism and osmoregulation can occur, with iron contaminated fish also being more susceptible to injury and disease. This

suggests that ferric hydroxides may be taken up by fish, despite their decreased bioavailability, and are exerting their toxic effects in that manner[23].

The effects of high iron levels in freshwater ecosystems not only impacts fish, but organisms at every trophic level. Adverse sublethal effects of high iron on developing nymphs, toads, planarian worms, and blackworms have been recorded, with a reduction in periphyton and macroinvertebrate community abundance and diversity (e.g., mayflies) detected following exposure to ferric iron (as a result of constraining their access to food on the sediments). Inhibition of algal growth has also been noted, in addition to iron-mediated damage of aquatic plants[19,23,38,39,42,63]. Iron contamination can thus affect benthic habitat and food sources[23].

The reason why iron can be so toxic is due to its redox-activity, which can promote free-radical production and subsequently induce lipid peroxidation, mitochondrial dysfunction, and DNA damage (e.g., altered DNA structure, base substitutions, DNA lesions), that can lead to tissue damage and potentially death of the fish[17,21,64]. The negative effects of metal contamination of freshwater systems, including iron, is likely more pronounced on developing fish, especially embryos, resulting in morphological and functional deformities. In fact, the post-natal period of developing fish is reported to be the most sensitive stage to any type of metal comtamination[65].

While iron is essential for developing fish as it plays a crucial role in many cellular processes, it is apparent that increased accumulation of iron in their bodies can be detrimental, as any increase in whole body iron levels beyond the normal physiological limit (i.e., iron overload) may compromise cell function and viability[2,6,15]. As a result, fish

possess a system in place to regulate iron homeostasis (at the cellular and organismal level), consisting of several iron transport and storage proteins.

1.3 Mammalian Regulation of Iron Homeostasis

1.3.1 Systemic and Cellular Iron Uptake, Storage, and Export

Iron homeostasis needs to be tightly regulated, and due to an absence of a regulatory iron excretion pathway, it is largely maintained by regulating iron absorption. Consequently, vertebrates can control and prevent the accumulation of excess free iron by controlling dietary iron uptake from the duodenum, its transport in the circulation, cellular iron uptake and utilization, macrophage recycling of iron, and storage of iron in liver. This is carried out by a set of iron transport and storage proteins, which include TfR, DMT1, IREG1, and ferritin.

The highest demand for iron in the body originates from erythropoiesis as iron is required for hemoglobin synthesis (which make up erythrocytes). In fact, 70% of the body's iron pool can be found as heme in erythrocytes. Iron released from senescent erythrocytes that have been phagocytosed by recycling macrophages is reutilized by the body, and this serum iron pool accounts for about 90% of daily iron requirements. Any additional iron needed is absorbed from the diet through the gut (10%) to compensate for the daily non-specific iron loss that may occur (e.g., blood loss, sweating, and sloughing of epithelial cells)[7,9,66,67]. Due to the lack of excretory pathways, organisms only absorb enough iron to offset daily iron loss and thus prevent the occurrence of iron overload[67]. Any excess iron is taken up by the liver and stored in ferritin until needed, or kept in the recycling macrophages (Fig. 2)[7,13,68].

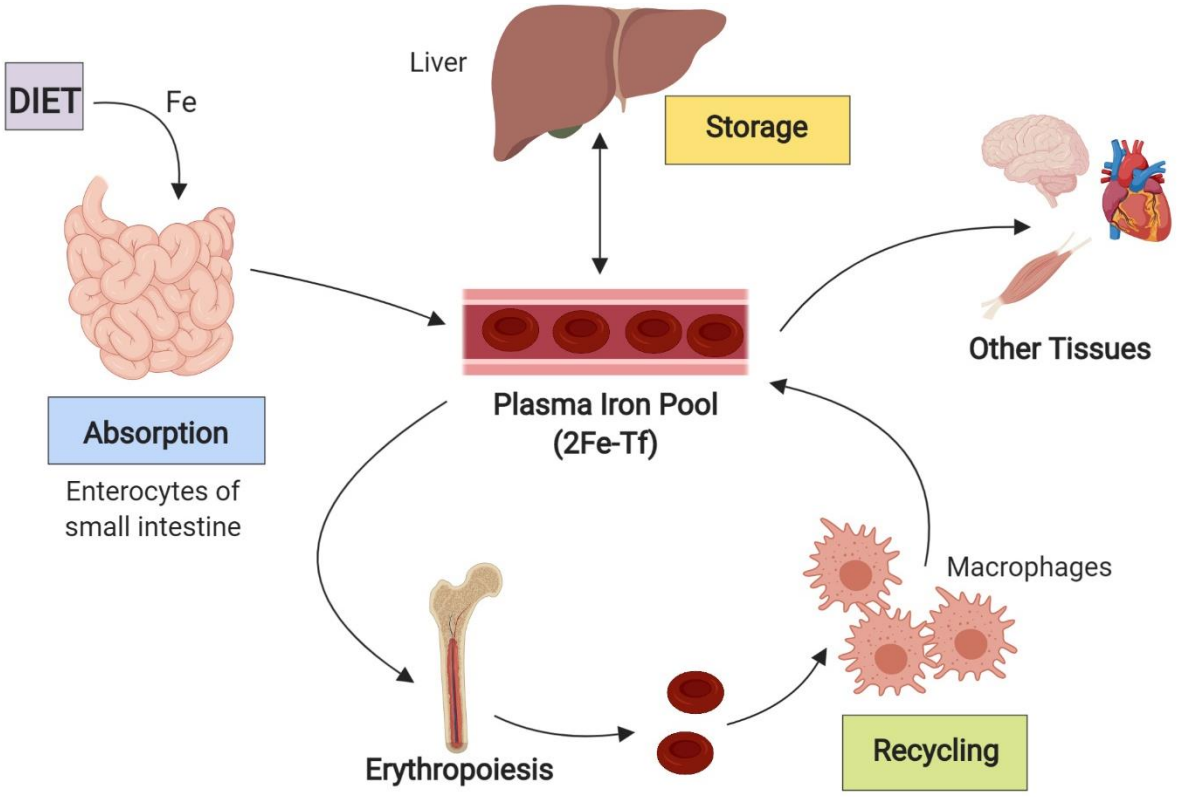

Figure 2. Systemic Control of Iron Levels.
Since there a regulated excretory pathway for iron does not exist, levels are controlled at the gut (dietary iron absorption), liver (cellular iron storage), and recycling macrophages (release of iron recycled from senescent erythrocytes), to maintain serum iron at homeostatic levels. This iron can be transported to target tissues via transferrin. 90% of iron utilized by the vertebrate derives from recycling macrophages; about 10% originates from the diet, just enough to offset any non-specific iron loss from the body. Any excess iron is stored in the liver until needed.
**Created using Biorender.com*

Vertebrates can acquire dietary iron as either non-heme iron salts or heme[69]. The inorganic dietary iron is mainly in the Fe^{3+} form and must be reduced to Fe^{2+} prior to uptake into the intestinal enterocytes via DMT1 (divalent metal transporter 1) by a ferric reductase (Dcytb; duodenal cytochrome b reductase 1) at the apical membrane. DMT1 is a proton-coupled (H^+/Fe^{2+}) symporter localized on the apical membrane of enterocytes that can only take up iron in the divalent form, utilizing the low acidity of the intestine to facilitate Fe^{2+} uptake. Once in these absorptive cells, Fe^{2+} can be utilized by the cell,

stored in a non-reactive form in ferritin (the main cellular iron storage protein), or released into the blood circulation through ferroportin (or IREG1, the iron exporter) at the basolateral membrane if needed elsewhere[13]. IREG1-mediated export of Fe^{2+} is coupled to a ferroxidase (either anchored to the membrane or free floating, e.g., hephaestin) that subsequently oxidizes Fe^{2+} to Fe^{3+}, so that it can be bound to the carrier protein transferrin (Tf)[70] (Fig. 3).

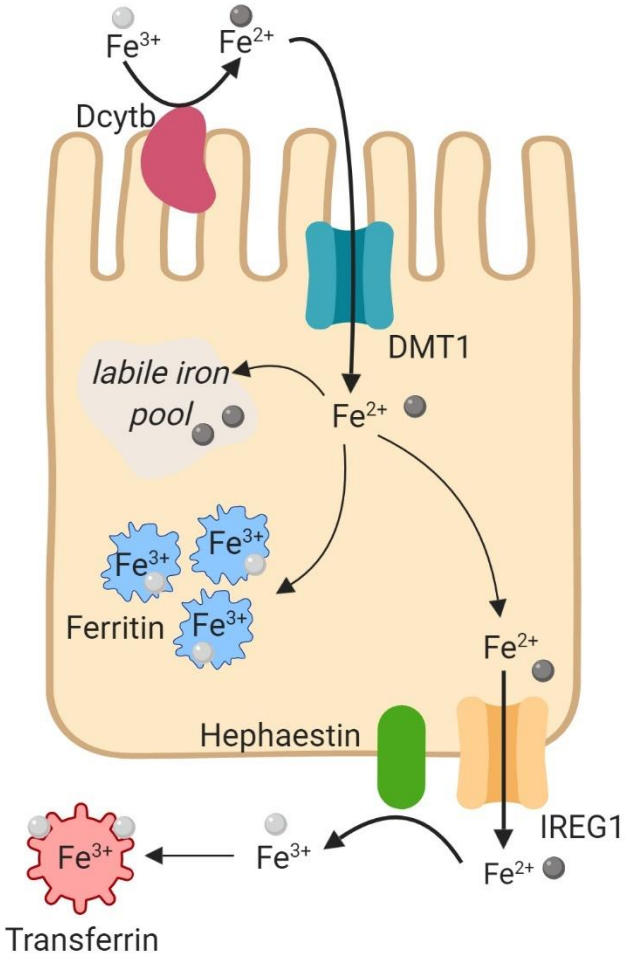

Figure 3. Mechanism of Iron Uptake and Export from Enterocytes of the Small Intestine.
Prior to uptake into the enterocyte via DMT1, Fe^{3+} is reduced to Fe^{2+} by Dcytb at the apical membrane. Subsequently after uptake, iron can be either stored in ferritin as Fe^{3+} or maintained in the labile iron pool for use by cellular proteins or enzymes. Cellular iron export into circulation occurs via IREG1 at the basolateral membrane of the enterocytes, where Fe^{2+} is then oxidized to Fe^{3+} by Hephaestin, a membrane-bound ferroxidase. Fe^{3+} is then bound to transferrin for subsequent delivery to target cells.
**Created using Biorender.com*

Tf is a single-chain glycoprotein with two hydrophilic iron binding sites. It binds Fe^{3+} iron for transport in a nonreactive state, while shielding them from potential hydrolysis. About 30-45% of circulating transferrin are usually occupied. Usually 1% of iron in circulation are non Tf-bound iron (NTBI), which are handled by low molecular weight ligands like citrate, ascorbate, ATP, ferritin, and albumin. Iron overload can be characterized by the appearance of NTBI when saturation of Tf surpasses 70%[67,71]. These can be taken up by cells via non-Tf mediated pathways. NTBI can enter the liver via a zinc transporter zip14; in the heart, NTBI can cross cardiomyocytes via voltage gated L- and T- type Ca^{2+} channels[71]. The liver plays an important role during iron overload by clearing any excess NTBI. However, if its ferritin storage capacity is exceeded, and its antioxidant defense system is overwhelmed, that could lead to oxidative stress and consequent cellular and tissue wide injury[1].

Once in circulation, iron is bound to transferrin (Tf; a carrier protein) which delivers iron to target tissues by binding to transferrin receptors (TfRs) on the target cell. TfR controls the absorption of iron into cells, thereby preventing excess cellular iron loading. Two receptor types exist: TfR1 is ubiquitously expressed in all cells requiring iron, while TfR2 is predominantly expressed in the liver[1]. Iron-bound Tf binds to TfR1 at the cell surface and is internalized into an endosome via clathrin-mediated endocytosis. The acidic pH of the endosome (pH 5.5 -6) leads to the dissociation of the iron from Tf. TfR1 has a high affinity for holo-Tf (Tf complexed with iron) but has a low affinity for apo-Tf (iron-free Tf) at neutral pH, to prevent competitive inhibition. The pH in the endosome is lowered via a proton pump, inducing a conformational change that results in the release of iron from Tf. Fe^{3+} is then reduced to Fe^{2+} by a metalloreductase STEAP 1-4 (six-

transmembrane epithelial antigen of prostate 1-4) and then released into the cytosol via DMT1[2]. This acidic milieu allows for Tf to remain bound to TfR1. Once the endosome undergoes exocytosis, the pH returns to neutral, which allows the release of apo-Tf from TfR1. Tf and TfR1 are then recycled back to the cell surface[72] (Fig. 4).

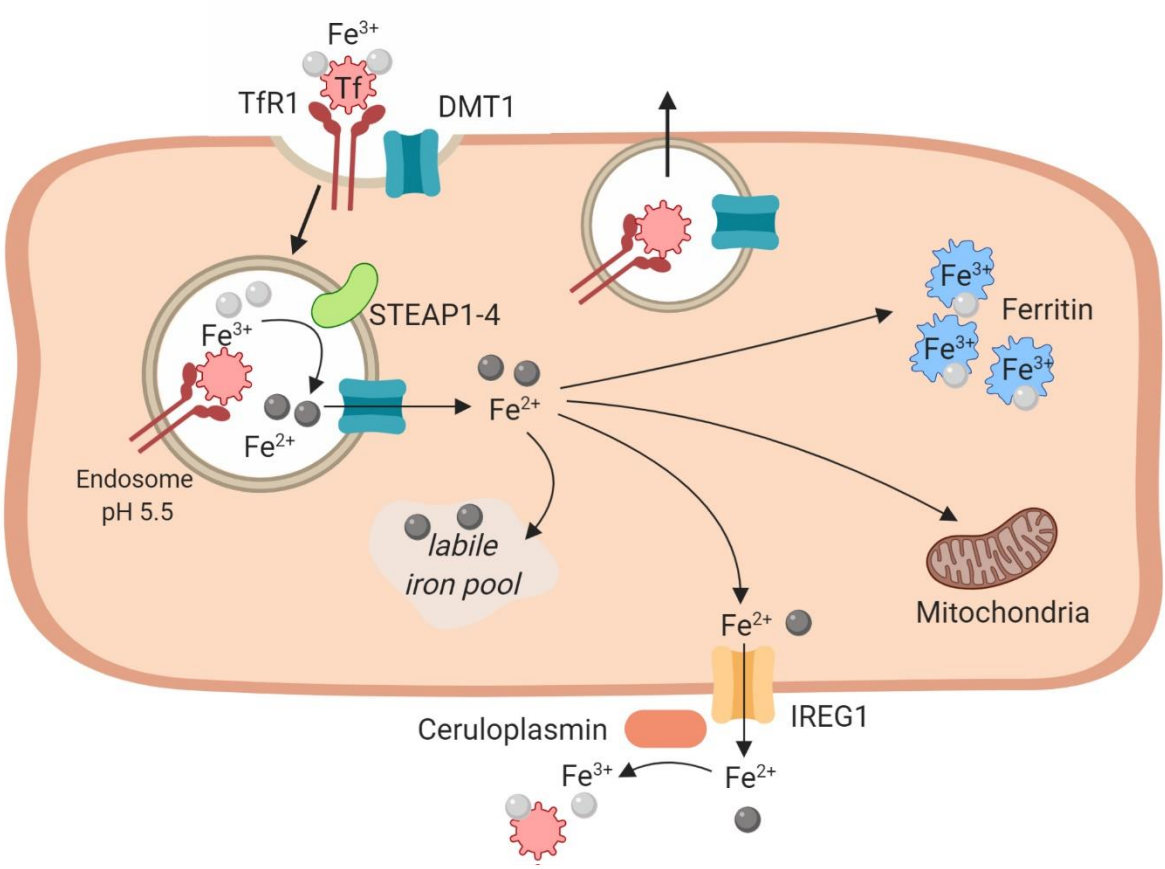

Figure 4. Cellular Iron Uptake, Storage, Utilization, and Export.
For uptake by target tissues (e.g. non-absorptive tissues like the heart), iron uptake is mediated by TfR1. Iron-bound Tf (holo-Tf) binds to the cell's TfR1, resulting in the clathrin-mediated endocytosis of the TfR1/holo-Tf complex into an endosome. The low pH allows for the dissociation of Fe^{3+} from Tf and is reduced to Fe^{2+} by STEAP1-4, a metalloreductase. The acidic milieu also permits for Fe^{2+} export into the cytosol via DMT1. The endosome is then recycled back to the cell surface and the apo-Tf is released back into circulation. Once in the cytosol, iron is stored in ferritin, maintained in the labile iron pool, or shuttled to the mitochondria for incorporation into Fe-S clusters or heme. Any excess iron not utilized by the cell is exported by IREG1 and subsequently oxidized to Fe^{3+} by a serum copper ferroxidase, ceruloplasmin, and bound to Tf.
**Created using Biorender.com*

Within the cytosol, Fe^{2+} can be shuttled off to the mitochondria for incorporation into Fe-S clusters and heme proteins, utilized by other proteins in the nucleus or cytosol (i.e., metalate non-heme iron enzymes), or stored in ferritin[2]. Ferritin is a heteropolymer comprised of two types of polypeptide chains, H (heavy) and L (light) chain which co-assemble to form a hollow sphere where iron can be deposited[69]. Ferritin can store up to 4500 iron atoms, averaging at 2000-2500 in tissues[7]. Its main purpose is to store excess iron in a non-reactive form, where it is still bioavailable to the organism when needed. The H chain (which possesses ferroxidase activity) binds Fe^{2+} ions and oxidizes them to the stable Fe^{3+} form. Fe^{3+} is then released from the ferroxidase site and transported to nucleation site in the L chain, where it is stored. Ferritin mainly localizes in the cytoplasm, but can be found in the serum, nucleus, or mitochondria[70]. Ferritin plays a key role during iron overload conditions. By binding excess cytosolic iron and storing it, it can prevent Fe^{2+} from indiscriminately undergoing redox reactions. Iron can also enter the labile iron pool (LIP), which is a ferritin-regulated cytosolic pool of available metabolically active iron for use by enzymes and proteins in various cellular processes[73,74]. Iron export from these cells are also mediated by IREG1 coupled to a ferroxidase, typically ceruloplasmin, which is a multicopper oxidase secreted by the liver[67].

It should be mentioned that the brain is the only organ that does not have direct access to iron as the central nervous system (CNS) is separated from the systemic circulation via the blood brain barrier (BBB). Therefore, transport of iron into the brain requires bypassing the BBB[69]. The BBB is the microvasculature of the brain, characterized by the presence of tight junction proteins between the endothelial cells. It controls iron efflux and influx since any changes in iron uptake (low or high) can lead to

neurophysiological dysfunctions[75]. The BBB mediates iron entry by utilizing TfR1 for iron uptake and IREG1 for export into the CNS interstitial fluid. Distinct brain regions and cell types also display differential expression of iron transport and storage proteins. For example, neuronal cells take up iron mainly via TfR1-mediated endocytosis (with some indications of minor NTBI uptake), whereas glial cells (oligodendrocytes, astrocytes, microglia) are devoid of TfR1, taking up predominately NTBI bound to ascorbate, citrate, or ATP[69,76]. Furthermore, ferritin is mainly expressed within glial cells, and only in a subset of neuronal cells. This suggests that glial cells are used for iron storage, while neuronal cells control iron uptake, only intaking what is required for cellular activity, and exporting residual iron from the cytosol rather than storing it[77].

1.3.2 Systemic and Cellular Regulation of Iron Homeostasis

In mammals, regulation of iron homeostasis occurs both at the systemic and cellular level. The major regulator of systemic iron homeostasis is hepcidin, a peptide hormone produced and secreted by the liver. Hepcidin controls iron absorption from the gut, recycling by macrophages, and storage in the liver, since a regulatory excretory pathway does not exist. In response to elevated iron levels (both serum and liver), hepcidin transcription is upregulated and is subsequently secreted, targeting intestinal, liver, and macrophage IREG1. It binds to, and ubiquinates IREG1, leading to its internalization and proteasomal degradation[15,67,73,78]. This prevents release of iron from enterocytes, liver hepatocytes, and macrophages, which averts efflux of iron into circulation[7]. This is accomplished in order to prevent Tf saturation, which can lead to increased levels of NTBI in circulation and potential uptake by other tissues[67]. Hepcidin essentially forces sequestration of iron in cells, within ferritin, until hepcidin levels are

reduced, where it can be released again. When no longer needed, hepcidin is cleared by the kidney[79]. In the gut, this stored iron can be lost during sloughing of the epithelial layer and excreted from the organism[7] (Figure 5).

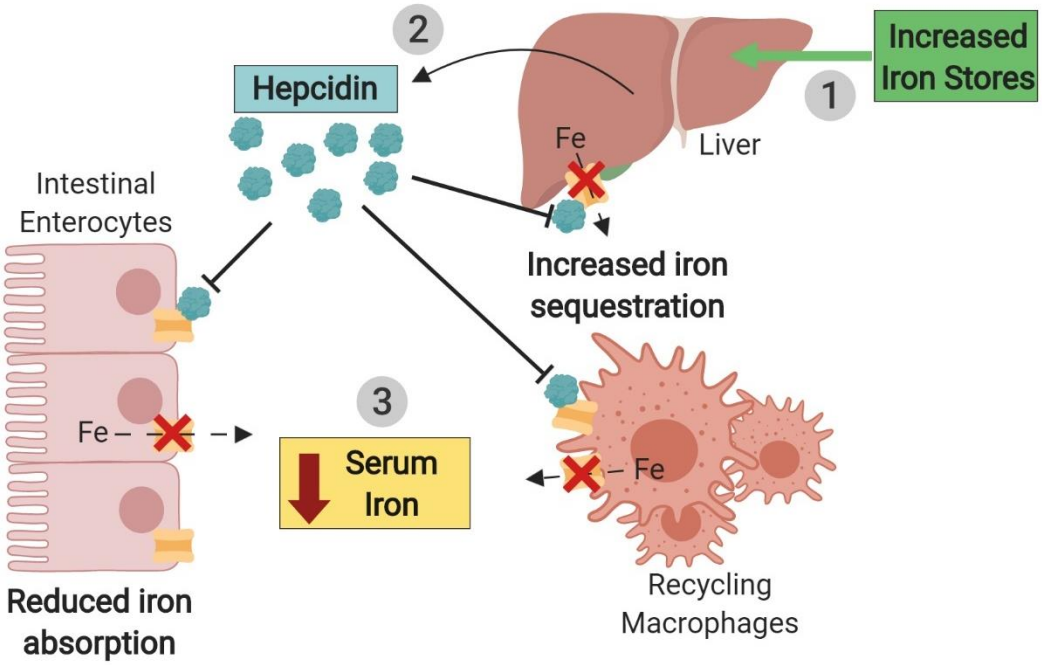

Figure 5. Systemic Regulation of Iron Homeostasis by Hepcidin.
(1) Increased serum iron or liver iron stores triggers the transcription and subsequent secretion of hepcidin by the liver. **(2)** Hepcidin then binds to IREG1 on its main targets: liver hepatocytes, recycling macrophages, and enterocytes of the small intestine. **(3)** This prevents iron export from these tissues, resulting in increased iron sequestration in the liver and recycling macrophages, and reduced iron absorption from the gut. This subsequently leads to decreased serum iron levels, which will prevent Tf saturation, increase of NTBI, and ensuing tissue iron loading.
**Created using Biorender.com*

The liver increases iron uptake during iron overload and can trigger hepcidin transcription; both hepatic and serum iron levels (via TfR2) can trigger hepcidin synthesis via alternate pathways[71]. Hepcidin is not only regulated by iron. It can be upregulated in response to inflammation and infection, while iron deficiency, hypoxia, and erythropoiesis lead to transcriptional inhibition[7].

Conversely, regulation of iron homeostasis at the cellular level involves post-transcriptional regulation of the iron transport and storage proteins, DMT1, TfR1, IREG1, and ferritin (Fig. 6). This occurs in all tissue and cell types. Post-transcriptional regulation occurs primarily via the interaction of iron-regulatory proteins (e.g., IRP1, IRP2) with iron-responsive elements (IRE) located on the mRNA (at the 3'- or 5'-UTR)[6]. The IRE is a conserved stem-loop structure, which by binding IRP, can modify the stability or translation efficiency of the mRNA. For example, the 3' untranslated region (UTR) forms stem loops in the mRNA of TfR1 and DMT1 and these are sensitive to degradation by ribonucleases due to the presence of instability elements in these stem loops. For IREG1 and ferritin, these stem loops are present at the 5' CAP of their translation start site (i.e., 5' UTR)[13,80].

In iron-replete cells, 4Fe-4S clusters bind to IRP1, initiating a conformational change which prevents IRP1 from interacting with the IRE on the target mRNA transcripts. IRP2 on the other hand, undergoes ubiquination following oxidation and subsequent degradation by proteasomes[2]. For DMT1 and TfR1, the dissociation of the IRPs from their IREs renders the transcripts more susceptible to degradation by endonucleases, leading to a decrease in the abundance of these transcripts[81]. For IREG1 and ferritin, this signals translational activation of their transcripts, since the IRPs are not blocking ribosomal assembly[7]. Together, this causes downregulation of TfR1 and DMT1 synthesis while upregulating IREG and ferritin synthesis, to increase iron storage and export, but decrease uptake to prevent cellular iron loading and potential oxidative stress damage[2,14]. Low cellular iron levels, on the other hand, allow binding of IRPs to IREs. This stabilizes and protects TfR1 and DMT1 mRNA from degradation, thus initiation translation, while

preventing ribosomal assembly on IREG1 and ferritin mRNA, resulting in translational repression. This upregulates synthesis of TfR1 and DMT1, and inhibits IREG1 and ferritin synthesis, to increase iron uptake but decreases export and storage[2,14].

TfR2 lacks an IRE, so it does not respond to cellular levels of iron, but rather acts as a 'sensor' for the liver, playing a role in initiating hepcidin synthesis or repression[180].

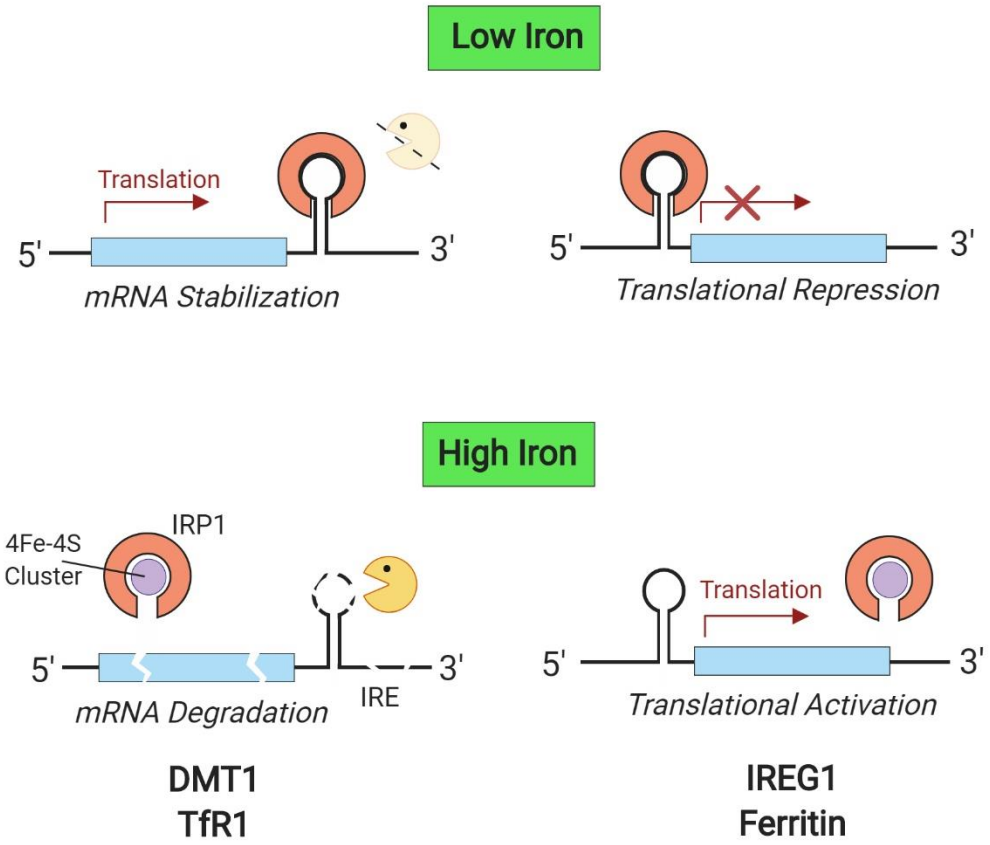

Figure 10. Cellular Regulation of Iron Homeostasis at the Post-Transcriptional Level by IRPs.
In response to low cellular iron levels (i.e., iron deficiency), the IRPs bind to the IREs of the target transcripts, either stabilizing and activating translation of DMT1 and TfR1 for increased iron uptake or inducing translational repression of IREG1 and ferritin to prevent iron export and storage. In iron replete cells (i.e., iron overload), iron (as a 4Fe-4S cluster) binds to IRP, preventing its binding to the IRE of the target transcripts. This leads to destabilization and consequent degradation of DMT1 and TfR1 to minimize iron uptake, while allowing translational activation of IREG1 and ferritin for increased iron export and storage, as ribosomal assembly on their promotor is no longer blocked by IRP.
**Created using Biorender.com*

1.3.3 Iron Homeostasis in Fish: What is known

What we know regarding iron regulation in fish mainly derives from zebrafish studies, as mammalian orthologues of many iron regulatory proteins are also present in zebrafish[82]. A summary of the homologous proteins discovered and characterized thus far in zebrafish can be found in Table 2.

Table 2. Iron Transport, Storage, and Regulatory Proteins in Zebrafish. Homologous proteins involved in regulation of iron homeostasis in zebrafish, and their localization within the fish. Localization information sourced from the online zebrafish database (ZFIN)[83].

Protein	Localization in Zebrafish[83]	Reference
DMT1	Gut, liver, gills, blood, lens	84,85
IREG1	CNS, liver, gut, gill	86
TfR1	Tfr1a: blood, blood island Tfr1b: ubiquitous	87
Tf	Liver, renal system, muscle	88
Hepcidin	Gut, liver	88
TfR2	Liver	87
Ferritin Heavy Chain	Fth1a: blood, eye Fth1b: undetermined	83
Ceruloplasmin	Gut, pancreas, liver, blood	89
STEAP1-4	Not determined	
Hephaestin	Not determined	
IRP1/IRP2	Blood	85
Dcytb	Not determined, but activity has been detected in gut[90] and gill[74]	

There is currently no information regarding a ferritin light chain sequence in fish; however an M chain (typically observed in lower vertebrates) has been discovered in numerous fish species, including zebrafish[89]. Additionally, an equivalent ferric reductase to Dcytb has not been cloned, but its activity has been detected in the gut and gill of

zebrafish[74,90]. However, the expression of a ferric chelate reductase has been discovered in larval zebrafish gut and gills[91]. Due to the whole genome duplication that transpired in teleosts, zebrafish possess paralogs for a subset of their genes. These include some of the mammalian orthologues of iron homeostatic proteins, for instance, TfR1. In zebrafish, TfR1a has a restricted expression within differentiating erythrocytes, whereas TfR1b displays ubiquitous expression[87]. Zebrafish also possess paralogs of the ferritin heavy chain gene[83].

It has been suggested that the mechanism of iron handling may likely be the same in fish, considering the proteins in fish are quite comparable to their mammalian counterparts. Similar to mammals, a regulated excretory pathway for iron may not exist; though small amounts of iron can be lost through non-specific means[82]. In contrast to mammals, fish can also absorb waterborne iron (either as Fe^{2+} or Fe^{3+}) from the gills (specifically the gill epithelium), in addition to uptake from the gut through dietary sources[74,92]. The mechanism by which this transpires is still under study, however it is suggested to be similar to the uptake pathway in the gut, most likely utilizing the same set of iron homeostatic proteins[74,93]. Whether fish can absorb Fe^{3+} directly is also currently unknown. In mammals, the integrin-mobilferrin pathway seems to be involved in direct Fe^{3+} uptake[73].

1.4 Iron and Oxidative Stress: The Link

Despite possessing an extensive regulatory system to maintain whole-body iron homeostasis, being exposed to iron at the concentrations found in contaminated freshwaters may lead to iron overload in fish. Iron overload is characterized by increased

systemic or cellular iron levels that exceeds ferritin's binding capacity, resulting in the deposition of free iron in tissues[94]. This can be dangerous since iron's redox-active state can render it toxic at high tissue concentrations, as it can promote the production of endogenous reactive oxygen species (ROS)[95].

1.4.1 Endogenous Production of ROS

ROS production is a result of an organism's regular cellular metabolism. At low to moderate concentrations, they are involved in physiological cell processes, but at elevated concentrations, they can have adverse effects on the cell[96]. ROS can be found in two forms: radical or non-radical form. Free-radicals are molecules that contain one or more unpaired electrons which renders the molecule reactive (OH•; hydroxyl radical, $O_2^{\bullet}$; superoxide anion); when two radicals combine, that gives rise to nonradical forms of these ROS (H_2O_2)[12]. In the presence of metals like iron, H_2O_2 can be converted to hydroxyl radical, OH•, the most reactive and damaging form of ROS (Table 3)[97].

Table 3. Types of ROS. Major endogenous oxidants and their key sites of production; studies in aquatic animals have mainly centred around these ROS types[98].

Oxidant (ROS)	Chemical Formula	Reaction Formula	Major Site of Production
Superoxide anion	$O_2^{-\bullet}$	$O_2 + e^- + H^+ \rightarrow HO_2\bullet \rightarrow H^+ + O_2^{-\bullet}$ $NADPH + 2O^2 \leftrightarrow NADP^+ + 2O_2^{-\bullet} + H^+$	Mitochondria/Cytosol
Hydrogen peroxide	H_2O_2	$2O_2^{-\bullet} + H^+ \rightarrow O_2 + H_2O_2$	Cytosol/Peroxisome
Hydroxyl radical	OH•	$Fe^{2+} + H_2O_2 \rightarrow Fe^{3+} + OH^- + OH\bullet$	Cytosol

All aerobic organisms require O_2 to live, however ROS can be formed as a by-product of cellular respiration. In the mitochondrial electron transport chain, some

electrons (~1-3%), during the process of reducing O_2 to H_2O, can leak from the cytochrome c oxidases and produce superoxide anions by the addition of an electron to molecular oxygen[95]. The major source of superoxide anions originates from the mitochondria, however they can also be formed as a by-product of enzyme activity, for example by NAD(P)H oxidases[99]. NAD(P)H forms superoxides when it metabolizes O_2 in order to activate defense mechanisms against invading pathogens. H_2O_2 can likewise be produced in the peroxisome during metabolic reactions involved O_2, or enzyme activity[99]. Additionally, ROS can be generated by the actions of environmental toxins and pollutants like pesticides, or alcohol[100].

ROS, specifically superoxide anions and H_2O_2, are also signalling molecules that mediate a wide variety of cellular activities including cell proliferation, migration, differentiation, signalling, apoptosis, and gene expression, in addition to pathogen defense (innate immunity)[96,101]. Superoxide anions are short lived, however H_2O_2 is quite stable and can traverse the cell membrane, extending the reach of its redox signalling capacity to distant targets[101,102].

Superoxide anions and H_2O_2 are not very reactive on their own, in fact low ROS levels are not deleterious. It is their transformation to OH• in the presence of iron (either free iron, low molecular weight iron chelates, or heme proteins) that gives rise to the increased reactivity[100]. This is known as the Fenton reaction (Fig. 7). Due to its ability to undergo redox cycling, iron is an intrinsic producer of ROS. Under physiological levels of O_2, iron can be found in its more stable form, Fe^{3+}. However, free Fe^{2+} (which is typically

sequestered by ferritin unless in iron overload conditions) can induce the reduction of O_2 or H_2O_2, leading to the formation of superoxide anion radicals or hydroxide radicals[95].

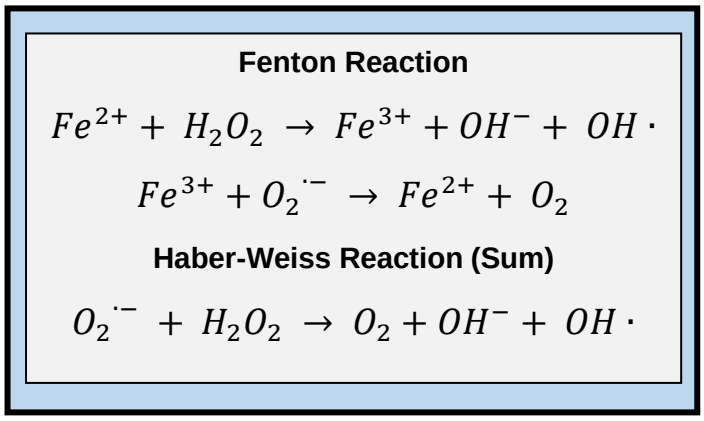

Figure 7. Iron and ROS Production.
Redox-reactions mediated by iron that result in increase of **(1)** ROS (OH·) production and **(2)** iron which can mediate further ROS production.

This iron-catalyzed ROS can also damage ferritin, or other iron containing proteins, releasing reactive iron to the labile iron pool (LIP), further increasing cellular reactive iron concentrations and thus amplifying ROS production in a continuous cycle, via the Haber-Weiss reaction as well[99]. It is a cyclic process whereby increased superoxide concentrations can lead to the release of iron (both Fe^{2+} and Fe^{3+}) from iron-containing molecules such as ferritin or Fe-S cluster-containing enzymes, rendering them inactive[95]. Superoxide anion radicals can also inactivate catalase and peroxidases, and oxidize antioxidant vitamins, thiols, and catecholamines[103]. These iron-mediated redox reactions can transpire anywhere within the cell, including the mitochondria and peroxisomes, and is thus not only limited to the cytosol[104].

The iron-catalyzed hydroxyl radicals are highly reactive (in fact the most reactive ROS), with a half-life of 1 ns in aqueous solution[95]. As a result, it tends to react with whatever is closest to its site of formation, reacting indiscriminately with cellular components including DNA, proteins, lipids, and enzymes, and also at a high rate due to

its reactivity and short half-life[100]. They can trigger DNA damage by adding double bonds to DNA bases, or by strand breaking. Furthermore, iron-catalyzed lipid peroxidation can lead to the formation of peroxyl radicals, and through a series of reactions, to the final product of this peroxidation process, malondialdehyde (MDA), which can also directly oxidize DNA[103]. In fact, lipids are the most sensitive to oxidative stress. Peroxidised membrane phospholipids can ensue, leading to plasma membrane leakage[103]. This can alter membrane permeability, and result in both decreased activity of membrane enzymes and dysfunctional membrane receptors[105]. Formation of carbonyl derivatives of proteins, peptide cleavage, amino acid modifications or unfolding of proteins can also occur following ROS-mediated attack on proteins[100,103]. If these ROS levels are not controlled, this may compromise cellular function, and if the damage occurs in neuronal tissues, for instance, it may result in neurobehavioral or neurodevelopmental impairments[56,95,106]. In fact, increased iron-mediated oxidative stress is associated with cancer, diabetes, coronary disease, myocardial infarction, rheumatoid arthritis, atherosclerosis, ischemia/reperfusion, and neurodegenerative disorders[95,107].

Biological systems exist in a steady state of formation of these oxidants (ROS) and their removal by the antioxidant defense system. Oxidative stress occurs when there is an imbalance in the system, favouring the production or activity of these oxidants. This occurs either because the overproduction of ROS exceeds the capacity of the antioxidant defense system to eliminate them or counteract their activity, or because there is a deficiency in the antioxidant defense system in effectively eliminating these oxidants (e.g., depletion of antioxidants or impaired antioxidant enzyme activity)[107]. Therefore, if the oxidants are not sufficiently metabolized or scavenged, this can result in cellular

damage[97]. In fact, iron-mediated ROS production can lead to ROS buildup, overwhelming the antioxidant system and causing oxidative stress[9].

1.4.2 The Antioxidant Defense System

The antioxidant defense system is composed of three main categories of antioxidants, which include non-enzymatic scavengers (i.e., antioxidants; GSH, α-tocopherol, vitamin E), enzymatic scavengers (e.g., GSH-peroxidases, superoxide dismutases, catalases), and conjugation enzymes (e.g., glutathione-s-transferases; GST)[96,100,107,108]. These can be further categorized by the role they play in dealing with oxidative stress. Phase I enzymes are ROS scavengers, involved in neutralizing ROS by converting it to non-reactive H_2O. These enzymes include superoxide dismutases (SODs) and catalases (CAT) and are considered the cell's 'first line of defense' against oxidative stress. Phase II enzymes are detoxification enzymes, with a role in clearing reactive oxidants and electrophilic compounds (e.g., lipid peroxides) from the cell. These include conjugation enzymes like GSTs[96,105,109–111]. Antioxidants are nucleophilic molecules, and that allows them to react with electrophilic oxidants and ROS, by donating 1-2 electrons[96]. There are numerous additional antioxidants involved in the elimination of ROS (in fact, a couple dozen exist), however the focus will be on those that are key players in the antioxidant defense system and are most commonly used as biomarkers of environmental toxicity in aquatic animals, which are SOD1, SOD2, CAT, and GST (Figure 8)[103,110,112].

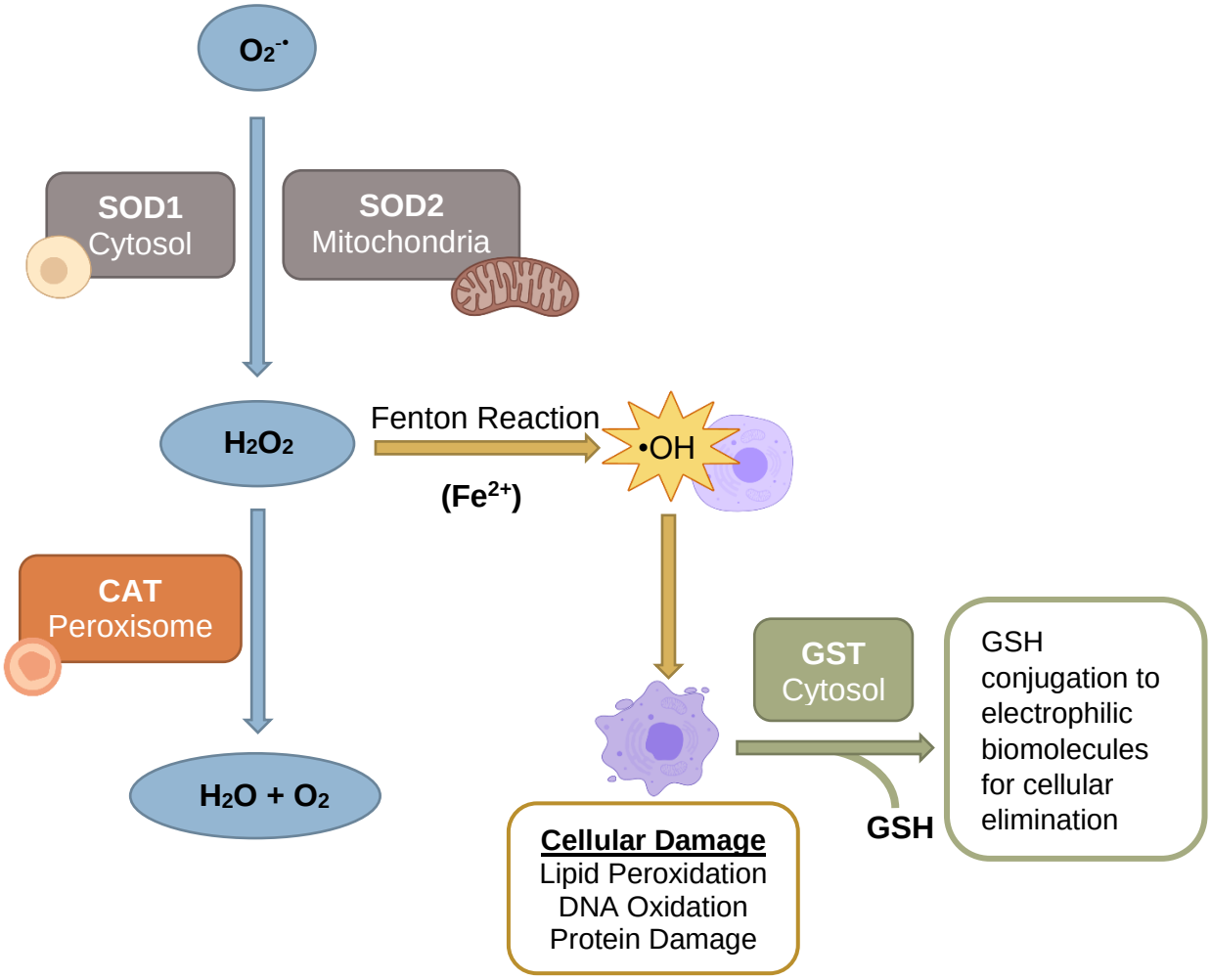

Figure 8. The Antioxidant Defense System.
Cellular production of superoxide anions ($O_2^{-\bullet}$) can result from cellular respiration, enzyme activity for pathogen defense, or environmental toxicants and pollution, including iron itself. Dismutation of $O_2^{-\bullet}$ is accomplished via SOD1 in the cytosol, and SOD2 in the mitochondria. The resulting H_2O_2 is catalyzed to H_2O and O_2 by CAT in peroxisomes. However, iron overload can increase cellular Fe^{2+} levels, which can convert the H_2O_2 to •OH before it can be neutralized. This leads to lipid peroxidation and oxidation of DNA and proteins, subsequently damaging the cell. In these circumstances Phase II antioxidants, like the detoxifying enzyme GST, can mediate the conjugation of GSH to these electrophilic molecules to (1) decrease their reactivity and prevent further cellular damage, and (2) increase their solubility for elimination from cells.

The first line of defense against oxidative stress is mediated by superoxide dismutases (SODs). Two main SODs exist in the cell: SOD1 and SOD2. SOD1 is a Cu/Zn SOD localizing in the cytosol (with a small fraction in the mitochondrial intermembrane space), whereas SOD2 is a Mn SOD found in the mitochondrial matrix near the electron transport chain, the main site of superoxide anion production[111]. SODs are metalloenzymes that catalyze the dismutation of two molecules of superoxide anions to H_2O_2 and water, utilizing a redox-active transition metal cofactor (Mn for SOD2, Cu and Zn for SOD1)[97,113,114]. Furthermore, SOD2 is crucial for cell functioning. A SOD2 knockout in mice was shown to induce lethality, due to its importance in controlling mitochondrial superoxide production (the predominant cellular ROS source). Conversely, cytosolic superoxide production under physiological conditions is comparatively lower, hence why SOD1 knockout, while producing numerous physiological issues, does not induce lethality[102].

While the resulting H_2O_2 from the dismutation reaction is a nonradical, it is highly reactive as it can be converted to •OH in the presence of Fe^{2+}. Thus, it is rapidly eliminated before such a reaction can occur. This process is typically mediated by catalase (CAT) in peroxisomes[97,113]. CAT continues the detoxification process started by SOD, by catalyzing the breakdown of H_2O_2 to H_2O and O_2, employing an iron cofactor (heme group). CAT plays a key role in capturing and converting H_2O_2 before it can diffuse out of the cell and cause damage elsewhere, and is thus crucial in protecting cells against severe levels of oxidative stress[96,111,115]. In fact, it can catalyze the breakdown of millions of H_2O_2 a second[105].

As previously mentioned, if ROS levels cannot be controlled and catalysis of high levels of •OH occur via iron-mediated redox-activity, this can lead to significant production of electrophilic molecules. Since ROS, the electrophilic compounds they produce, and iron itself are highly reactive and can catalyze further damaging reactions in the cell, adaptive responses are activated. This involves upregulation of phase II detoxification enzymes by the antioxidant defense system, for example, GSTs[116,117].

GSTs (glutathione-s-transferases) are phase II detoxification enzymes that detoxify both endobiotic and xenobiotic electrophiles[118]. They have peroxidase, isomerase, and ligand binding activity, and can also modulate apoptotic and cell survival signal transduction pathways when activated[119]. They conjugate GSH, via nucleophilic attack of the sulfur atom of GSH (reduced glutathione), to the electrophilic group on the exogenous or endogenous xenobiotic. Conjugation of GSH to electrophilic molecules by GST generates compounds that are less toxic and more hydrophilic. For example, GST prevents further oxidative damage by conjugating breakdown products of lipid peroxidation to GSH. These are subsequently converted to mercapturic acids and excreted in bile and urine, via the activity of Phase III detoxification enzymes[120]. GST can also protect the nucleophilic groups of proteins and nucleic acids and repair macromolecules damaged by ROS[121].

Three GST subtypes exist: cytosolic, microsomal, and mitochondrial. Some of its endogenous conjugation targets include peroxidised lipids and DNA hydroperoxides, while exogenous ones are heavy metals, carcinogens, and drugs[119]. The most studied are the five cytosolic mammalian classes: Alpha, Mu, Pi, Theta and Sigma[122]. These GST subunits are differentially expressed in diverse tissues, and respond to different types of

xenobiotics[108]. The commonly studied one in fish is GSTP, as it can be readily activated following exposure to toxicants. Its expression can be induced by drugs, metals, xenobiotics, and food additives, is ubiquitously expressed and developmentally regulated[119]**.**

The activity of these antioxidants is controlled by numerous ROS-sensitive transcription factors. ROS can act as secondary messengers to activate these transcription factors, which leads to the transcriptional activation and modulation of a wide variety of antioxidant genes. Whether this involves direct activation by ROS itself or via redox-regulated enzymes is still being studied[123]. The signalling effects of ROS can be far-reaching, as they can also upregulate pro-inflammatory pathways as well[124]. In fact, if ROS levels become uncontrollably high, they can mediate the activation of apoptotic cell death[111]. AP-1 (c-Fos, c-Jun, JunB, JunD), Nrf2, HIF-1, p53, NF-κB, SP1, and CREB-1 just are some of the transcription factors sensitive to H_2O_2[12,107,125]. They induce the expression of antioxidant genes to detoxify the oxidizing molecules (both ROS and electrophilic compounds) and also maintain cellular functions like cell proliferation, differentiation, and apoptosis, with numerous cross-interactions between signalling pathways (e.g., Nrf2 and NF-κB)[96,126,127]. Some transcription factors, like c-fos, are negative regulators, to ensure basal levels of ROS are still present (following detoxification processes) for physiological cellular processes[111]. In fact, antioxidant genes, for instance, SOD1, SOD2, and CAT, can be acted on by many of the above transcription factors. Consequently, each of them can be differentially regulated, however the details are still being elucidated[114,115].

All transcription factors but Nrf2 are involved in modulating cellular responses to intermediate levels of oxidative stress. However, with increasing levels of oxidative stress, the Nrf2 pathway is activated to induce antioxidant defenses (specifically phase II and III enzymes like GST) and minimize oxidative damage[96]. Nrf2 is the best characterized pathway in the antioxidant defense system. It binds to antioxidant response elements (ARE) on target genes, and can be activated by ROS, oxidants, and xenobiotics (including metals)[96,111,128]. There is a tight link between ROS, iron, and the antioxidant defense system, which also extends to regulation of iron homeostasis. Iron can, in fact, activate Nrf2, which itself modulates the expression of select iron homeostatic proteins including ferritin[116].

Antioxidant defense mechanisms are conserved amongst vertebrates, including fish, and have been extensively characterized in zebrafish[98,129]. The Nrf2 pathway especially has been heavily studied, showing similar patterns of activity between fish and mammals (i.e., GST activation by Nrf2 activity via ARE binding)[130]. Forms of ROS production are also conserved[98]. Transition metals, like iron, are known for their redox-cycling abilities and thus their potential to induce oxidative stress. CAT, SOD, GST, and GSH are recognised molecular biomarkers employed to monitor the oxidative stress responses of aquatic organisms exposed to environmental pollutants, including metals[103]. They provide an indication of the antioxidant status of the aquatic organism. Elevated exposure to trace metals (e.g., Cr and Cu) can lead to ROS overproduction and activation of the antioxidant defense system. In some cases, inhibition of antioxidase activity can occur following metal exposure. However, under certain conditions, their activity may remain elevated in an attempt by the organism to maintain oxidative balance[18,131,132].

1.5 Interplay between Iron and Essential Trace Metal Homeostasis

Iron overload may not only induce oxidative stress but may also influence the homeostasis of other essential trace metals utilized by organisms, such as copper (Cu), zinc (Zn), chromium (Cr), selenium (Se), nickel (Ni), cobalt (Co), and manganese (Mn)[18]. These trace metals have important biological roles and their deficiencies or excess can lead to adverse health effects. For example, Cu is a key constituent of metabolic enzymes (e.g., ferroxidases) and thus crucial for cellular metabolism, while Zn acts as a catalyst for numerous metalloenzymes, is involved in the metabolism of nucleic acids and proteins, and plays a role in the immune function, neurotransmission and cell signalling[18,65]. Mn, another key trace metal, is a cofactor for several enzymes involved in metabolic activities, and antioxidant defence, while also playing a functional role in bone maturation[133].

In fish, numerous studies have revealed that the regulation and homeostasis of several divalent metals are interconnected and can be affected by iron status. For example, Mn^{2+}, Co^{2+} , Cu^{2+} , Zn^{2+} , Ni^{2+}, and Cr^{2+} can utilize DMT1 for cellular entry, with increased exposure to any of these metals blocking iron uptake through DMT1, to different extents[134]. Ni^{2+}, Cu^{2+}, and Zn^{2+} were also shown to inhibit Fe^{2+} intestinal uptake via DMT1 in freshwater rainbow trout (*Oncorhynchus mykiss*)[135]. Altered regulation of Cu transporters can transpire following increased iron exposure, while iron overload conditions can lead to decreased Mn transport[24,136]. In fact, modulation of essential metal homeostasis can affect iron metabolism. For example Zn^{2+}, Cu^{2+}, and Mn^{2+} can regulate the transcription of IREG1 or even utilize it as an exporter[137–140]. Competitive binding to

transferrin with other trace metals including Cr^{2+}, Mn^{2+}, Cu^{2+}, and Co^{2+}, has also been demonstrated[67]. Transcriptional activation of hepcidin by Cu^{2+} and Zn^{2+} has been observed in cell culture studies, whereas Co^{2+} inhibits it[67]. Lastly, Mn exposure can alter the expression of Tfr1[141].

It is evident that due to such a close link between the homeostasis of iron and other essential trace metals (and crosstalk between pathways), perturbations in iron metabolism may affect regulation of other trace metals.

1.6 Iron overload and neurophysiological impairment? A potential link.

1.6.1 Iron Exposure and Altered Physiological and Oxidative Stress Responses

There is an assumption in the scientific community that waterborne ferric iron uptake is unlikely to occur and can thus only be found accumulating on external surfaces of skin and gills, exerting its toxic effects in that manner. This assumption stems from ferric iron's relatively lower bioavailability, and the high incidences of its polymerization in freshwater systems, which results in the formation of large molecular weight ferric hydroxides[11]. However, colloidal ferric iron can be small enough to pass through a 0.45 μm filter (a criteria used to determine whether iron is in soluble form or exists as precipitates), so while not considered 'dissolved' like Fe^{2+}, it can exist in a form small enough to be taken up by fish[11,42,82,142]. In fact, studies have revealed the potential existence of a ferric reductase in gut enterocytes of rainbow trout and branchial epithelium of zebrafish gills, mediating the reduction of Fe^{3+} to Fe^{2+} for subsequent uptake into DMT1, however at a slower rate than direct waterborne Fe^{2+} uptake due to limitations of

enzyme kinetics[74,143]. This is corroborated by a handful of studies which have demonstrated that while non-lethal, exposure to ferric iron in the form of ferric hydroxides does seem to have detrimental effects on the biochemistry and physiology of fish, including developing fish[3818]. For example, altered haematology in tilapia has been recorded following exposure to ferric iron, while brown trout in iron (magnetite, hematite) contaminated waters in Newfoundland displayed elevated plasma leukocytes, associated with increased liver inflammation[32,144]. Short-term exposure to ferric iron also suppressed thyroid activity of African catfish, as seen by decreased plasma T3 and T4 levels, and induced hyperglycemia, indicating a disturbed metabolic regulation[145].

Some studies have also demonstrated that exposure to waterborne ferric iron may alter stress and hormonal responses in fish. Developing carp embryos and larvae exposed to ferric sulphate exhibited increased whole body cortisol levels[50]. Increased production of cortisol and estradiol in whitefish when compared to control, following handling stress, has also been confirmed. These fish also displayed altered liver function, characterized by impaired steroid and xenobiotic metabolism, and decreased glycogen phosphorylase and phosphorylase *a* activities[21]. Another study displayed no change in estradiol concentrations and catecholamine levels before and after handling in iron exposed whitefish, whereas a distinct difference was observed in the reference groups. Seasonally related differences in fish physiology (e.g., plasma catecholamines, Na^+/K^+-ATPase activities) following acute stress were also neutralized, displaying an attenuated response. This, in conjunction with their diminished liver GPase activity, seemed to suggest that iron exposure resulted in impairments in the adrenergically mediated stress

response, as one of its key roles is to mobilize glycogen from liver by stimulating GPase activity[146].

There also seem to be indications of altered antioxidant capacity and increased oxidative stress following ferric iron exposure[17]. Induction of oxidative stress and lipid peroxidation in embryonic and adult medaka (transient; in brain and liver) was demonstrated after exposure to iron nanoparticles, in conjunction with altered antioxidants and antioxidant enzyme activity. High lipid peroxide levels in erythrocytes, in addition to differential activation of antioxidant enzymes, were also detected in cichlid fish reared in a contaminated river containing elevated iron levels[31,147].

Despite existing literature linking elevated iron exposure to altered physiological responses and induction of oxidative stress, studies have not examined whether neurophysiological functions of fish are also affected as a result, especially developing fish, as egg and early alevin stage are possibly more susceptible to iron toxicity compared to other developmental stages[23]. When examining mammalian models of iron overload, a potential link between elevated iron exposure (both during development and aging) and altered neurophysiological functions does seem to exist.

1.6.2 Iron Overload and Impaired Neurophysiological Function: Mammalian Models

Excess brain iron has been implicated in the pathogenesis of numerous neurophysiological and neurodegenerative disorders, either due to deposition of excess iron, dysregulation of iron homeostasis, or mutations of genes involved in iron homeostasis[148]. These include Alzheimer's, Parkinson's (age-related neurodegenerative disorders), Friederichs ataxia, and neurodegeneration with brain iron accumulation

(NBIA) diseases (e.g., neuroferritinopathy). Iron-induced oxidative stress plays a key role in the neurodegeneration, resulting in altered behavioural phenotypes[3,69,106,148–155]. These diseases display a link between increased iron levels mediating oxidative damage and resulting neurophysiological dysfunction.

The susceptibility for neurophysiological impairments resulting from increased iron levels in the central nervous system (CNS) is due to numerous factors. The brain is the most metabolically active organ in the body, so it possesses a high internal iron concentration. This is especially the case during development, as iron is the enzymatic cofactor for myelinogenesis[156]. As a result, the rate of iron influx to the brain during CNS development (as NTBI) is particularly elevated, with any iron uptake into the brain remaining there (iron levels in the adult brain are established during weaning period of a mammal)[2,157,158]. However, only a subset of neuronal cells (in both developing and adult CNS) possess ferritin for iron storage and thus possess a decreased ability to buffer the high levels of iron if it does occur[156,159].

It has also been proposed that the barrier mechanisms in developing brains are different than those in adults and may be more susceptible to disruptions and neurological damage[160]. The immature tight junctions of the BBB surrounding the brain in a developing organism puts it at risk for entry of NTBI into the developing brain (if iron levels are high enough to saturate transferrin) and are therefore susceptible to neurotoxins until the BBB is complete[77,156]. Furthermore, developing brains (including the BBB) have shifting temporal and regional patterns of iron transport and storage protein expression, which may render them more vulnerable to perturbations in iron metabolism[156,161].

The central nervous system (CNS) is also vulnerable to oxidative stress, due to the high oxygen needed to carry out its metabolic activities (e.g., great energy demands are required for synaptic activity). In fact, 20% of the body's oxygen supply is routed to the brain in order to keep up with the higher aerobic metabolism[99,128]. This, in addition to autooxidation of neurotransmitters and ROS release during neurotransmitter synthesis, means that the CNS contains a comparatively higher level of oxygen radicals under normal physiological conditions than other tissues. Furthermore, the CNS possesses a weak and easily oxidized antioxidant defense system[162]. While SOD levels are comparatively normal, it possesses low basal levels of CAT, and GSH due to a minimal content and activity level of Nrf2. This low GSH content can also restrict GPX activity, making the capability of the CNS to neutralize H_2O_2 minimal. Low GSH levels also means that the brain's ability to eliminate electrophilic compounds is not optimal[12,128]. Lastly, the CNS is predominantly composed of lipids (polyunsaturated fatty acids), which renders it prone to oxidative stress/ROS mediated damage[12,99,128,163].

Systemic iron overload can lead to iron accumulation in subregions of the brain like the basal ganglia, despite the protective BBB, in adult humans[164]. This has also been illustrated in numerous rodent models of iron overload (both developmental and adult models), where iron had a tendency to accumulate in brain regions that are iron-rich (basal ganglia, red nucleus, cortex, hippocampus) following systemic exposure to iron[156]. In fact, there is a comparatively greater accumulation of iron in the post natal period (as shown in rodent studies) during the first year window where the BBB is still developing[158,165–167]. Not only did iron loading occur in such rodent models, but differential expression of iron homeostatic genes and proteins (e.g., transferrin, TfR, ferritin, hepcidin,

DMT1) transpired, with impaired neurophysiological functioning (reduced motor coordination, startle response, locomotor activity) also occuring[149,165,166,168–171]. Deficits in complex behaviours like learning and memory were also impacted in rodent models of systemic iron overload (during postnatal development and adulthood), in addition to heighted anxiety[151,172,173]. In fact, children being fed infant formula with high levels of iron (12.7 mg/L iron sulphate) from 6 to 12 months scored lower in many neurodevelopmental measures such as visual-motor integration and motor functioning after a 10 year follow-up[174]. Interestingly, altered transcriptomics involved in learning/memory in brain of mice models of iron overload also arose, despite a lack of iron accumulation in the brain[164].

These altered neurophysiological functions have been linked to increased oxidative stress. Sub-chronic iron overload in rats (via intraperitoneal iron injection) lead to transient oxidative stress in the brain, displaying differential activity of CAT and SOD (both regional and temporal)[163]. Regional and temporal changes of these antioxidant enzymes in postnatal rat pups exposed to elevated iron levels were observed as well[158]. Iron uptake during neonatal period also led to oxidative stress damage to neuronal cells, with behavioural impairments mirroring those observed with Parkinson's[157]. Altered neurotransmitter homeostasis (characterized as decreased brain serotonin and dopamine levels) were likewise recorded, as iron can increase oxidation of monoamines in iron overload conditions[4,151].

1.7 Larval Zebrafish, a Powerful Model for the Study of Iron Overload

Zebrafish (*Danio rerio*) is a freshwater teleost native to South Asia, especially India, Nepal, and Bangladesh. Owing to the exposure to anthropogenic compounds released from waste water sources into their freshwater ecosystems, fish are often utilized as a biomonitoring tool to check water quality, with developing zebrafish being recently suggested as a potential candidate organism[175–178]. They have become an emerging model in developmental studies, and have been widely used to investigate the pathophysiology of trace metals, and to examine the embryotoxic and neurotoxic effects (including oxidative stress responses, or any toxicant-related stress responses) of effluents from various anthropogenic sources, including metals[85,175,179–181]. Transcriptional profiling, enzyme activity analysis, and behavioural neurotoxicity tests are typically carried out, in addition to the examination of key developmental endpoints, morphology, cardiac activity, and neurophysiological functioning (e.g., neuronal development). Larval zebrafish have also been employed to study the effects of iron overload, however its impact on neurophysiological function has not been examined[182–185]. On the other hand, zebrafish may prove useful in modeling iron overload-related diseases due to the close genetic similarity with humans[66,85,87,186,187].

Zebrafish show 70% genetic homology with humans (with large regions of conserved synteny with human chromosomes) which also extends to its neurophysiology. This is advantageous for while iron's effect on fish neurophysiology has not been examined, we may reference mammalian and human models of iron overload to interpret our results and make comparisons. Anatomical and physiological features of zebrafish

are similar to that of mammals. For example, key signalling pathways, metabolic pathways, cognitive behaviours, developmental process, cardiovascular function, and sensory systems are conserved. There is also existing homology between the antioxidant defense systems (e.g., expression patterns, activity levels, and antioxidant genes) of humans and zebrafish[91,112,129]. Mammalian and zebrafish brains are also quite similar with respect to functional components, with zebrafish also possessing a forebrain (diencephalon and telencephalon), midbrain, and hindbrain. They even possess a BBB similar to humans. Neurotransmitters, cell types (neurons, glial cells, oligodendrocytes, and astrocytes), and the neurological system itself are also conserved between zebrafish and mammals (including humans)[188]. In fact, larval zebrafish are used to model neurological and psychiatric disorders[66,189]. However, unlike its mammalian counterparts, zebrafish possess a marked capacity for adult neurogenesis and regenerative ability in the brain[190].

The use of zebrafish larvae confers many other advantages. Zebrafish's external development can allow us to monitor changes in response to iron overload throughout their developmental stages, while their transparency can enable us to directly observe internal structures through light microscopy (e.g., heart). Since iron overload has been shown to induce cardiac dysfunction in mammals, we can use this opportunity to examine larval zebrafish cardiac function[191]. Additionally, *in vivo* imaging of the body can also be achieved using vital fluorescent dyes (e.g., labelling ROS). Furthermore, frequent spawning, large spawns, and rapid development (e.g., maturation of the BBB occurs between 3 to 10 dpf[192,193]) make zebrafish a more powerful animal model as it allows for increased throughput of study (e.g., monitoring in multi-well plates) that cannot be

accomplished with other vertebrate models, like rodents[66,194,195]. For example, embryogenesis is completed within the first 72 hours and major organs can be detected by 5 dpf (days post fertilization), at which point they can begin exogenous feeding. Prior to this point, nutrients are supplied by their yolk sac[196].

1.8 Objectives and Hypothesis

As previously discussed, exposure to high levels of ferric iron may potentially affect fish fitness and physiological performance. Impaired neurophysiological functioning may render developing fish unable to effectively respond to external stimuli, which may decrease its viability (e.g., fail to escape from adverse conditions such as predation). Despite iron contamination of freshwater ecosystems remaining a pressing environmental concern, this aspect of iron toxicity on fish has never be explored. Consequently, the objective of this study was to examine the effects of ferric iron exposure on 1) regulation of iron homeostasis, 2) oxidative stress responses, and 3) physiological and behavioural phenotypes during early development, using larval zebrafish as our model organism.

As developing fish are likely more vulnerable to environmental contaminants, we will examine whether they can maintain iron homeostasis in the face of elevated waterborne iron levels. Therefore, in addition to measuring whole-body total iron loading, the mRNA expression of key iron transport and storage proteins, including DMT1, TfR1, IREG1, and ferritin, will be assessed. Furthermore, if whole-body iron loading does occur, we want to ascertain whether they are able to effectively mitigate any potential iron-mediated ROS damage by launching an effective oxidative stress response. Therefore, whole-body ROS levels will be measured to determine the extent of ROS production if it

does transpire. We speculated that if fish experience elevated ROS, then the mRNA expression of oxidative stress-response proteins will increase. Therefore, SOD1, SOD2, CAT and GSTP will be examined. Notably, these genes are also commonly used as environmental contamination biomarkers. To determine whether the neurophysiological functioning of developing zebrafish was altered following iron overload, their swimming activity, escape responses, and stress responses will be examined. Key physiological performance (e.g., heart rate, hatching rate) will be evaluated as well.

Since developing rodent models of iron overload exhibit altered behavioural phenotypes, and because tissue iron loading and oxidative stress have been shown to transpire in ferric iron-treated fish, we hypothesize that exposure to elevated ferric iron levels in developing zebrafish will result in altered neurophysiological functioning stemming from elevated whole body iron levels and iron-mediated induction of oxidative stress.

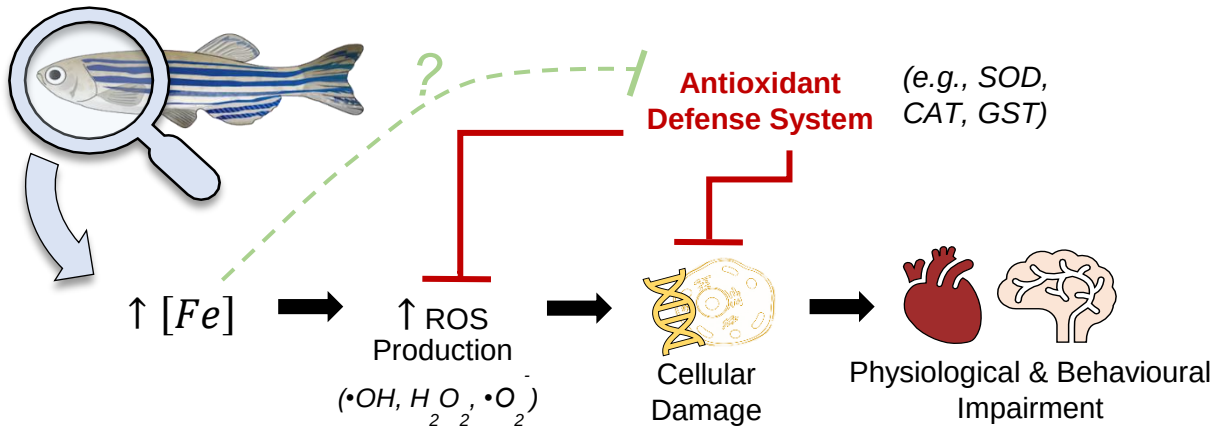

Figure 9. Hypothesis.
Exposure to elevated waterborne iron will lead to tissue iron loading and oxidative stress, by amplifying ROS production, and via modulation of the antioxidant defense system. This will compromise cellular functioning, and subsequently lead to physiological and behavioural impairments in developing zebrafish.

2 Materials and Methods

2.1 Zebrafish Husbandry and Embryo Collection

Adult zebrafish (TL strain) were housed in re-circulating aquaria maintained at 28℃, pH 7.4, and in a 14 h light/10 h dark cycle. In order to collect eggs, males and females were placed in breeding cages the afternoon prior to breeding, with a ratio of 2 females: 1 male, and separated by a mesh divider. Spawning was induced the next morning once the light was turned on and mesh divider removed. Zebrafish were allowed to spawn for 1-2 hours. Fertilized eggs were collected within an hour and placed in Petri dishes (50-100 per 50 mL). Embryos were subsequently examined under a dissecting microscope, and dead or unfertilized embryos were removed prior to treatment.

2.2 Exposure Regime

Ferric ammonium citrate (FAC, Alfa Aesar) was used as our iron source in this exposure study. A stock solution of 100 g/L FAC was made by dissolving FAC in Milli-Q water. Stock solution was kept at room temperature and in the dark until use. A previous study reported that exposure to 100 mg/L of FAC significantly increases whole body iron levels in larval zebrafish[182]. In the present study, 0 (control), 10, 50, and 100 mg/L FAC were tested. The FAC exposure water was prepared with deionized water supplemented with NaCl, $CaSO_4 \cdot 2H_2O$, $MgSO_4 \cdot 7H2O$, K_2HPO_4, and KH_2PO_4 (artificial freshwater; AF). The ionic composition of the water was (in µM): 800 Na^+, 250 Ca^{2+}, 62 K^+, and 150 Mg^{2+}. The pH of both exposure and control waters were adjusted to 6.8-6.85 using H_2SO_4, which is the pH of the solution containing the highest iron concentration. Adding iron to

water decreases its pH, so to isolate the possible effects of pH from that of iron and pH on the larvae, the pH of the control AF was also reduced to the same amount and not kept at around 7 or higher[23]. This is supported by studies suggesting that the pH of the ferric iron exposure water should be kept between 6.5 to 9 to minimize any confounding effects of pH on the results[19]. Furthermore, zebrafish can function normally in pH 6.5 to 8 waters as characterized in standardized toxicity tests[188,197,198]. Because we observed that exposure to 50 mg/L FAC was sufficient to increase whole-body iron levels in larval zebrafish (see Results), this concentration was chosen for all subsequent experiments, unless mentioned otherwise.

Within 3 h post-fertilization (hpf), embryos were placed in new Petri dishes (40 larvae per Petri dish, N=1) containing either 40 mL of 0 or 50 mg/L FAC water. Embryos/larvae were maintained in an incubator at 28^{o}C, set up with a 14 h light/10 h dark cycle. Over the course of the exposure (from 0 to 5 days post fertilization; dpf), the exposure and control waters were made fresh and changed daily. Experimental timeline is shown below:

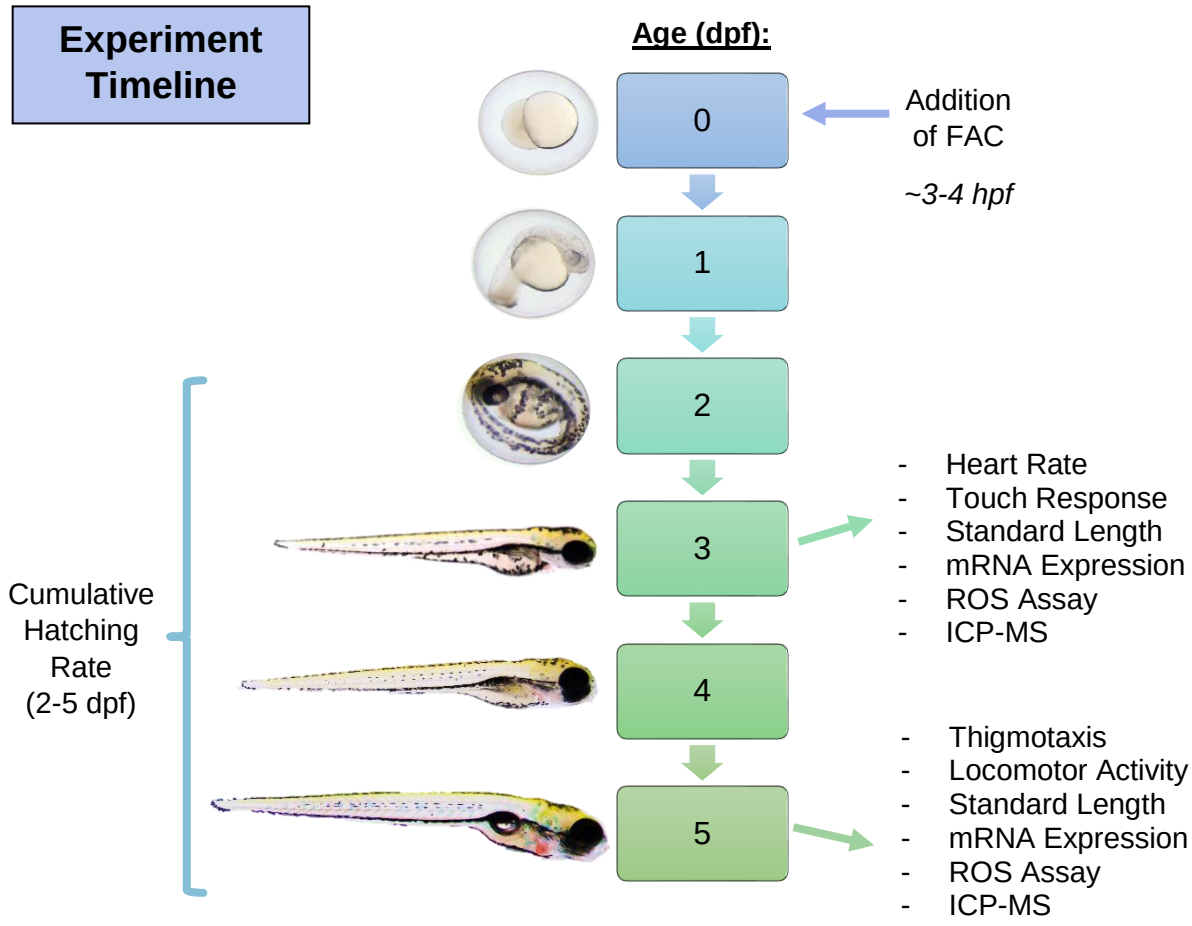

Figure 10. Experimental Timeline.
Key physiological, molecular, and behavioural parameters were assessed on either 3 dpf, 5 dpf, or both. Cumulative hatching rate was examined from 2-5 dpf. FAC exposure water was added by 3 hpf and changed daily; control water was also changed daily.

2.3 Measurements of Water and Whole-body Iron Levels

To determine total iron levels in the exposure water, a quantitative colorimetric iron assay was carried out, using the QuantiChrome™ Iron Assay Kit (DIFE-250, BioAssay Systems). The absorbance was measured at 590 nm using a microplate reader (Gen5, BioTek). Whole body iron burden was determined in 3 and 5 dpf larvae (control and FAC treated). After euthanization with MS-222, larvae were washed twice with iron-free AF, and transferred to 1.5 mL microfuge tubes with excess water removed. Twenty fish were pooled as one sample, and a total of five to six samples (N=5-6) were analyzed in this experiment. Firstly, tissues were dehydrated for 24 h at 65^{o}C, followed by digestion with 200 µl 6N HNO_3 at 65^{o}C for an additional 48 h. Samples were diluted appropriately with 2% HNO_3 and then filtered. Trace metal levels were analysed using an inductively coupled plasma mass spectrometry (ICP-MS) at Trent University. The essential trace metals examined, in addition to iron, were Mn, Zu, Cu, Co, and Ni – this was carried out to determine whether exposure to elevated levels of iron can alter the homeostasis of essential metals. Levels of essential ions, Ca^{2+}, K^{+}, Mg^{2+}, and Na^{+} were also measured to check for any changes in ionoregulation following iron exposure. To examine total iron content in 5 dpf larval heads, the head regions of the larva (including the brain and eyes) were isolated using a razor blade, following euthanization with MS-222, ensuring that the gut, yolk sac, or other tissues were not included. Twenty larval heads were pooled as one sample (N=3-7).

2.4 Physiological Conditions

Larvae were examined daily to check for any morphological changes or deformities, and whole-body length was measured at 3 and 5 dpf (standard length). Standard length is defined as the tip of the snout to the base of the tail, not including the length of the caudal fin.

Heart rate was measured in 3 dpf larval zebrafish – because inflation of the swim bladder and active swimming behaviour occur at 4 dpf and beyond – to examine whether iron overload altered cardiac function in developing zebrafish. Each Petri dish containing larvae was first allowed to acclimate under the microscope (Leica) for 10 min. A 1-1.5 min video of each larva (5 larvae/dish, n=9-15 per treatment) was then recorded using the LAS X software. The number of heart beats were counted and documented as beats/min.

To determine whether iron overload can delay hatching time, the cumulative hatching rate, the percentage of larvae that hatched (including the survivors and those that died after hatching) out of the total number of embryos initially placed in each Petri dish, were recorded from 2 dpf to 5 dpf, at the same time each day. Under normal conditions, larvae typically hatch between 2-3 dpf.

2.5 Behavioural Responses

To examine developmental neurotoxicity as a result of iron overload, diverse parameters were utilized, already established in the field of zebrafish neurotoxicity. Neurotoxicity is not only limited to the brain, but includes any component of the CNS, PNS or sensory organs[188]. Accordingly, response to tactile stimuli, general locomotor activity, and anxiety using thigmotaxis were the parameters utilized in this study[181,199].

2.5.1 Touch Response

Zebrafish larvae can respond to touch stimuli by 2 dpf, and by 3 dpf they display a startle or escape response when touched, reacting swiftly to tactile stimuli by swimming away[181]. This touch response test can thus be utilized to check for defects in sensory-motor function. Following the exposure (control or 50 mg/L FAC treatment), zebrafish larvae at 3 dpf were transferred to a new Petri dish containing only AF and allowed to acclimate under the microscope for 10 min. Tactile stimulus consisting of a light touch was applied to the tail of each larva (8-21 larvae/dish, N=6) using a microloader pipette tip. Their responses were recorded using the LASX software. The touch-evoked responses were categorized into two groups: i) larvae swam away immediately after a single touch (immediate response), or ii) larvae responded after 2-3 touches or showed no response to touch (delayed/unresponsive).

2.5.2 Free Swimming Activity

All subsequent behavioural tests were carried out in the DanioVision™ tracking chamber (Noldus) and analyzed using the EthoVision Software. The tracking chamber is a light-tight box, with infrared illumination from the bottom to allow for recording in the dark, as well as visible light illumination for recording in a light setting. In order to assess larval locomotor activity, general swimming activity was examined using this set up, on 5 dpf larvae. Robust locomotor activity arises at 5 dpf and its behavioural repertoire continues to stabilize until 7 dpf. On the other hand, only burst locomotor activity are witnessed in 3 dpf larvae, thus the behavioural repertoire they display is limited and not consistent for study purposes[200]. Furthermore, 4 dpf larvae were not used due to the high variability seen at that age, resulting from the transition to an inflated swim bladder

(characterized as free swimming) from an inactive swim bladder. The timing at which this begins is not synchronized between larvae, thus some may be more active than others, resulting in an inconsistent and highly variable dataset[201].

Larvae at 5 dpf were examined under the microscope to ensure normal morphology, as any malformations will affect locomotor activity, and consequently accuracy of the behavioural readout[202]. A single larva (12 larvae from each treatment per plate) was placed per well, in a 24 well plate containing 1 mL of its respective exposure water. Four plates were prepared for four separate trials, as large sample sizes are required due to the high intra- and inter-larval variability that exists with respect to locomotor activity[201,203]. Furthermore, the choice for 24-well plates rather than 96 or 48 stems from literature showing that improving the ratio of larvae body length to well diameter (6.8 mm:4 mm in 96-well plate versus 16.5 mm:4mm in 24-well plates) results in a comparatively more accurate readout of locomotor activity (e.g., speed and duration of locomotion)[200,202,203].

These plates were subsequently placed in the incubator for 2 hours in order to acclimate and reduce the stressful effects of transferring the larvae[204]. Following this, each plate was placed inside the tracking chamber and allowed to acclimate for 5-10 minutes at room lighting (500-650 lux). After acclimation, larvae were exposed to the dark (0 lux) for 10 min followed by light (4, 000 lux) for 10 min, alternating between light and dark cycles for 30 mins, and the swimming activity recorded, with a sampling rate of 25 frames/sec. Average swimming velocity, total distance moved, and percent cumulative duration larvae spent either moving or not moving, under both light and dark conditions, were analyzed on excel. Any wells showing incorrect tracking by the software was

discarded from the final data set. For all experiments, testing began after 13:00 in the afternoon as larvae during that diurnal period exhibit stable activity[205].

2.5.3 Thigmotaxis

To assess larval stress responses at 5 dpf, the same set-up and protocol stated in the previous section was utilized. Here, a stress response was triggered by turning the light off for 5 mins (0 lux), after having kept it on for 10 min (10,000 lux). Four trials were carried out. Percent time spent in each zone of the well, as well as percent distance moved, defined as the outer zone (4 mm-wide outer perimeter of well; equivalent to standard length of 5 dpf larval zebrafish) and inner zone (centre of well; diameter=8.5 mm), were determined using the EthoVision software. For larval zebrafish, sudden darkness induces a stress response characterized by hyperactivity. When stressed, larval zebrafish display thigmotactic behaviour, where they will spend a higher percentage of their time swimming near the edges of the well, rather than in an open space (centre of well). While studies have mentioned that thigmotactic behaviour is also shown in zebrafish larvae after sudden light stimulus, their basal locomotor activity in the light is quite low, and thus not considered a reliable readout of their behaviour[206]. The set up for both thigmotaxis and locomotor activity is below:

Experimental Outline

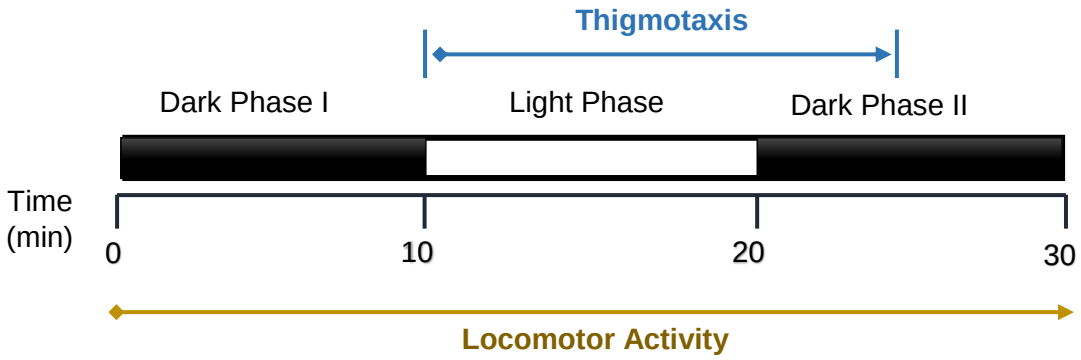

Plate Set-Up

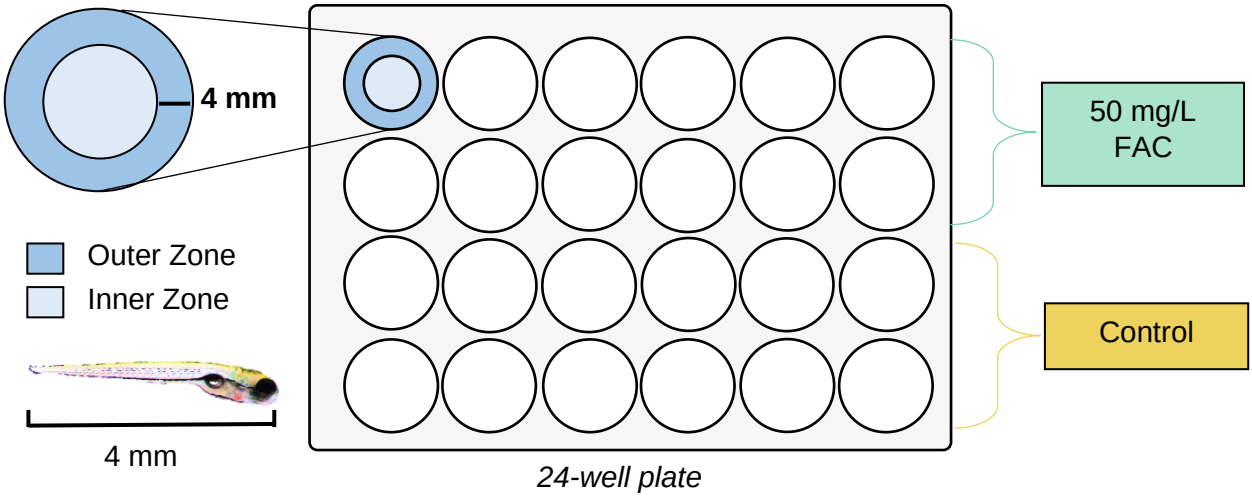

Figure 11. Set-up for the behavioural tracking chamber.

2.6 ddPCR (droplet digital PCR)

Control and FAC-exposed larvae (3 and 5 dpf) were euthanized and total RNA was isolated from pools of 20 larvae (20 larvae per replicate, total of 3 replicates per treatment) using the Monarch Total RNA Miniprep Kit (New England BioLabs), and purified. cDNA (from 1 μg RNA) was subsequently synthesized using the iScript cDNA Synthesis Kit (Bio-Rad). ddPCR (digital droplet PCR) was employed to quantify changes in mRNA expression levels between control and FAC treated larvae. The mRNA expression levels of iron transport and storage genes, DMT1 (*dmt1)*, TfR1b (*tfr1b)*, ferroportin (*ireg1)*, and ferritin1a and 1b heavy chains (*fth1a, fth1b)* were examined (Primer sequences are listed in Table 4). Several oxidative stress-response genes, including SOD (*sod1, sod2*), CAT (*cat*), and GST (*gstp1*) were also evaluated. To examine both phases of the antioxidant response, phase I antioxidant enzymes involved in ROS neutralization (i.e., SOD, CAT) and a phase II enzyme involved in elimination of electrophilic compounds (i.e., GST), were examined. *Gstp1* was used since it is the *gst* variant that is ubiquitously expressed in larval zebrafish and has shown strong involvement in metal, electrophilic compound, and xenobiotic metabolism[119].

First, PCR products of control 5 dpf larvae were purified and sent for sequencing (Centre for Applied Genomics; The Hospital for Sick Kids, Toronto) to confirm whether the designed primers amplified the correct genes of interest. Once confirmed, samples were prepped using the QX200™ddPCR™ EvaGreen® Supermix (Bio-Rad) and emulsified with Droplet Generation Oil for EvaGreen (Bio-Rad) into nanolitre-sized droplets using the QX200™ddPCR™ Droplet Generator (Bio-Rad). Emulsified droplets from each sample were pipetted into a 96-well plate, sealed, and amplified using a

thermocycler (Bio-Rad). Thermal cycle was as follows: enzyme activation for 5 min at 95℃, denaturation for 30 s at 95℃ for 40 cycles, annealing/extension for 1 min at 60℃ for 40 cycles, followed by signal stabilization for 5 min at 4℃ and 5 min at 90℃. Ramp rate of 2℃/sec was utilized between steps. Droplets were subsequently read after amplification, using the QX200™ Droplet Reader (Bio-Rad), with values given as number of copies/μL. Three biological replicates (per treatment) for each gene of interest were used and fold-changes averaged, relative to control. The expression levels of the target genes were normalized to the mRNA content of our reference gene, Ef1a (*ef1a*). Two-way analysis was performed to check the stability of this housekeeping gene under both control and FAC conditions (see Fig. S1 for details). The results demonstrated that *ef1a* displays a stable expression profile in both control and FAC-treated larvae when measured using ddPCR. This indicates that iron exposure does not affect the expression of *ef1a* and can thus be employed as a reference gene in our study.

Table 4. ddPCR Primer Sets. Corresponding primer sequences of iron transport/storage and oxidative stress response genes expressed in zebrafish larvae, for ddPCR.

Gene	*Encoded Protein*	*Accession Number*	*Primer Sequence (5'-3')*
dmt1	Divalent Metal Transporter 1	AF529267.1	**F:** CCAGCAAACAACGAGACCCT **R:** CAGGAAACCCTCCATCACAAAC
tfr1b	Transferrin Receptor 1b	NM_001009918.2	**F:** AATGGCTTGAGGGATACTGGG **R:** AGCATGGGTGCTTTGACCTT
fth1a	Ferritin1a heavy chain	XM_017356903.2	**F:** GCTGGCATCTCAACACAACG **R:** CTTGTCGAACATGTACTCGGC
fth1b	Ferritin 1b heavy chain	XM_017356903.2	**F:** TCAAGGAGCTGTCGGATTGG **R:** CCCTGCATATGGCTGACTGA
ireg1	Ferroportin/IREG1	HM068067.1	**F:** CCTACAACTGAACCCCCGAT **R:** CGAAGGACCAAAGACCAACTCT
sod1	Superoxide Dismutase 1 (Cu/Zn SOD)	NM_131294.1	**F:** GGTGACAACACAAACGGCTG **R:** AGGTCTCCGACGTGTCTCA
sod2	Superoxide Dismutase 2 (Mn SOD)	NM_199976.1	**F:** GAACCACAGGGTGAGCTGTT **R:** GCTGCAATCCTCAATCTTCCG
cat	Catalase	NM_130912.2	**F:** TCTCCTGATGTGGCCCGATA **R:** TTTGCACCATGCGTTTCTGG
gstp1	Glutathione-S-Transferase Pi	NM_131734.3	**F:** CTTCGCAGTCAAAGGCAGATG **R:** CGCCCTTCATCCACTCTTCA
ef1a	Elongation Factor 1 alpha	FJ915061.1	**F:** CCTCTTGGTCGCTTTGCTGT **R:** GAGTTGGGAAGAACACGCC

2.7 ROS Assay

To evaluate the presence of ROS at the whole-body level between control and FAC-exposed larvae, at 3 and 5 dpf, under in vivo condition, CM-H_2-DCFDA (chloromethyl -2',7'-dichlorodihydrofluorescein diacetate; Invitrogen) was employed. CM-H_2-DCFDA is a fluorescent dye-based ROS indicator that passively enters cells and fluoresces upon oxidation by intracellular ROS, following its cleavage by intracellular esterase. It was used rather than H_2-DCFDA for improved retention in the cell, which would allow for long term imaging since its thiol-reactive chloromeythyl group (that becomes exposed following cleavage) can allow it to covalently bond to intracellular glutathione or other thiols. As a positive control, zebrafish larvae exposed to 2 mM H_2O_2 for 1 hour (to induce oxidative stress) were used[207].

Control zebrafish larvae were incubated in 10 µM CM-H_2-DCFDA for two hours in 2 mL microfuge tubes (10 larvae/tube in 1 mL of 10 µM CM-H_2-DCFDA)[207]. Previous testing with H_2O_2 -exposed larvae showed improved uptake and longer retention following a longer incubation. FAC- and H_2O_2-exposed larvae were first washed with AF and then incubated with CM-H_2-DCFDA, for also two hours. Exposure was carried out in the dark and inside the incubator to maintain optimal ambient conditions. After exposure to CM-H_2-DCFDA, larvae were washed twice with AF, then placed in respective Petri dishes, containing system water with MS-222. MS-222 anaesthetizes the larvae to minimize larvae movement during image acquisition. Both whole body and head of larvae were imaged using a fluorescent microscope (Leica). Additionally, larvae without CM-H_2-DCFDA exposure (negative control) were imaged. For quantitative determination of ROS levels, these larvae were also placed in 96 well plates, one larva per well (n=35-37 larvae

per treatment). The plate was positioned in the microplate reader (Gen5, Biotek) fitted with a green filter, and ROS levels measured at an excitation of 485/20 nm and emission of 528/20 nm. Two readings were carried out and averaged. Values were normalized to a blank (well containing AF/MS-222 mix) and fold changes in fluorescence intensity of FAC-exposed larvae were determined relative to control.

2.8 Statistical Analysis

Sigmaplot software was used for all statistical analyses and graphing. Data were checked for normality and equal variance. If failed, non-parametric tests were used. Statistical differences between groups were determined using student's t-test, one-way, two- way ANOVA or two-way RM ANOVA, followed by the post hoc Holm-Sidak test. $p < 0.05$ was defined as statistically significant. Data are expressed as mean ± SEM (standard error of the mean).

3 Results

3.1 Iron Analysis

To determine whether exposure to high FAC concentrations lead to increased iron accumulation in the larval zebrafish, trace metal analyses on 5 dpf larvae exposed to 0, 10, 50, and 100 mg/L FAC were carried out using ICP-MS. The results show that exposure to 50 mg/L or 100 mg/L FAC resulted in a similar elevation of total iron levels in zebrafish larvae (Figure 12). Because exposure to 50 mg/L and 100 mg/L FAC were found to similarly increase total iron levels in the body (P=0.230), 50 mg/L was chosen for subsequent experiments.

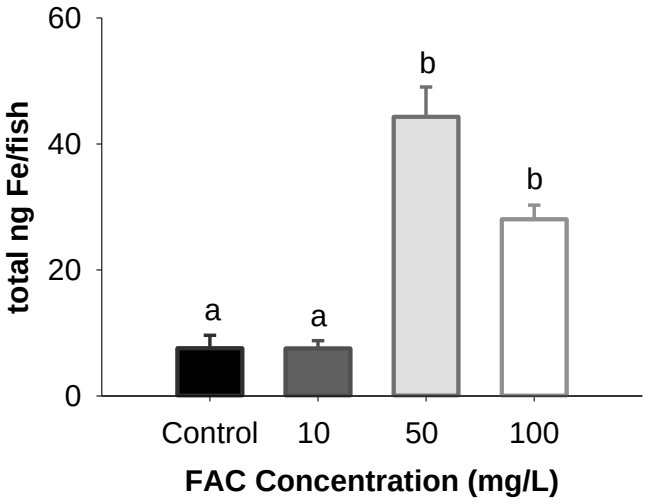

Figure 12. Effects of FAC exposure on whole body iron level in zebrafish larvae
Five-day exposure to 50 mg/L or 100 mg/L FAC caused a significant increase in whole-body iron levels of 5 dpf larvae, compared to control. Data are mean ± SEM, N=5-6 per treatment, with 20 pooled larvae per replicate. Bars not sharing the same letter are significantly different from each other (one-way ANOVA, $p<0.05$).

When a colorimetric iron assay was carried out to determine the total iron concentration in the FAC exposure water, results showed that 50 mg/L FAC contained about 12.1 mg/L Fe, which falls within the range of iron found in contaminated freshwaters (refer to Table 1). This FAC concentration employed can thus be considered environmentally relevant (Table 5).

Table 5. Total iron content of the exposure water (FAC dissolved in AF). Data represents mean ± SEM of six technical replicates.

Concentration of FAC used in Exposure Water (mg/L)	Total Iron Content in Exposure Water (mg/L)
0	0
10	2.8 ± 0.1
50	12.1 ± 0.1
100	23.5 ± 1

Five-day exposure (from 0 to 5 dpf) to 50 mg/L FAC increased whole body iron levels in both 3 and 5 dpf larvae, compared to control (Fig. 13a). There was a significant 3-fold increase in whole body iron levels in FAC-exposed 3 dpf larvae, when compared to control. However, difference in tissue iron loading between control and FAC-exposed larvae was even larger at 5 dpf, with FAC-exposed larvae exhibiting a 6-fold increase in whole body iron levels. To compare, there was no significant difference in iron levels between control groups (3 dpf versus 5 dpf; p=0.366).

To check for general tissue distribution of iron, iron levels in the head region were also measured in 5 dpf larvae and compared to whole body iron levels (Fig. 13b). The head region of larvae exposed to 50 mg/L FAC displayed a 3-fold increase in total iron levels, compared to control, while whole-body measurements showed a 6-fold increase in total iron levels.

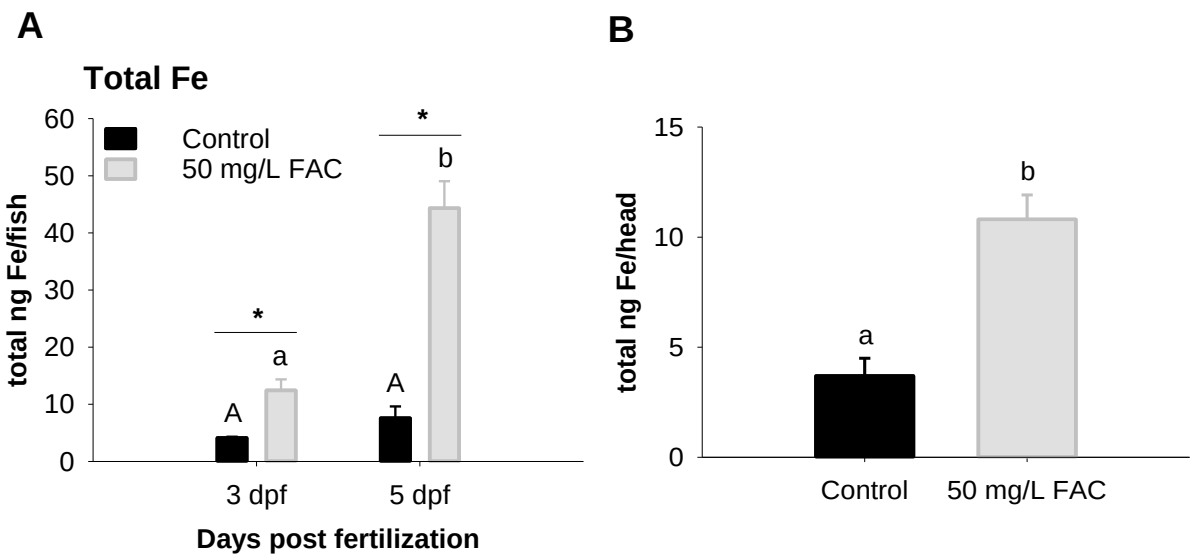

Figure 13. Iron loading in whole body and head of iron-exposed larvae.
(A) Mean± SEM of total Fe (in ng) per larva, at 3 and 5 dpf, measured using ICP-MS. N=5-6 per treatment, pooled sample of 20 larvae per replicate. Letters compare within treatments; asterisk within the same developmental age. ($p<0.05$, two-way ANOVA). **(B)** Tissue iron loading in 5 dpf larval heads after exposure to 0 or 50 mg/L FAC. Mean ± SEM. N=3-7 per treatment, 20 pooled larvae per replicate. Bars not sharing the same letter are significantly different from each other (student's t-test, $p<0.001$).

3.2 Trace Metal and Ion Homeostasis

Since iron transport proteins like DMT1 and IREG1 may mediate the transport of other divalent metals across cells, and potentially impact their homeostasis, whole body Ni^{2+}, Mn^{2+}, Zn^{2+}, Cu^{2+}, and Co^{2+} levels were measured using ICP-MS. Both 3 dpf and 5 dpf FAC-exposed larvae showed increased whole-body Mn levels when compared to control. Two-way ANOVA showed a significant interaction between iron exposure and developmental age, with increased Mn retention observed at both 3 and 5 dpf; however, the increase (1.7-fold compared to control) was only statistically significant at 5 dpf following a post-hoc test (Fig. 14a). For the other trace metals, no significant interaction was detected, therefore a student's t-test was carried out. The results demonstrate that

whole body iron loading resulted in a significant 1.2-fold increase in whole body Zn^{2+} levels in 3 dpf larvae, when compared to control (Fig. 14b) and a 1.6-fold increase in whole body Ni^{2+} levels in 5 dpf larvae (Fig. 14c). No difference in Zn^{2+} levels at 5 dpf or Ni^{2+} levels at 3 dpf were seen. Cu^{2+} (Fig.14d) and Co^{2+} (Fig. 14e) displayed no significant difference in levels when compared to control, on either day.

With respect to major ion homeostasis, there was no significant difference in Na^{+}, K^{+}, or Mg^{2+} whole body levels in either 3 dpf or 5 dpf FAC-exposed larvae, when compared to control (Fig. 15b-d). However, there was a significant 1.4-fold increase in Ca^{2+} levels in 3 dpf larvae when compared to control (Fig. 15a), while levels were no different from control at 5 dpf.

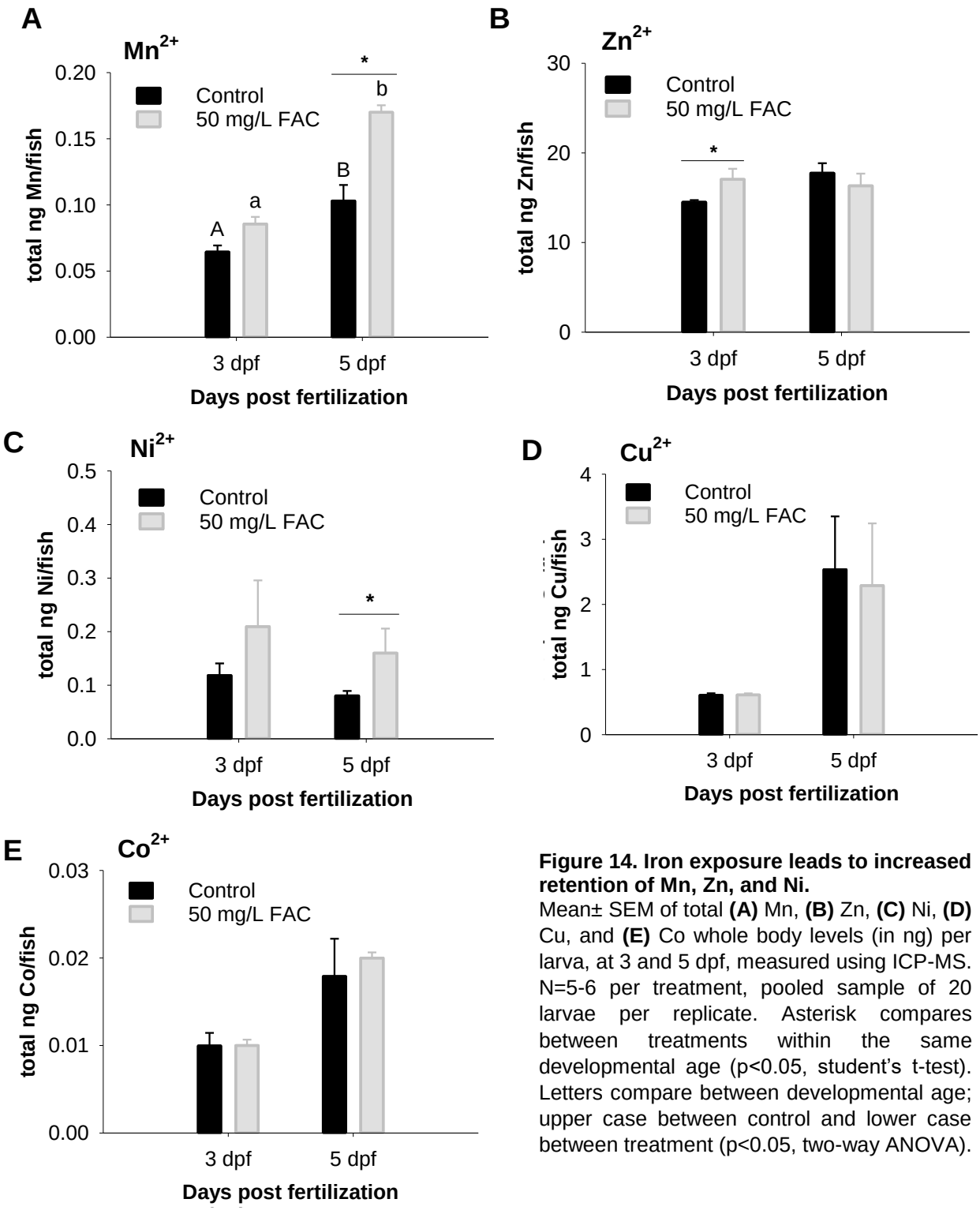

Figure 14. Iron exposure leads to increased retention of Mn, Zn, and Ni.
Mean± SEM of total **(A)** Mn, **(B)** Zn, **(C)** Ni, **(D)** Cu, and **(E)** Co whole body levels (in ng) per larva, at 3 and 5 dpf, measured using ICP-MS. N=5-6 per treatment, pooled sample of 20 larvae per replicate. Asterisk compares between treatments within the same developmental age ($p<0.05$, student's t-test). Letters compare between developmental age; upper case between control and lower case between treatment ($p<0.05$, two-way ANOVA).

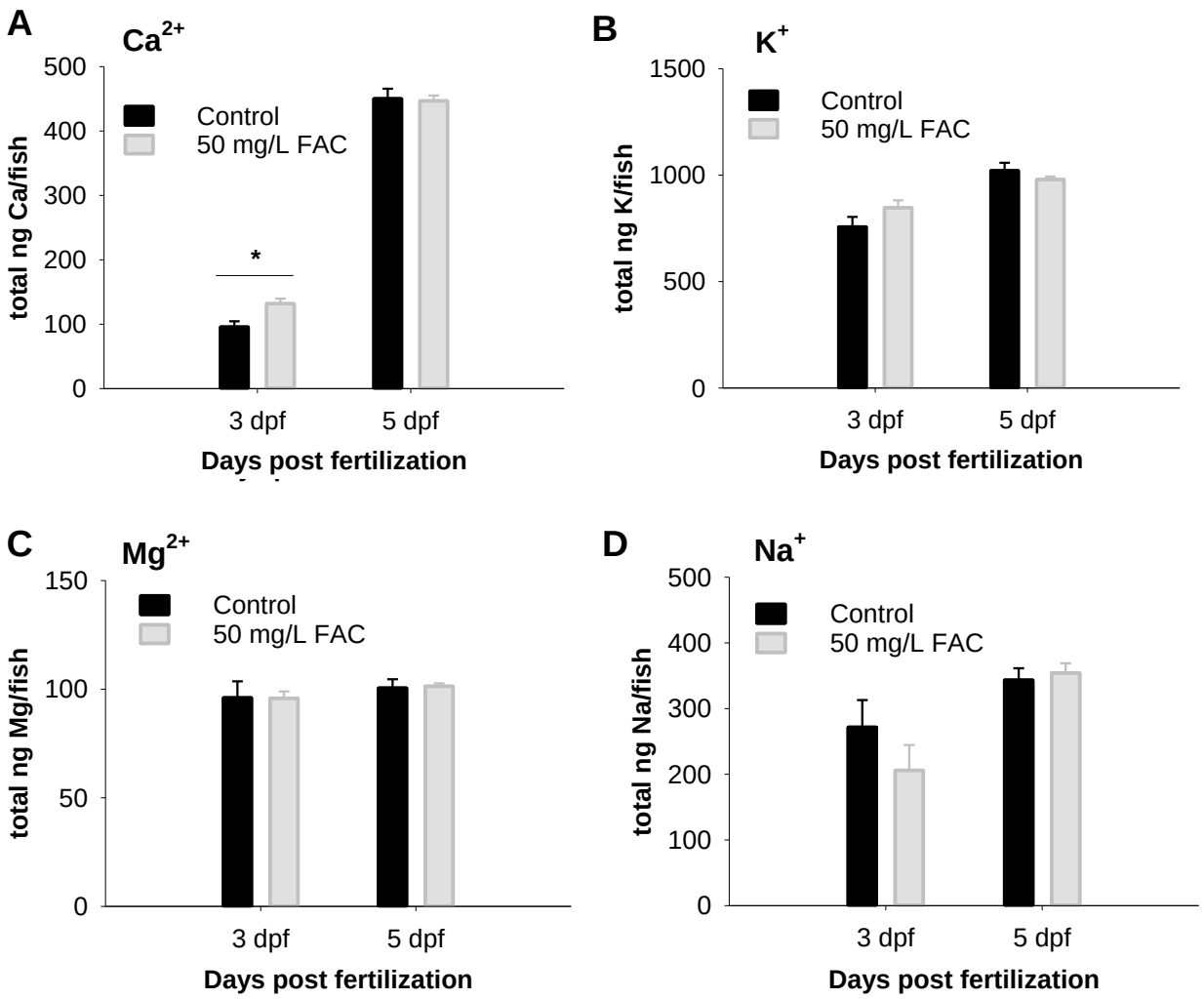

Figure 15. Iron exposure causes increased retention of Ca^{2+} at 3 dpf.
Mean± SEM of total **(A)** Ca^{2+}, **(B)** K^{+}, **(C)** Mg^{2+}, and **(D)** Na^{+} whole body levels (in ng) per larva, at 3 and 5 dpf measured using ICP-MS. N=5-6 per treatment, pooled sample of 20 larvae per replicate. (*p<0.05, student's t-test).

3.3 Physiological Endpoints

The effects of FAC exposure on cumulative hatching rate is illustrated in Figure 16a. The cumulative hatching rate of larvae exposed to 50 mg/L FAC was significantly lower at both 2 and 3 dpf compared to control (3.9% versus 35.3% and 74.7% versus 100%). Interestingly, the delay in hatching did not appear to be permanent, as cumulative hatching rate of 50 mg/L FAC-exposed larvae reached 100% by 5 dpf. The mortality of zebrafish embryos/larvae was also recorded in this experiment. At 1 dpf, the mortality rate for control embryo was 4.13 ± 0.92 %, and 9.46 ± 1.47% for 50 mg/L FAC exposed embryo (N=17-25, 30-40 larvae per replicate). However, after 1 dpf, no further mortality was observed in both control and 50 mg/L FAC treated larvae. Zebrafish larvae typically experience what is termed a 'mortality wave' within the first 24 hpf, where mortality is the highest, ranging from 5-40% for control larvae[195]. Differences can range by how thoroughly the egg screening was carried out, with embryo sensitivity to external factors highest the first 4 hpf[208].

Similar trends with respect to standard length were observed (Fig. 16b). At 3 dpf, FAC-exposed larvae were significantly smaller than control. However, by 5 dpf, there was no significant difference in standard length between control and FAC-exposed larvae. FAC-exposed larvae also displayed normal morphological phenotypes, showing a clear lack of pericardial edema, spinal curvature, or tail deformities (Fig. 16c). However, accumulation of ferric precipitates can be seen covering the chorion of 3 dpf FAC-exposed larvae (Fig. S2).

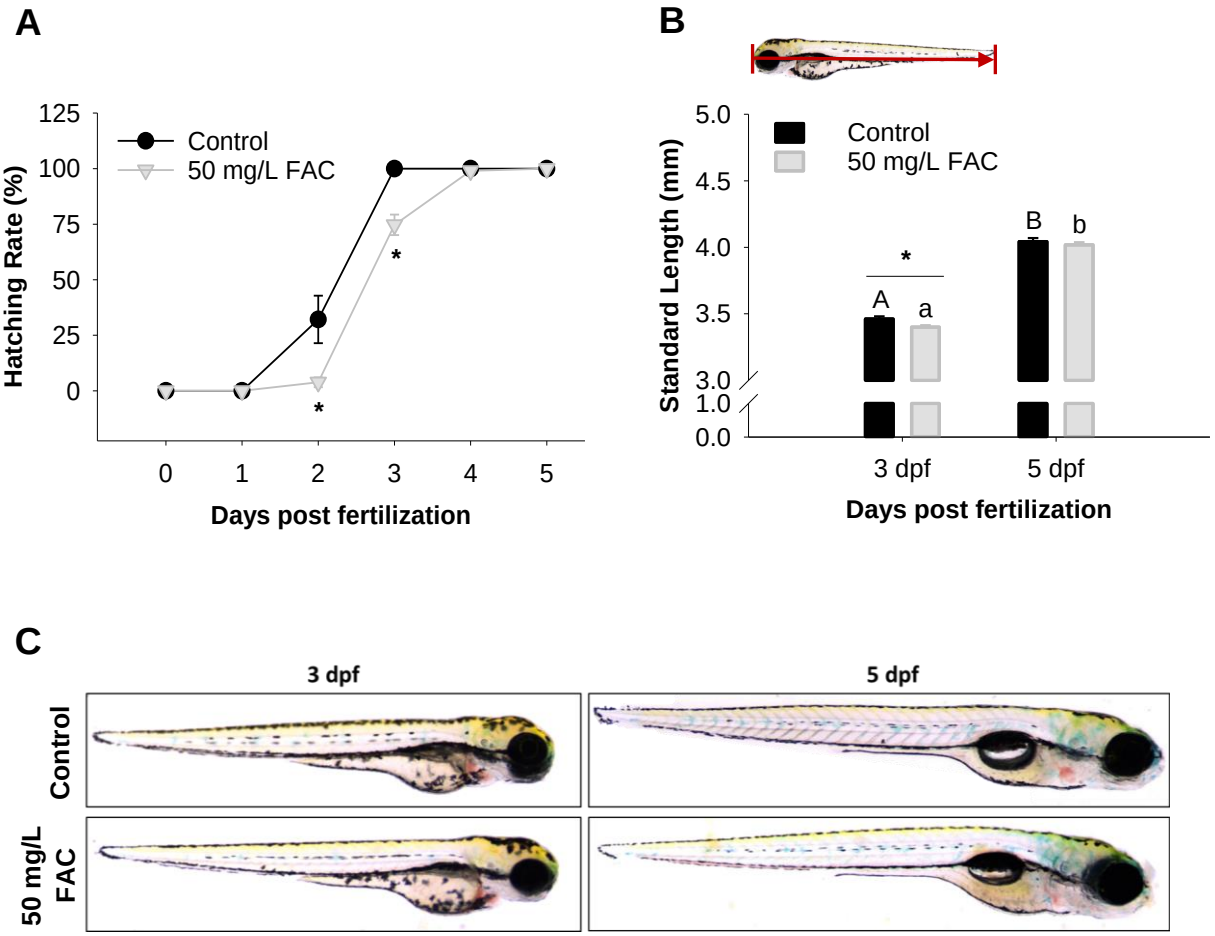

Figure 16. Delayed hatching rate and shorter standard length (at 3 dpf) following iron exposure.
(A) Hatching rate (%) of zebrafish embryos exposed to 0 and 50 mg/L FAC, from 0 to 5 dpf. Data are mean ± SEM, N=7 (30-40 fish in the same dish are considered as one replicate). *, $p<0.05$ (one-way ANOVA) **(B)** Mean ± SEM standard length (mm) of 3 and 5 dpf control and FAC-exposed larvae. N=37-75 larvae/treatment ($p<0.05$, student's t test). Letters compare within treatments; asterisk within the same developmental age. **(C)** Morphology of 3 and 5 dpf control and FAC-exposed larvae.

With respect to larval heart rate, we observed a significant effect of iron exposure on heart rate measurements at 3 dpf, with a 21 beats/min decrease in average heart rate in FAC-exposed larvae compared to control (117 vs. 138 beats/min; Fig. 17).

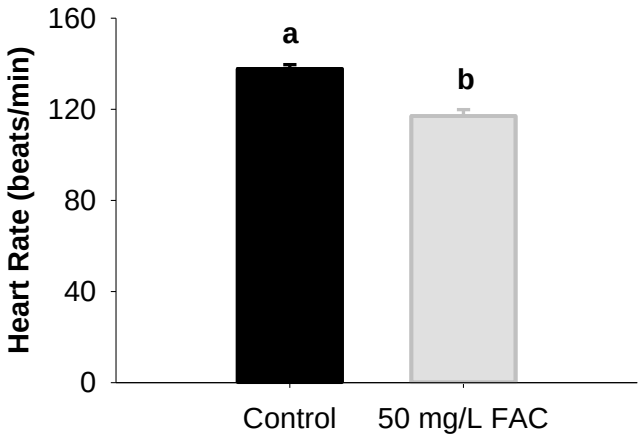

Figure 17. Decreased 3 dpf larval heart rate following iron exposure. Mean ± SEM heart rate (in beats/min) of 3 dpf control and 50 mg/L FAC exposed larvae. Values are expressed as mean ± SEM of triplicates. N=9-15, 3-5 fish per replicate ($p<0.001$, student's t-test). Bars not sharing the same letter are significantly different from each other.

3.4 Regulation of Cellular Iron Uptake, Export and Storage Genes

To examine the regulation of iron homeostasis by larval zebrafish following iron exposure, the mRNA expression of *dmt1*, *tfr1b*, *ireg1*, *and fth1a and 1b* were determined using ddPCR. Following exposure to 50 mg/L FAC, 3 dpf FAC-exposed larvae displayed no significant difference in mRNA expression levels of *dmt1*, *tfr1b*, and *fth1b*. However, expression levels for *ireg1* and *fth1a* were lower at that age, showing a 0.66- and 0.82-fold decrease, respectively, when compared to control (Fig. 18a). By 5 dpf, results demonstrated further decrease in *ireg1* expression (0.17-fold). Reduction in *fth1a* mRNA expression was not as extensive, but still significant, dropping to 0.52-fold of control mRNA expression. Unlike at 3 dpf, 5 dpf FAC-exposed larvae exhibited a significant drop in *dmt1*, *tfr1b*, and *fth1b* mRNA expression, compared to control (Fig. 18b).

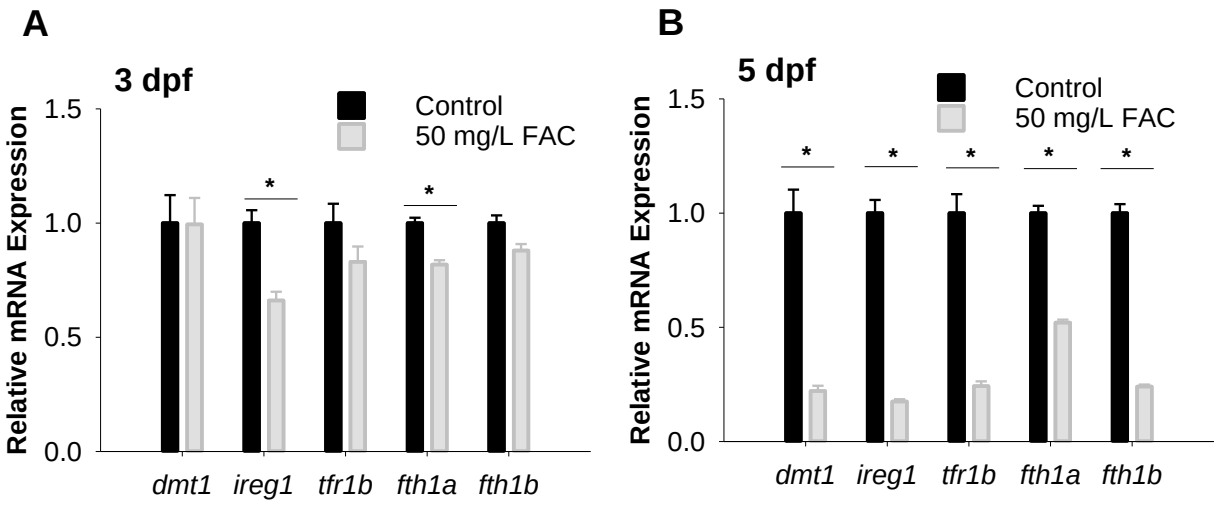

Figure 18. Downregulation of iron transport and storage proteins in 5 dpf larval zebrafish following iron exposure.
Relative mRNA expression of cellular iron uptake (*dmt1*, *tfr1b*), export (*ireg1*) and storage (*fth1a, fth1b*) genes in **(A)** 3dpf and **(B)** 5 dpf control and FAC-exposed larvae (whole-body). Fold changes relative to control. Genes normalized to *ef1a* (reference gene). N=3 per treatment, pooled sample of 20 larvae per replicate. (*p<0.05, students t-test).

3.5 Regulation of Oxidative Stress-Response Genes

With respect to larval zebrafish oxidative-stress responses following exposure to 50 mg/L FAC, 3 dpf, FAC-exposed larvae displayed decreased mRNA expression of *sod1* (0.52-fold), while mRNA expression for *sod2* and *cat* were upregulated at that point (1.17- and 1.4-fold) when compared to control. Furthermore, there was no significant difference in the expression of *gstp1* in FAC-exposed larvae (Fig. 19a).

However, by 5 dpf, there was a change in the expression profile of these same set of genes. Both *cat* and *sod2* mRNA expression decreased, showing no significant difference between levels in control larvae. Additionally, there was a small, however

significant, increase in *sod1* expression when compared to their levels at 3 dpf (0.70- versus 0.52-fold), however levels were still no where near control. The biggest change was a significant 2-fold increase in the expression of *gstp1* in FAC-exposed larvae (Fig. 19b).

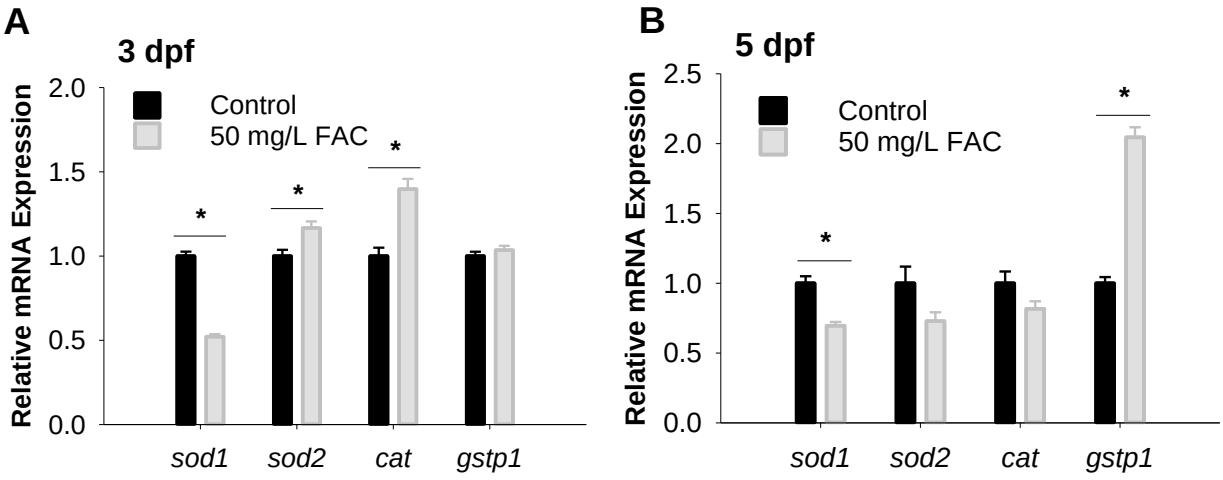

Figure 19. Differential regulation of oxidative stress-response genes in iron-exposed developing zebrafish.
Relative mRNA expression of select oxidative stress-response genes in **(A)** 3dpf and **(B)** 5 dpf control and FAC-exposed larvae (whole-body). Fold changes relative to control. Genes normalized to *ef1a* (reference gene). N=3 per treatment, pooled sample of 20 larvae per replicate. (*p<0.05, students t-test).

3.6 Touch Response

To examine whether iron exposure caused defects in sensory-motor function, the larvae's responses to touch were recorded at 3 dpf. Tactile stimulus was applied to the tail and escape behaviour was analyzed. Our data demonstrates that FAC-exposed larvae appeared to exhibit a delayed response after application of tactile stimulus to the tail, (about 58 ± 4.6 %; control: 16 ± 3.0 %; Fig. 20a). In some cases, 5-6 applications of stimuli would be required before the FAC-exposed larvae would swim away. On the other hand, control larvae generally displayed immediate escape responses, rapidly swimming

away after application of tactile stimuli (84 ± 3.0 %; FAC: 42 ± 4.6%), displaying the stereotyped c-start that characterizes the escape reflex of healthy larval zebrafish (Fig. 20b).

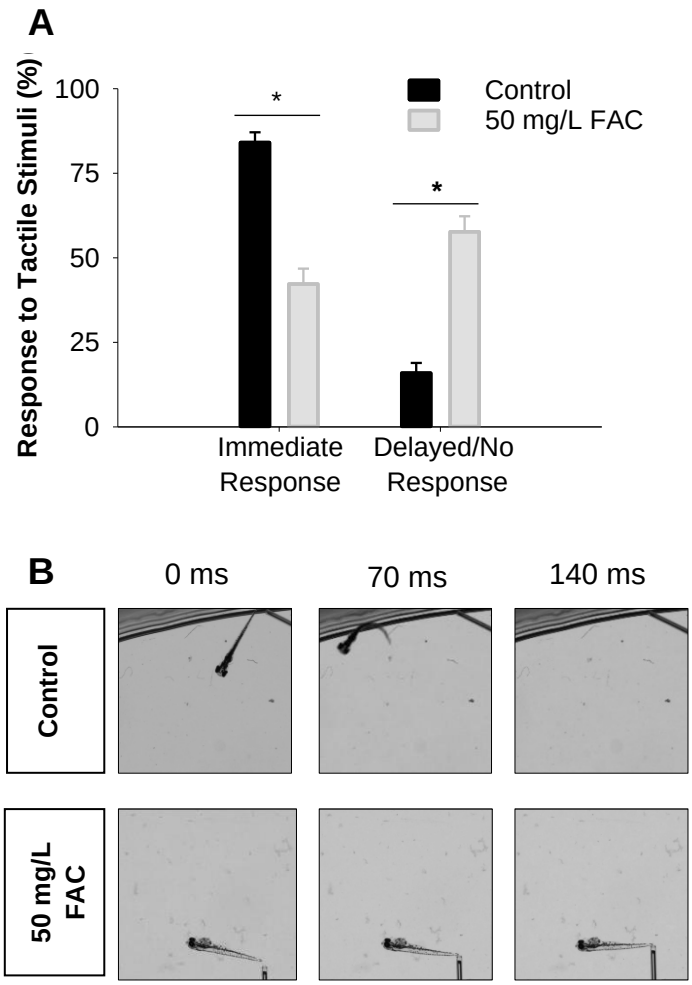

Figure 20. 3 dpf zebrafish larvae displayed delayed touch-evoked escape responses following iron exposure.
(A) Response of control and FAC-exposed 3 dpf larvae, after tactile stimuli to the tail. N=6 per treatment (replicate represents an individual Petri dish), 8-21 larvae per replicate. Immediate; larvae swim away right after tactile stimuli. Delayed/no response; >1 applications of tactile stimuli before larvae swim away (*p<0.001 student's t-test). **(B)** Representative images demonstrating the responses of control and FAC-exposed larvae following tactile stimuli.

3.7 General Swimming Activity

Exposing 5 dpf zebrafish larvae to cycles of light and dark elicited stereotyped and consistent behavioural responses[209]. In control larvae, exposure to light instigated an initial decrease, followed by increase in activity over the 10 min period. When darkness

was introduced, a marked increase in locomotor activity in control larvae was produced, which slowly abated over the 10 min period. FAC-exposed larvae displayed similar pattern of locomotor activity; however, the magnitude of response was significantly lower. FAC-exposed larvae travelled less distance while swimming in the well during both light and dark cycles, compared to control (Fig. 21a), moving a total average distance of 490 ± 30 mm over all four trials while in the dark, and 170 ± 17 mm during the light cycle (control: 758 ± 34 mm in the dark, 537 ± 73 mm in the light). Furthermore, FAC-exposed larvae also displayed a consistently slower average velocity irrespective of light stimulus, when compared to control, at all time points (Fig. 21b). Further analysis revealed that control larvae's total average velocity was 2.5 ± 0.11 mm/s in the dark, while 0.9 ± 0.03 mm/s in the light. Conversely, FAC-exposed larvae's average velocity was 1.6 ± 0.1 mm/s in the dark, and 0.28 ± 0.03 mm/s upon exposure to light. In addition to moving slower, these FAC-exposed larvae spent more of their time immobile rather than actively swimming (Fig. 21c), especially in the dark which typically elicits hyperactivity (67%; control: 48%).

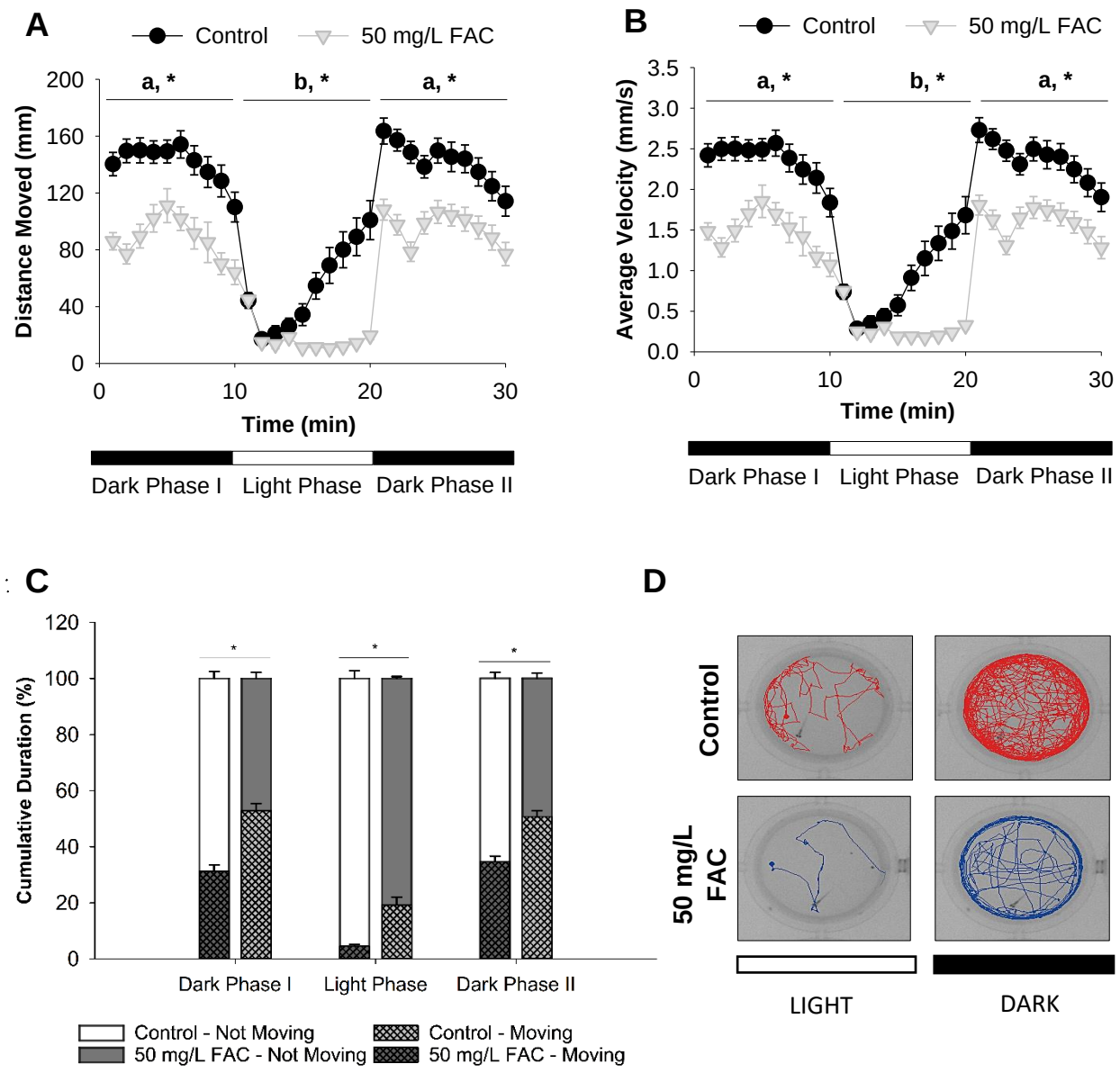

Figure 21. Iron-exposed 5 dpf larval zebrafish exhibited impaired locomotor activity, characterized by decreased distance moved, velocity, and % time spent moving.
(A) Distance moved (mm) per min, **(B)** average velocity (mm/s) per min and **(C) %** cumulative duration spent moving/not moving (s), of 5 dpf control and FAC-exposed larvae, during cyclic periods of dark/light exposure (two-way RM ANOVA, $p<0.001$). * indicates difference between treatments, while different letters show significance between light/dark exposure. Data represents mean ± SEM of four trials, 11-12 larvae per trial and per treatment. N=45-46 **(D)** Representative images showing path travelled (i.e., activity level) of control and FAC-exposed larvae during periods of dark and light exposure (10 min).

3.8 Thigmotactic Response

After induction of sudden darkness, control larvae showed a clear preference for the outer zone (Fig. 22a), spending 68.4 ± 2.1 % of the 5 min dark period in this zone actively swimming, while FAC-exposed larvae spent 61.0 ± 2.6 % of their time instead. This decrease in time spent in the outer zone by the FAC-exposed larvae was due to a relatively higher incidence of time spent not moving while in the inner zone, when compared to control (Fig. S3). However, with respect to the distance moved per zone, there was no significant difference between control and FAC-exposed larvae (Fig. 22b).

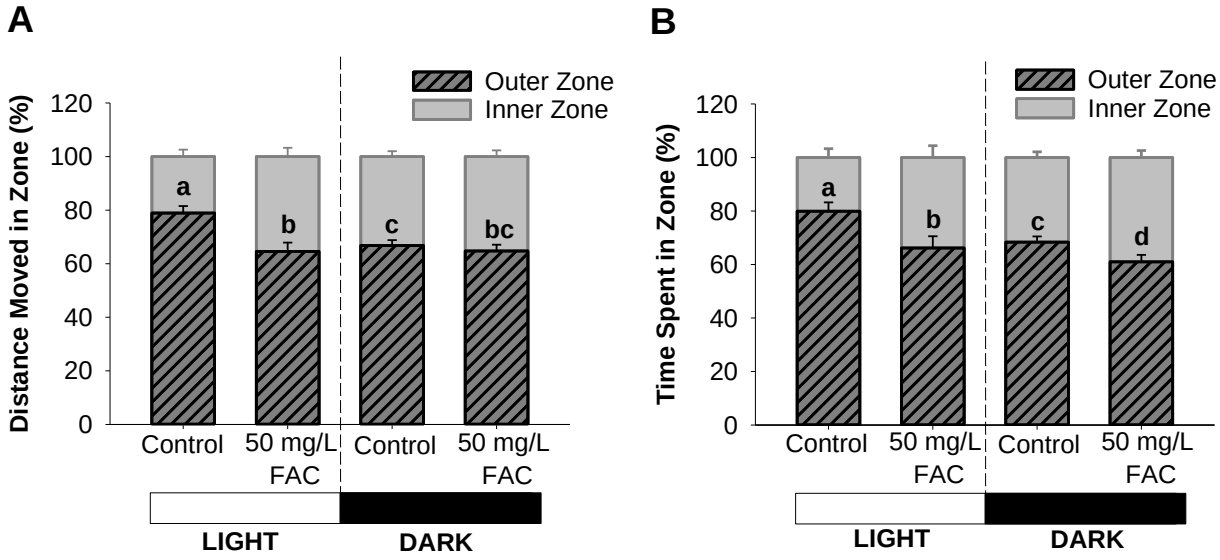

Figure 22. Iron-exposed 5 dpf larval zebrafish spend less time in outer zone compared to control; no changes in % distance moved.
Thigmotactic response of 5 dpf control and FAC-exposed larvae, measured as **(A)** % time spent per zone (in s) and **(B)** % distance travelled per zone, after induction of sudden darkness (dark phase 2) for 5 min, compared to light. Data represents mean± SEM of four trials, 11-12 larvae per trial and per treatment. N=45-46. Outer Zone: 4 mm-wide outer perimeter of well; Inner Zone: centre of well (diameter = 8mm). Bars not sharing the same letter are significantly different from each other (two-way RM ANOVA, $p<0.05$).

3.9 ROS Generation Following Iron Exposure

Exposure to 50 mg/L FAC resulted in a significant 2.83-fold increase in ROS levels in 3 dpf larvae when compared to control (Fig. 23a; N=37) when fluorescence intensity was measured in a plate reader. Generated ROS levels were still elevated in 5 dpf larvae, however the fold change was about 1.54 when compared to control (Fig. 23b; N=35). When examining the localization of ROS in 3 dpf and 5 dpf iron exposed larvae under the fluorescent microscope, the highest intensity was in the gut (Fig. 23e, f). ROS was also seen in the gut of control larvae, but to a lesser extent (Fig. 23c, d). Both control and iron exposed 3 dpf larvae displayed elevated ROS levels in their yolk sac, however the fluorescence intensity was relatively higher in iron-exposed larvae when compared to control (Fig. 23c, e). The increased fluorescence in these regions may be a result of dye accumulation and consequent autofluorescence.

Lowest ROS intensity seemed to be in the skeletal muscle tissues of both 3 dpf and 5 dpf iron-exposed larvae, almost comparable to control larvae (Fig. 23c-f). However, small evenly spaced points of increased fluorescence along their tails can be observed, once the magnification was increased (Fig. 23i, m). These were apparent in all 3 and 5 dpf iron-exposed larvae, but at varying intensities (not shown). These were not visible in the control larvae on either day. While hard to detect the liver at 3 dpf since it is still developing, the liver in 5 dpf displayed elevated ROS levels when compared to control (Fig. 23d, f, l). In 3 and 5 dpf larvae, while still higher than control, ROS levels were not as elevated in the heart when compared to other tissues. When examining the heart in the 3 dpf at increased magnification (the day heart rate measurements were carried out),

ROS levels seemed to be higher around the pericardium than within the heart itself (Fig. 23g).

Increased ROS levels were visible in the head regions of both 3 and 5 dpf iron-exposed larvae (Fig. 23g, h, j, k). Even more so, the ROS seemed to be within the brain, as neuronal tracts can be detected due to the increased fluorescence. Patterning and intensity of neuronal staining between 3 dpf and 5 dpf larvae also slightly differed. In some cases, generalized increase in fluorescence in the head would be seen, without neuronal tracks being detected (not shown). ROS was not observed in the head region of control larvae on either day (Fig. 23c, d). Reference to general organ location within 3 dpf and 5 dpf larvae can be found below.

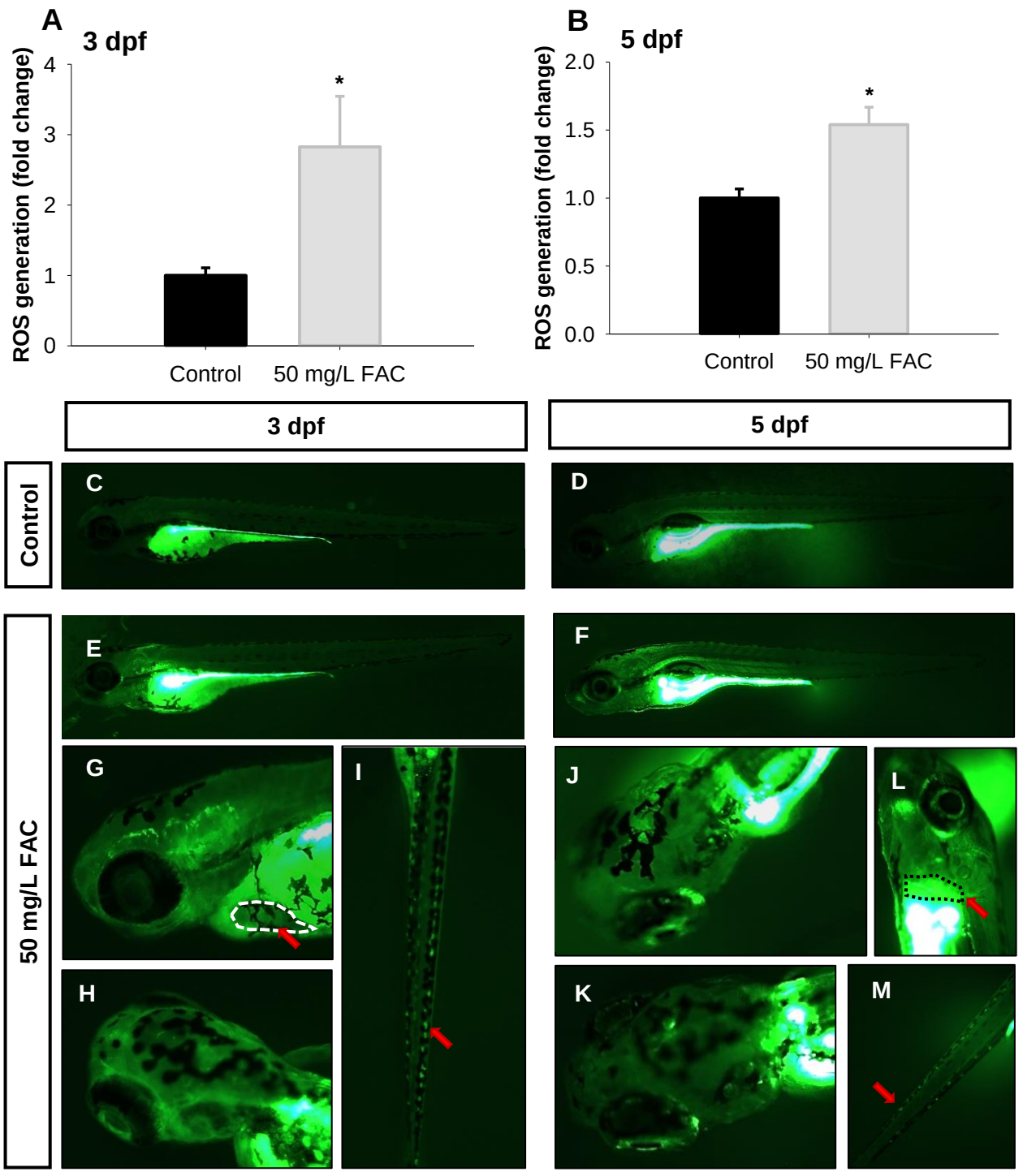
A
3 dpf
ROS generation (fold change)
0
1
2
3
4
*
Control
50 mg/L FAC
B
5 dpf
ROS generation (fold change)
0.0
0.5
1.0
1.5
2.0
*
Control
50 mg/L FAC
3 dpf
5 dpf
Control
50 mg/L FAC
C
D
E
F
G
H
I
J
K
L
M
gut
heart
Yolk sac
brain
eye
hear
liver
gut

Figure 23. Increased ROS levels in 3 and 5 dpf zebrafish larvae following iron exposure.
Mean ± SEM fluorescence intensity in **(A)** 3 dpf and **(B)** 5 dpf control and iron-exposed larvae stained with CM-H_2-DCFDA and quantified using a plate reader. Values were expressed as fold change in fluorescence intensity relative to contrsol. N=35-37 per treatment (*p<0.05, student's t-test). **C-F**, lateral view of control and iron-exposed ROS generation in CM-H_2-DCFDA-stained larvae at 3 dpf and 5 dpf (2.5 X). **G-M**, closeup of (**G, H)** 3 dpf iron-exposed and **(J, K)** 5 dpf larval heads (5X) both dorsal and lateral. The heart can be viewed in **G** (red arrow). **(I, M)** lateral view of 3 dpf and 5 dpf iron-exposed larval tails (2.5X). **(L)** Ventrolateral view of 5 dpf iron-exposed larval zebrafish displaying fluorescing liver (red arrow) (2.5X).

4 Discussion

4.1 Regulation of Iron Homeostasis

Exposure to 50 mg/L FAC was able to induce iron overload in developing zebrafish, causing a 6-time increase in whole body iron levels by 5 dpf. This seems to indicate a lack of homeostatic control of iron levels by the larvae following exposure to high environmental iron levels.

There was a 3.6-time increase in whole body iron burden between 3 and 5 dpf FAC exposed larvae (12.44 versus 44.33 ng Fe/fish) that cannot be accounted by differences in size, as there was only a modest increase in standard body length (about 0.5 mm) and similar total protein content (Table S1) between developmental age. This rapid and dramatic increase in iron content may be due to two reasons: formation of the gut, and breakout from the chorion. For example, while the larvae were exposed to FAC from 3-4 hpf, there was only a comparatively moderate increase in iron levels by 3 dpf, shortly (i.e., within 12-24 hours) after having hatched from the chorion. It seems like the chorion may have been the reason for the slow uptake. Developing zebrafish are enveloped in the chorion until hatching – it is a noncellular envelope, about 1.25-2.5 μm thick, consisting of three layers. Piercing these layers are evenly spaced pores (0.5-0.7 μm and 1.5-2.5 μm apart; the ionic form of iron is in the pm scale) that range in size depending on the developmental stage[195]. Not only does the pore size change, but so does the chorion's overall permeability and stability throughout this developmental stage[208,210]. The negative surface charge of the chorion may allow it to preferentially attract, and bind to, positively charged particles like metal ions. This, however, potentially

limits their entry across the chorion[51,211]. Studies have shown that small hydrophilic molecules and metals can cross the chorion, however with some restriction, meaning that the chorion does confer some protection[211–214]. Furthermore, the cell membrane of embryos in other organisms (carp, brown trout) can limit entry of iron precipitates, with most of the accumulated iron localizing on the egg membrane, and some (4-5%) reaching the embryo[50,51]. This may be possible as the size of ferric hydroxide precipitates can range from 0.03 to 500 μm[215].

Before gut formation, the main route of exposure for any waterborne toxicant (including metals) is dermal until 3 dpf, as that is when the mouth opens and oral uptake of metals is possible – at this point enteral becomes another available uptake route[18,177,216–218]. The first formation of the gut can be seen at 60 hpf in larvae, while still in the chorion. The gut continues to develop from 3 hpf to 5 dpf, with the complete digestive system fully functional by 5 dpf for exogenous feeding to begin[181,218–220]. The increase in iron content from 3 to 5 dpf may then have been the result of waterborne iron uptake from the gut, in addition to dermal uptake. In fact, Prussian blue staining of larval zebrafish following exposure to 100 μmol/L FAC (from 3 to 6 dpf) showed localization of iron in the gut[183]. Metals can also be taken up from the gills. However, while the presence of gill slits can be detected at 72 hpf, they do not gain functionality until 14 dpf. Therefore, we cannot confirm whether gill uptake of iron also contributed to iron loading at this point[221]. However one study demonstrated that waterborne iron uptake and accumulation of iron was detected in brown trout start-fed fry, at which stage the gills are starting to develop and, according to the authors, may be involved in the iron accumulation[51].

Such iron loading in the larvae suggests altered iron homeostatic mechanisms, which was corroborated by our ddPCR data. A reduction in mRNA expression of the iron import proteins, DMT1 and TfR1b, did not occur until age 5 dpf, five days into our exposure protocol, while 3X iron loading was detected at 3 dpf. What produced that delay in downregulation is not clear. However, during periods of high cellular iron concentrations, the mRNA of these iron importers can be exposed for degradation. By binding to iron regulatory proteins (IRPs), iron can inhibit IRP binding to iron response elements (3'-IREs) on their mRNA, resulting in mRNA destabilization and consequent degradation. This in turn blocks the translation of these iron import proteins, in order to prevent further iron uptake during periods of iron overload[13,222]. As a result, this may account for the decrease in mRNA levels of *dmt1* and *tfr1b* in 5 dpf iron-exposed larvae.

Our results also demonstrated a continual decrease in the mRNA expression levels of *ireg1* and *fth1a/b*, slight at 3 dpf, but more significant by 5 dpf. However, studies show that during iron overload, ferritin expression is upregulated to increase iron storage, while export from tissues into circulation is increased via upregulation of IREG1, to prevent cellular iron loading. This is accomplished by the same IRP/IRE mechanism mentioned above, where inhibition of IRP binding to the 5'-IRE by iron, in this case, promotes translation of ireg1 and ferritin (and not their degradation)[81]. Other regulatory pathways may therefore be involved in their expression.

With regards to IREG1, it has a couple of unique characteristics that renders its regulation more complex, being the only known cellular iron exporter. First, IREG1 has tissue specific differences in expression, with the highest expression observed in the intestinal lumen, liver, and macrophages[223,224]. In the lumen, IREG1 modulates the export

of iron absorbed from duodenum enterocytes into the circulation. So, we may assume that IREG1 can be downregulated, specifically in gut enterocytes in response to iron overload, to prevent further iron uptake into the body (something our results seem to hint at)[225]. Interestingly, that may be possible. One study has demonstrated decreased *ireg1* mRNA expression in mouse enterocytes in response to a high iron diet[226]. Furthermore, post-transcriptional modification of IREG1 has been shown to occur in rodent duodenal mucosal cells, creating a –IRE splice variant of *ireg1* (i.e. mRNA lacking the IRE) that does not respond to levels of cytosolic iron[227]. To further tease apart the effects of local (cellular-level) and systemic signals of iron status on *ireg1* expression in intestinal enterocytes, another study utilized a *sla* mouse (sex-linked anemia characterized by a deletion in the hephaestin gene) which displays normal iron uptake, but impairments in iron export, resulting in increased cellular iron loading, but low systemic iron levels. After a high iron diet feeding, they noted decreased mRNA expression of *ireg1* despite increased enterocyte iron levels, thus indicating they are responding to the iron deficiency at the systemic level. The same change in expression levels were not seen with DMT1 or TfR1[226]. These results suggest that *ireg1* expression can be independently regulated via other pathways, in a tissue dependent manner, for example, through the peptide hormone hepcidin[228]. In fish, IREG1 can be regulated systemically at the post-translational level by hepcidin, which in response to high iron, promotes the internalization and degradation of IREG1 in enterocytes, to modulate iron absorption from the gut[7,229]. Whether this can also signal the downregulation of *ireg1* gene expression in the gut, in order to prevent further production of IREG1 protein, is not clear. However, it may be possible, as injecting hepcidin in sea bass following induction of iron overload (via 2 mg intraperitoneal injection

of iron dextran) resulted in decreased mRNA expression of intestinal and liver *ireg1*[224]. It seems that the hepcidin-mediated internalization of IREG1 during iron overload may initiate changes at the transcriptional level that may also trigger a reduction in *ireg1* transcripts. Since zebrafish do express hepcidin (low levels can be seen starting at 48-66 hpf) this may explain the decreased *ireg1* mRNA transcripts detected at the whole-body level[230].

Ferritin plays a key role in mitigating ROS production by sequestering the labile iron pool in order to minimize iron's interaction with superoxide radicals, while also defending against cellular stress and inflammation. As a result, it is a protein that can be regulated by many different pathways. In fact, its expression can be regulated by cytokines (TNF; tumor necrosis factor), oxidative stress (e.g., Nrf2), ROS, oncogenes, growth factors, and hypoxia, at the transcriptional and post-transcriptional level[231,232]. However, ferritin's involvement in regulating both iron homeostasis and oxidative stress (which go hand in hand during iron overload) make it difficult to elucidate which pathway is predominantly affecting ferritin expression, especially since these pathways typically upregulate ferritin levels during iron overload, stress, and inflammation. It has likewise been suggested that the regulatory response to iron by ferritin is mainly at the post-transcriptional level, and does not affect mRNA expression[232,233].

So far, literature has not indicated a pathway by which ferritin transcription can be inhibited in response to iron overload. Whether ROS could have played a role in its activation or inhibition is also not clear. What we can surmise is that this downregulation of *fth1a/b* in our developing zebrafish may increase the level of free iron in the cytoplasm, which might lead to ROS production. Conversely, there are cases where mRNA

expression may not match protein levels, so it may simply be a case of ferritin protein expression being increased to such high levels that its mRNA expression was downregulated, signalling a reduced need for more protein. However, without looking at protein expression levels, we cannot make any definitive conclusions. Unfortunately, there is no existing antibody for zebrafish FTHA or FTHB, therefore, western blotting may not presently be possible. Nevertheless, studies examining iron overload in other fish species, like salmon, have made use of species-specific ferritin heavy chain antibody[51]. Whether that would work on zebrafish remains to be seen.

Without examining ferritin heavy chain protein levels, we also cannot determine whether the accumulated iron in the larvae were either in free form or bound to ferritin. For example, one rodent study stained for the FTH antibody, while measuring total iron levels. They subsequently calculated the ratio of ferritin to iron levels in order to determine how effective the tissue and/or organism was in stabilizing the excess free iron[234]. Also, ICP-MS does not differentiate between ferritin-bound and free iron – they are all measured as total iron[164]. It may be interesting to see if there is a way to quantify the iron contained in ferritin (which would be in the Fe^{3+} form) versus free cytosolic iron (Fe^{2+} form). In rodents, histological sectioning and staining using Prussian blue to check regional deposits/accumulation of iron can be done, as it stains for ferric iron (essentially ferritin-bound iron)[69,235]. This could also be an option for larval zebrafish as well.

For future research, examining the potential iron absorption pathways in larval zebrafish can be done. For example, it is not known how dermal uptake of iron occurs (e.g., via paracellular routes, or competitive uptake through ionocyte ion transporters). While literature does not make mention of paracellular routes of metal uptake by fish

(including iron), metals (e.g., Cd and Zn) can be taken up through ionocyte Ca^{2+} channels localized on freshwater fish gill epithelium[236,237]. While it is not clear whether iron can also enter through these channels, ferric iron exposure has been shown to limit Ca^{2+} uptake through ionocytes in the inanga fish (*Galaxias maculatus*)[238]. Larval zebrafish do possess ionocytes on their skin, so cutaneous iron uptake by developing zebrafish may be another avenue to investigate in the future[239].

Overall, we can surmise from this dataset that zebrafish are unable to effectively regulate iron balance during early development and the decreased *dmt1* and *ireg1* expression are likely compensatory responses to reduce the iron loading that transpired. This is important to note as it indicates that developing fish in iron contaminated freshwater ecosystems may fail to maintain iron homeostasis in the face of elevated waterborne iron levels. These findings thus emphasize the need to understand the potential consequences of iron loading in developing fish.

Furthermore, while our results indicate a delayed (and potentially impaired) homeostatic control of iron homeostasis, an iron overload study in tilapia *(Tilapia sparrmanii)* mention that fish can acclimatize to long-term iron exposure. After a four-week exposure to 18.6 mg/L Fe, the bioconcentration of serum iron in these tilapia returned to control levels, showing fish can regulate toxic concentrations of iron – it is just a slow process[60]. The decreased mRNA expression of *dmt1, ireg1* and *tfr1b* at 5 dpf might imply that the developing zebrafish may be in the process (or just beginning the process) of restoring iron homeostasis.

4.2 Iron Overload and Trace Metal Homeostasis

Our trace metal analysis seems to suggest that exposure to high iron can alter Mn homeostasis. Iron-exposed larvae displayed a significantly consistent increase in whole-body Mn levels, at 3 and 5 dpf, following a similar trend in whole-body iron levels. Our statistical analysis show that not only is the data significant, but also displays interactive effects between iron treatment and developmental age, with increasing Mn accumulation detected with growth of the larvae during iron exposure. This increased tissue Mn may be due to decreased cellular export and consequent reduction in excretion from their body (as we did not add Mn to the water). Studies have shown that Mn homeostasis is similar to iron's and iron status can affect Mn levels through regulation of iron transport proteins[67,133,136]. In fact, entry of divalent metals, like Mn^{2+}, into cells through DMT1 have been shown to occur[7,134,222,240]. Moreover, there is some evidence linking Mn export through IREG1. In vitro studies have shown mutations in *ireg1* leading to increased intracellular Mn level[241]. Additionally, increased expression of *ireg1* in cell lines displayed potential cytoprotective effects against Mn toxicity[138]. An in vivo study also demonstrated that *ireg1* deficiency can result in decreased intestinal uptake of Mn in mice, with a potential involvement of IREG1 in biliary excretion of Mn[242]. Consequently, a possible downregulation of IREG1 during iron overload may have resulted in decreased excretion of Mn, and consequent Mn accumulation in the larvae.

However, conflicting studies do exist. One study showed that the role of IREG1 in cellular export of Mn may be minor under normal physiological conditions, with other Mn-specific pathways likely being more involved in Mn export, such as SLC30A10, the main cellular exporter of Mn[240,243]. This is corroborated by another study suggesting that the

affinity of IREG1 for Mn is lower than that for iron, by three orders of magnitude[244]. However, robust *slc30a10* mRNA expression in zebrafish is not detected until 5 dpf[245]. As a result, we can for now only speculate about the hypothesized link between the dysregulation of Mn homeostasis and decreased *ireg1* expression. We may conclude, however, that in addition to dysregulation of Fe, larvae in iron-polluted environments may exhibit altered Mn balance. Conversely, it would be interesting to further investigate whether Mn exposure can modify iron balance in larvae, as rodent models of Mn exposure display altered iron levels, expression of DMT1 and TfR, and competitive binding of Mn to Fe-binding sites[133].

We also noticed a tendency of the larva to retain more Ni^{2+} at 5 dpf and Zn^{2+} at 3 dpf. While previous studies have not examined Ni^{2+} and iron homeostasis as extensively, there has been a link between Zn^{2+} and its export through IREG1 shown in cell culture studies[137,139]. Changes in Zn^{2+} levels at 3 dpf versus 5 dpf may be possible since expression of zinc transporters (especially cellular exporters ZnT1, ZnT2, ZnT4) do not peak until 5 dpf, for the exception of one, at 2 dpf[85]. Thus, Zn export at 5 dpf will likely be controlled by its own exporters. However, at 3 dpf, IREG1 (or another protein whose expression is controlled by iron) may play a bigger role, which may lead to increased Zn retention if these proteins are downregulated. No significant change was seen with Co^{2+} or Cu^{2+} homeostasis on either day, following iron exposure. Interestingly, a study conducted on zebrafish demonstrated that feeding fish a high iron diet increases the mRNA expression level of Cu transporters (both importers and exporters) to ensure that there is sufficient Cu for ferroxidase synthesis following increased iron uptake[24]. This illustrates that Cu levels can remain at homeostatic levels despite iron overload

conditions. Remarkably, a rodent model of chronic iron overload demonstrated that Zn and Mn can accumulate in the liver and spleen (but not the brain) of rodents, whereas Cu levels remain unaltered[246].

While some conflicting studies exist regarding altered ion homeostasis following iron overload, we also saw no significant difference in the levels of key ions, including K^+, Mg^{2+}, and Na^+, following elevated iron exposure. This seems to indicate that the larval zebrafish can regulate ion homeostasis effectively during iron overload. However, Ca^{2+} levels at 3 dpf showed a significant increase when compared to control. This may be possible as iron is recognized to affect Ca^{2+} homeostasis by either causing cellular retention of Ca^{2+} or competing for cellular uptake[247,248]. However, it is not definite whether the increased whole body Ca^{2+} detected was due to an increase in serum Ca^{2+} (indicating impaired entry) or within the cells (indicating increased Ca^{2+} retention). This potential link will be elaborated further in the next sections.

4.3 Iron Overload and Physiological Responses

The hatching period of zebrafish development is considered as one of the seven stages of embryogenesis and occurs between 48-72 hpf[195,218]. It has been suggested that delays in hatching (extending past 72 hpf) may indicate developmental delays and can be a result of exposure to environmental stressors (e.g., toxicants)[194,249]. Consequently, hatching rate has been used as a measure for determining developmental toxicity (including neurotoxicity) and is often used in toxicity studies as a toxicity endpoint for trace metals such as aluminum, mercury, and cadmium[195,196,250]. Our results indicated that high iron exposure resulted in delayed hatching, with about 75% of larvae hatching by 3 dpf.

However, this delay in hatching was not sustained and the rest of the larvae were able to hatch within the next 24 hours. The documented delay in hatching caused by exposure to elevated levels of trace metals may be due to their involvement in the hatching process[251–254]. Hatching is both a behavioural and biochemical process, with enzymes synthesized by the embryo digesting the chorion and the larvae then tearing up the chorion by twisting out[252]. Exposure to trace metals such as cadmium, mercury, zinc, and manganese was found to delay hatching by either affecting the larvae's swimming activity or inhibiting the proteolytic function of the hatching enzymes[28,252]. However, the exact mechanisms by which iron exposure affects hatching rate has yet to be explored. Interestingly, a study examining hatching of shishamo smelt (*Spirinchus lanceolatus)* eggs in river water containing iron at concentrations ranging from 0.54 to 2.04 mg/L noted that iron can decrease the hatching rate of these embryos. It has been suggested that iron can harden the chorion, which in turn increases pressure on the embryos and delays hatching[29]. It has also been suggested that colloidal iron on the membrane of the egg can negatively impact gas exchange, resulting in decreased O_2 uptake which can delay hatching[11,18,50]. This may be what occurred with our larvae, since ferric iron precipitates can be seen accumulating on the chorion surface (Fig. S2).

Conversely, the effect of iron exposure on the hatchability on fish may also be species specific, with exposure to 3 mg/L and 0.75-12 mg/L ferric hydroxide having no impact on coho salmon (*Oncorhynchus kisutch*) and brook trout (*Salvelinus fontinalis*) hatching rate, respectively, while exposure to 1.5 mg/L iron hydroxide decreased the hatchability and growth of fathead minnows (*Pimephales promelas*)[22,61]. In the case of

the fathead minnows, they have suggested that the colloidal iron may have blocked the pores of the chorion.

Like hatching rate, heart rate is also considered a toxicity endpoint with respect to embryo development, with any deviations from normal heart rate potentially indicating impairments with embryogenesis and therefore cardiac development[252]. Cardiac development commences at 15 hpf and the first heart beat can be measured at 48 hpf, after the formation of the two chambered heart tube (atria and ventricle separated by AV canal)[255–257]. Larval heart rate can range from 120-180 beats/min, depending on the experimental conditions/environments[252,258–260]. In our experiment, we observed that control larvae at 3 dpf exhibited a heart rate of approximately 138 beats/min. Importantly, exposure to high iron significantly decreased average heart rate by 21 beats/min, down to 117 beats/min. This finding suggests that high iron exposure may potentially affect cardiac function in developing zebrafish.

It has been documented that iron overload can lead to iron overload cardiomyopathy (IOC) in humans[56,191]. In IOC, excess iron enters the heart, with iron deposition occurring in the conduction pathway or cardiomyocytes. Due to the varied etiology, the consequences on cardiac function can be diverse (e.g., left ventricular hypertrophy, brady- and tachycardias, arrhythmias)[191,243,]. However, rodent studies (both in vivo and in vitro) have revealed that iron can enter the heart during iron overload through L-type calcium channels localized in sinoatrial node myocytes that are used to maintain electrical rhythmicity. This results in decreased entry of calcium through the channels, leading to sinus bradycardia[261,262,227]. Additionally, iron overload-induced ROS production can affect the proteins involved in excitation-contraction coupling (e.g.

SERCA; sarcoplasmic-endoplasmic reticulum Ca^{2+} ATPase, NCXs; Na^{+}-Ca^{2+} exchangers), impacting cardiac contractility as a result of altered Ca^{2+} currents[248,263]. Rodent cell culture studies have also shown high iron exposure leading to a decrease in mitochondrial respiratory enzyme activity in cardiomyocytes[244]. However, cardiac dysfunction can also occur indirectly via iron-mediated damage to other tissues, such as the liver (e.g., hepatic dysfunction)[56]. Although simpler in structure, the zebrafish heart is functionally and structurally analogous to the mammalian heart, and displays similar molecular and cellular processes during cardiac development[255,257,266,267]. In fact, cardiovascular physiology of humans, including electrical properties (e.g., L-type Ca^{2+} currents) are more comparable to that of zebrafish than rodents. For example humans and zebrafish display similar embryonic heart rates[195]. But despite these similarities, it is not certain whether the perceived decrease in larval heart rate in our study was due to iron overload-induced cardiac dysfunction, as iron overload can have varied effects on heart function.

As a final point, this decrease in heart rate could simply be due to high iron exposure affecting heart development during embryogenesis, as exposure to pollutants and toxicants can affect the biochemical and molecular processes involved in embryogenesis[252]. However, whether iron can have such effects has not been established in studies yet. This is the first study to demonstrate that iron exposure reduces heart rate in fish. Further study would be required to understand the effects of iron on cardiac function and the underlying mechanism in zebrafish.

Toxicity studies also examine general morphology of developing zebrafish in response to toxicant and trace metal exposure, while also measuring their standard body

length, as each developmental stage is associated with an optimal size the developing zebrafish should reach[253,254]. Our results demonstrated that iron-exposed larvae did not exhibit gross morphological changes as a result of iron overload throughout the five-day exposure period, however their body length was significantly shorter than control at 3 dpf. This reduction in standard length at 3 dpf may be due to the delayed hatching at 3 dpf, which may have resulted in a slightly slower development in some of the iron-exposed larvae. However, by 5 dpf, iron-exposed larvae seemed to show no difference in length between control, potentially indicating that they were able to catch up in terms of development.

4.4 Iron Overload and ROS Generation

The present study also revealed that the increased whole-body iron burden following iron exposure resulted in a consequent increase in the production of ROS (e.g., either as $O_2^{-\cdot}$ via the Haber Weiss reaction, or OH• via the Fenton reaction). Using a ROS florescent assay, we demonstrated that iron exposure led to a 2.8-fold increase in ROS levels at 3 dpf, and 1.54-fold increase at 5 dpf. Exposure to 100 mg/L FAC in 6 dpf and 10 dpf zebrafish larvae was likewise able to increase ROS levels (4.2- and 2.4-fold change, respectively) in another study[184]. Our ROS assay data is in support of our ddPCR results demonstrating the induction of *sod2, cat,* and *gstp1* antioxidant gene expression. It is hard to say whether ROS levels were lower at 5 dpf because they were actively being scavenged, or whether this was a transient change in ROS levels that may increase at a later timepoint. It is well established that the half-life of ROS is quite short, and the cell can experience ROS fluxes[95].

Furthermore, the increased ROS levels detected suggests that ferritin storage may not have been enough in the subset of tissues that experienced increased ROS production, leading to deposition of free iron in the cells. It also suggests that uptake and export mechanisms were not optimal either, since some regions displayed tissue-specific ROS accumulation. When looking at the patterning of ROS localization, there is a tendency for the highest fluorescence to be emanating from the regions involved in iron uptake and storage, which are the gut and liver, respectively. Iron tends to accumulate in the liver of fish, leading to oxidative stress-mediated hepatocellular changes since iron uptake into the liver during iron overload can occur via NTBI uptake through transporters such as zip14[25,49,71]. This may also suggest that iron uptake from the gut may have been able to occur in developing zebrafish. A general and modest increase in ROS was detected in the region containing the heart, however, it is not clear whether ROS was within the heart tissue itself (but at low levels) or the surrounding pericardium only. This suggests that iron's impact on heart rate (e.g., induction of bradycardia) can be either from ROS mediated damage, or potential iron entry though VGCCs. Additionally, minimal ROS was detected in skeletal muscle tissues, suggesting iron may not accumulate as much in muscles, as supported by other fish studies of iron overload[21,26]. It should be noted that in all cases, some inter-larval differences existed with respect to fluorescence intensity, and thus ROS levels, in certain regions (e.g., brain, heart), while consistent ROS levels in the gut, liver, and tail skeletal muscles were observed. This seems to indicate inter-larval differences in iron handling and oxidative stress responses.

The most interesting discovery was the presence of ROS in the brain and peripheral nervous system. Both 3 dpf and 5 dpf larvae displayed localized elevated ROS

generation in evenly spaced regions on their tail, dorsolaterally. When reviewing literature, and the zebrafish database (ZFIN), these regions appear to generally correlate to the location of mechanosensory Rohon Beard (RB) cells, involved in mediating the touch-evoked escape response. To confirm, co-localization studies using RB cell-specific antibodies for immunohistochemistry can be conducted[83,268,269]. This lends support (however tentatively) to a potential impairment of sensory function playing a role in the delayed escape response witnessed in 3 dpf larvae. However, since a ROS assay does not measure nor indicate damage of cellular components, we cannot make any definitive links. The potential for these cells to experience elevated ROS may be due to the close localization of their nerve endings to the skin surface, which may mediate iron entry through any surface ion channels. However, this is only speculation at this point.

ROS was also detected in the brain and eye of the developing zebrafish at 3 and 5 dpf, indicating that iron can accumulate and induce the generation of ROS in these regions. This may be due to a lack of a fully functional BBB, which consequently allowed iron uptake into the brain, a trend observed in rodent models of postnatal iron exposure[156]. In zebrafish, the BBB begins to be formed at 3 dpf, but is not fully developed until 10 dpf[192,270]. This also suggests that developing zebrafish brains are susceptible to oxidative stress, similar to mammalian brains. Furthermore, this can potentially imply that iron overload in the brain may have played a role in the altered behavioural phenotypes witnessed. However, ROS levels are relatively lower in the brain when compared to other regions. Unfortunately, since the brain tissue was very dense in 5 dpf larvae, and the fluorescence intensity relatively weak, it was challenging to acquire a detailed image of the brain structures. As a result, we cannot with certainty specify which neuronal

pathways demonstrated elevated ROS production in the subset of larval zebrafish that displayed more specific ROS patterning, and due to the localization of the fluorescence, dopaminergic, serotonergic, or noradrenergic neuronal groups are all possible candidates[271,272]. Though we can confirm that the faint fluorescence of neuronal tracts was localized in the forebrain region, with stronger intensity tracts in the midbrain and hindbrain.

The ROS detected in 3 dpf were localized in another region of the brain, with a higher intensity, when compared to 5 dpf. The difference in ROS patterning between 3 and 5 dpf is possible since the CNS and PNS are still undergoing development, with continuous growth and acquisition of neurons, which is not completed until 5 dpf[181]. While the head region in some larvae displayed general increase in ROS fluorescence when compared to control, a subset showed a consistent patterning of fluorescent tracks on the lateral side of the brain (midbrain and hindbrain). Numerous catecholaminergic tracts are known to pass that area, in addition to reticulospinal neurons[272–274]. Future studies should examine the precise neuronal networks that are adversely influenced by iron overload.

Live imaging of ROS cannot be carried out in mammalian models of iron overload; thus, we do not have a comparison of regions where oxidative stress occurred, especially when it comes to the brain. However, the use of larval zebrafish does offer us this advantage of examining in real-time (while the larvae are still alive) regional changes in ROS production that can provide us with a further understanding of altered iron homeostasis and its effects on oxidative stress responses in various organs or tissues. Hence, the use of larval zebrafish may prove useful in furthering our understanding of iron overloading and its detrimental effects.

However, a few limitations should be highlighted. First, there may exist potential regional differences in larval epithelial permeability with respect to the uptake of CM-H_2DCFDA, which could play a role in the regional variances in ROS levels detected. Secondly, studies have indicated that H_2DCFDA can be oxidized by Fe^{2+} in the presence of low H_2O_2 levels, increasing fluorescence levels, while co-exposure of H_2O_2 with Fe^{2+} may considerably amplify the fluorescence emitted then with H_2O_2 alone[275]. While increased *cat* expression in our FAC-exposed larvae indicates increased H_2O_2 production, we cannot confirm whether H_2O_2 levels were sufficiently elevated to prevent iron-mediated oxidation of CM-H_2DCFDA. Utilizing ROS subtype-specific dyes may help eliminate this confounding factor. Lastly, it should also be noted that CM-H_2DCFDA measures ROS content, which is the difference between ROS production and scavenging by the antioxidant system, rather than total ROS production.

Overall, our findings propose that exposure to environmentally relevant concentrations of ferric iron will lead to cellular iron loading and subsequent increase in iron-catalyzed ROS production in developing zebrafish. Further investigations will involve examining the consequences of this increased ROS production, as both this dataset and the mRNA expression profile of the antioxidant genes cannot confirm whether any cellular damage were induced in these iron-exposed larval zebrafish. Assays examining lipid peroxidation, DNA oxidation, or protein damage is recommended. Remarkably, preliminary apoptosis assay data conducted using acridine orange (AO) staining of whole-body larvae show no evident differences in apoptosis at first glance (Fig. S4). Conversely, iron can also induce ferroptosis. Therefore, conducting necrosis assays may be another avenue follow, in order to further elucidate the type of impact iron has on the larvae[148].

4.5 Differential Regulation of Oxidative Stress-Responses

Not only did the five-day exposure to 50 mg/L FAC lead to iron overload, dysregulation of iron homeostasis, and elevated ROS production, we also observed an induction of the antioxidant defense system by the larvae, likely in response to the increased iron-mediated ROS production. The increased expression of *sod2* and *cat* (Phase I detoxification enzymes) at 3 dpf in iron-exposed larvae indicates that there was an active attempt by the larvae to neutralize the iron-induced ROS. The enhanced *sod2* and *cat* expression suggests the presence of higher superoxide anion and H_2O_2 concentrations, respectively. Their expression patterns are typically linked – it has been suggested that SOD is activated first to deal with the increased superoxide anions and that the increased H_2O_2 that results subsequently activates CAT[163].

Furthermore, expression of *gstp1* (Phase II detoxification enzyme) did not significantly change at 3 dpf, likely because the production of electrophilic compounds may not yet have reached adequate levels to activate *gstp1* expression. *gstp1* possesses an antioxidant response element in its promotor which can be induced by electrophilic compounds, metals, and H_2O_2 via Nrf2, the main transcription factor that mediates cellular responses to environmental toxicants[126]. However, increased mRNA expression of *gstp1* detected at 5 dpf consequently means that ROS reached levels high enough to cause cellular damage, such as lipid peroxidation and DNA oxidation, whose degradation products can lead to *gstp1* activation. GSTP1 is crucial for the detoxification of these electrophilic molecules via their conjunction to GSH[130]. This indicates that the larvae were attempting to mitigate the damage induced by excess ROS via the activation of *gstp1*[119]*.* For example, the induction of *gstp* expression in liver of mice exposed to iron overload

was mediated by iron-induced peroxidised lipid products[118,276]. Additionally, since *gstp1* also possesses peroxidase activity, its activation could have played a role in the relatively lower ROS levels detected in 5 dpf larvae (when compared to 3 dpf), despite decreased *sod1*, *sod2*, and *cat* levels[119]. *Gstp1* expression is high in the liver, kidney, gills, brain, and intestines of larval zebrafish, which are regions that tend to accumulate iron and/or require rapid detoxification abilities[119].

Increase in *gstp1* transcript levels may also explain the decreased *sod2* and *cat* levels observed in 5 dpf iron-exposed larvae. The fact that *gstp1* was upregulated at 5 dpf can lead us to assume that *cat* and *sod2* were not downregulated due to their success in eliminating ROS, but rather the excess ROS could have led to their inhibition via a negative feedback mechanism directly by ROS, or via oxidative stress-mediated damage or modification of the corresponding protein[121]. This is further supported by our ROS assay which demonstrated that ROS levels were still elevated in 5 dpf FAC-exposed larvae, when compared to control. Essentially, phase I scavenging activity was inhibited, leading to increased need for phase II detoxification activity[119]. This may be possible, as studies have revealed downregulation of *cat* expression after prolonged exposure to elevated ROS (either via hypermethylation of the promotor by ROS, or transcriptional repression by the H_2O_2 sensitive PI3K-AKT signalling pathway)[115,277–279]. CAT enzyme activity can also be inactivated, either by metal ion binding to -SH group of CAT or by H_2O_2/superoxide radicals[31,280]. Studies have not examined as extensively how *sod2* can be downregulated in response to elevated ROS levels, however, SOD protein activity can be inhibited following long-term exposure to highly concentrated toxicants[147,281–283]. For example, mis-metallation of SOD2 can occur[12]. Iron can bind to the active site of SOD2

(i.e., Mn SOD) instead of Mn, which inactivates the enzyme during conditions of altered iron homeostasis[114]. In fact, decreased SOD and CAT activity was detected in freshwater rohu fish (*Labeo rohita)* liver and gill following exposure to ferrous iron, suggesting possible inhibition of the enzymes by Fe[49]. Another study, however, demonstrated increased activity in flathead grey mullet fish (*Mugil cephalus)*, which may indicate that the fish was able to launch an adaptive response to iron overload in that case[64].

What is interesting is that their expression level (both mRNA and protein) may depend on the length of toxicant exposure time and level of oxidative stress that is induced. For example, exposure to low dose of Zn and Pb in sharptooth catfish (*Clarias gariepinus*) resulted in an initial increase, followed by a decrease (by 28 days) of SOD and CAT activity. Decrease in activity occurred faster when the metal concentration was higher[284]. This suggests that long term exposure to toxicants can inhibit antioxidant enzyme activity. It has also been suggested that the activity of antioxidant enzymes can be inhibited under high levels of oxidative stress, whereas moderate oxidative stress can increase their activity[97]. This change in activity may translate to changes at the transcriptional level as well[285]. For example, Co exposure elevated *cat* and *sod2* mRNA expression at 24 hpf, with a small reduction in *sod2* expression detected by 72 hpf in larval zebrafish[286].

This trend in differential and tissue specific activation or inhibition of antioxidant enzyme activities has been seen on other occasions. Tilapia exposed to contaminated river water containing high levels of Fe, Mn, Cu, and Zn displayed tissue specific differences in activity. There was a decrease in SOD activity in the liver and muscle during the warmer seasons while CAT activity was elevated, whereas both SOD and CAT activity

were lower in the gills. On the other hand, GST activity levels tend to stay elevated irrespective of tissue type and season, most likely to handle the continued flux of electrophilic compounds[121].

Our results also show that, interestingly, unlike *sod2*, *sod1* was significantly downregulated even earlier, at 3 dpf. Its downregulation could have contributed to the sustained ROS levels that lead to *gstp1* expression and potential inhibition of the other phase I detoxification enzymes at 5 dpf.

The difference in SOD response to iron-mediated ROS production can be possible, for while they share similar names and function, their structure, regulation, roles, and localization within the cell do differ. For example, SOD1 is localized predominantly in the cytosol, is constitutively expressed, and not as inducible as other SODs. It is fundamentally considered a housekeeping gene. Furthermore, its promotor is not as sensitive to external stimuli, but can be activated by ROS. On the other hand, SOD2 is found in the mitochondrial matrix and its gene exhibits an inducible expression profile in response to oxidative stress[114,125]. ,SOD2 is involved in rapidly dismutating any superoxide radicals that are released from the electron transport chain during cellular respiration and thus plays a key role in managing ROS levels, since the highest ROS production is from the mitochondria[102]. As a result, they could be differentially regulated by ROS. In fact, a study examining the effects of sub-lethal heavy metal exposure (Cu, Cd, Cr, Pb) on antioxidant activity in adult zebrafish saw a rapid increase in *sod2* expression, whereas induction of *sod1* mRNA expression was delayed, indicating a sensitivity to metals with SOD2 that is not seen with SOD1[197]. On the other hand, it has been shown that at the protein level, SOD1 can be readily inactivated by H_2O_2 by oxidizing

the Cu cofactor, which can lead to the subsequent oxidation of SOD1[111,287]. Whether that translates to changes at the transcriptional level is not clear. What caused the differential response of these SODs to iron-induced oxidative stress, and through which transcriptional regulatory pathway, cannot be determined from these results, since numerous redox-sensitive transcription factors are involved in regulating these antioxidant genes (e.g., Nrf2, AP-1, NF-kB, p53, PI3K-Akt, and HIF)[114,125,288–290].

To finalize, our results demonstrate that zebrafish larvae were able to activate their antioxidant defense system with the intention of mounting an oxidative stress response against the increased ROS production, following iron exposure. However, a reduction in the expression of phase I antioxidant genes (*sod1*, *sod2*, *cat*) suggests that the larval ROS scavenging capabilities in the face of increasing whole body iron levels can become overwhelmed. However, increased expression of *gstp1* indicates attempts by the larvae to mitigate any potential ROS-mediate damage to cellular components, which may help stave off potential cellular dysfunction or apoptotic cell death. This data proposes that larval fish in iron-contaminated freshwater systems may not be able to effectively mitigate iron-mediated ROS production. Further investigations can be carried out to determine whether expression of *gstp1* and other phase II detoxification enzymes can be maintained following iron exposure extending past 5 dpf. Furthermore, conducting a time point expression profile (from 0-5) to check for day-to-day transcriptional changes could be useful, especially for antioxidant genes, since they do show transient expression at the mRNA level. This may allow us to check whether *sod1* expression could have been activated earlier (i.e., prior to 3 dpf) before its levels decreased. For example, a rodent

study of iron overload showed that SOD activity increases before CAT, and starts to decrease by the time CAT activity increases[163].

4.6 Effects of Iron Overload on Behavioural Phenotypes

4.6.1 Locomotor Activity

Examining locomotor function is a standard neurotoxicity test and it allows us to determine whether larval zebrafish displayed defects in swimming activity following iron exposure. Larvae are typically hypoactive in the light, while displaying increased locomotor activity in the dark, so examining their behaviours during both light and dark conditions provides a more complete dataset. Our results show that alternating light and dark periods resulted in consistent and stereotyped locomotor activity in control larvae that has been characterized in numerous studies. Locomotor activity becomes elevated for first 4-6 minutes and slowly declines to baseline after 10 min, following exposure to darkness, which elicits hyperactivity. This is followed by a drop in locomotor activity after induction of light – initiating a startle response – that slowly increases over the exposure period[202,205,209,291]. While iron-exposed larvae showed the same response to changes in photic stimuli as control (e.g., lower activity in light, higher activity in dark), the magnitude of activity was considerably less. They displayed a significantly lower average velocity and total distance moved, irrespective of changes in photic stimuli. Furthermore, they would spend up to two thirds of their time immobile, rather than actively swimming while in the dark period. Together, these results seem to indicate that the iron-exposed larvae developed defects in motility as a result of iron overload. From this dataset we cannot differentiate between whether the larvae displayed a hypokinetic (decreased number of

movements) or bradykinetic (slower movements) phenotype or both[203]. In our case, average velocity is an integrated measurement of the larval activity comprising of immobility, low speed mobility, and high speed mobility[292]. Due to the frame rate speed, instantaneous velocities cannot be determined. Future work can involve finding a means to elucidate the type of kinetic phenotype exhibited by the iron-exposed larvae. Nevertheless, the iron-exposed larvae were still able to respond to changes in light, indicating a functional visual system.

Changes in spontaneous swimming movement and swimming speed in dark/light have been shown to occur in developing zebrafish following exposure to environmental toxicants, such as heavy metals (cadmium, chromium, inorganic mercury, nickel chloride), polybrominated diphenyl ethers, and herbicides[4,28,253,293–298]. In fact, there is a known relationship between neurotoxicity induced by environmental toxicants and resulting behavioural changes in developing zebrafish[299]. These behavioural changes have been linked to toxicant-mediated ROS-induced damage. Iron overload and its effect on the swimming activity of fish has yet to be investigated – this is the first study examining the neurobehavioural effects of iron exposure in fish. However, mammalian studies of post-natal iron overload hint at a potential defect in the dopaminergic system from iron-induced oxidative stress damage[167]. After post-natal exposure to high iron, rodents exhibited periods of hypoactivity correlating with increased iron deposits in the basal ganglia, hippocampus, and striatum, resulting in ROS-mediated dopaminergic neuronal damage[157,300–304]. Weanling rats exposed to 20 mg/L of dietary iron for 12 weeks also exhibited behavioural changes, including decreased locomotor activity during the exploratory phase of an activity test, and occasional instances of decreased habituation.

This was also correlated to a slight increase in brain iron levels[166]. These are similar behavioural patterns witnessed with the iron-exposed zebrafish larvae. Interestingly, increased cellular iron levels in dopaminergic neurons, and consequent oxidative stress damage that results, is also a hallmark of neurological diseases such as Parkinson's, which is characterized by bradykinesia and rigidity[113,301,302].

In zebrafish, the dopaminergic system begins to develop by 18 hpf, and is fully formed by 96 hpf, which fits the time frame of our behavioural analysis (5 dpf or 120 hpf)[293,305]. In fact, the major dopaminergic pathways in mammals can also be found in the zebrafish brain. The topography of zebrafish brain does differ from mammalian brains, but homologous regions have been identified[306–308]. For example, areas believed to resemble the human basal ganglia, which controls voluntary motor function, have been localized in the zebrafish forebrain[181,306,309–312]. The basal ganglia is highly conserved in zebrafish, where its dopaminergic projections are involved in numerous locomotor functions including modulating locomotor activity (e.g., initiation and execution of movement), somatosensory processing, mechanosensory processing, and autonomic output[313–316]. Interestingly, ablation of the dopaminergic supraspinal neurons in developing zebrafish results in decreased total distance swam in addition to a decrease in the proportion of time spent swimming (characterized as beat-glide swimming), similar to what transpired with our iron-exposed larvae[314]. Furthermore, acute exposure to dopaminergic antagonists (which inhibit dopaminergic activity by targeting dopaminergic receptors involved in execution and initiation of movement) in 6-7 dpf zebrafish larvae led to marked dose-dependent decrease in locomotor activity in both light and dark conditions[203,317,318]. Injection of dopaminergic neurotoxins in adult zebrafish also gave rise

to altered locomotor activity, with fish displaying reductions in distance moved and velocity[203,319,320]. This seems to further support the hypothesis that the dopaminergic system in developing zebrafish may be the potential pathway affected by elevated exposure to iron, similar to what is seen in rodent and human models of postnatal iron overload.

Dopaminergic regions of the brain (e.g., basal ganglia) readily experience iron loading and oxidative stress damage (compared to other regions) for a few reasons[321]: (i) non-heme iron preferentially localizes in dopaminergic neurons, since they require high iron content for dopamine synthesis and (ii) dopaminergic neurons possess little to no ferritin[69,77,322]. Iron levels in these dopaminergic regions can be as high as the liver, however they have a decreased capacity to bind any of the free iron due to low ferritin levels, meaning they have a reduced ability to buffer high levels of iron if it does occur[77,156]. In fact, entry of iron into these cells are also comparatively easier. Dopaminergic activity is required for execution of voluntary movement and is dependent on Ca^{2+} and electrical activity. While all neuronal cells utilize extracellular and intracellular Ca^{2+} sources, a continuous flux of Ca^{2+} is required to modulate dopamine release in dopaminergic neurons at a higher flux compared to other neuronal types[323]. A steady and continuous Ca^{2+} influx is also required for membrane potential, and autonomous pacemaking activity in a subset of dopaminergic neurons[323]. This is accomplished via the plasma membrane L-type Ca^{2+} channel. This L-type Ca^{2+} channel based pacemaking activity of dopaminergic neurons is linked to a mitochondrial $O_{2}^{\cdot -}/H_2O_2$ axis, meaning that they are always on the edge of oxidative stress[12]. Dopamine metabolism itself generates high H_2O_2 levels as well, further increasing basal ROS levels[324].

Studies have shown that iron can enter neuronal cells via voltage gated Ca^{2+} channels (VGCC's) during iron overload (similar to what is observed in the heart), and for cells that require high Ca^{2+} flux to function, the increased iron levels can be detrimental. For example, an in vitro cell culture model demonstrated increased Fe^{2+} uptake during neuronal membrane depolarization, competing with (and consequently inhibiting) Ca^{2+} entry into these cells, following exposure to elevated Fe^{2+} (in the mM range). This behaviour was successfully abrogated by using a L-type Ca^{2+} channel blocker, nicardipine[321]. Decreased intracellular Ca^{2+} levels were also detected in rat hippocampal primary cultures following exposure to Fe^{2+} (from 1-100 μM) which were further reduced when the cells were pre-treated with agents that induce depolarization (and activates VGCCs). Neuronal pre-treatment with a cocktail of VGCC blockers (L-, T-, P-, N-, Q-types) resulted in decreased Fe^{2+} flux during both resting and depolarization conditions. Treatment with CM-H_2DCFDA showed that this increased Fe^{2+} influx resulted in amplified production of ROS, as well, which was elevated even further during depolarization[325]. In fact, an in vivo model of iron overload noted that nicardipine treatment following intraperitoneal injection of iron can prevent accumulation of iron, and subsequent ROS-induced damage, in dopaminergic neurons. This suggests iron uptake through VGCCs plays a key role in its accumulation in these neurons[326].

Iron-mediated ROS production and damage of dopaminergic neurons can lead to either their loss (via apoptosis or ferroptosis, an iron-mediated form of necrosis) or decreased dopamine content (via dopamine oxidation), which is likely the source of the hypoactive tendencies witnessed in rodent models[148,157,327]. Alternatively, iron could have impacted Ca^{2+} signalling and potentially led to delayed depolarization or neurotransmitter

release. Studies have also implicated altered Ca^{2+} homeostasis in potentiating the iron-mediated neuronal damage. For example, PMCA (plasma membrane Ca^{2+} ATPases) in neuronal cells can become inhibited following iron-induced oxidative stress. ROS, like H_2O_2, can downregulate PMCA in hippocampal neurons as well[328]. This results in decreased Ca^{2+} clearance and subsequent Ca^{2+} accumulation in neuronal cells [148,329].

Furthermore, we must also not rule out potential impairments in mitochondrial bioenergetics, considering ROS production and accumulation first begins in the mitochondria and can damage components of the respiratory transport chain. Increased iron flux into the mitochondria following elevated cytoplasmic iron during iron overload can also occur[148]. Mitochondrial damage is also not regional specific and can transpire in all tissues[153]. Lastly, a few studies have suggested that the neurobehavioural dysfunctions witnessed in rat models of iron overload may be due to, or associated with, peripheral effects from iron toxicity of other organs (e.g., liver toxicity, neuroendocrine dysfunction), since iron loading in the brain, and lipid peroxidation, are only slight[164,166]. For example, some transcriptomic changes can occur that may affect behaviours such as learning and memory, following systemic iron overload, without a concurrent increase in brain iron levels[164].

However, whether any of these defects also occur in fish, and are the cause of the altered motor function, require further investigation. What can be addressed in future studies is the mechanisms behind the altered larval locomotor function and the involvement of dopamine. Consequently, in addition to measuring dopamine content in larval zebrafish, mRNA expression of its receptors (D1 and D2), transporters (DAT; dopamine transporter), and genes involved in its biosynthesis (TH, tyrosine hydroxylase)

and degradation (MAO; monoamine oxidase) can also be examined[330,331]. These known dopamine biomarkers have been comprehensively utilized to understand the effects of high environmental selenium levels on dopaminergic function and behaviour in adult zebrafish, and can thus be utilized in larval zebrafish as well[332,333]. If a link can be shown between iron exposure and altered dopaminergic function in larval zebrafish, then the next route would be to examine whether altered Ca^{2+} homeostasis is a key player in the pathophysiology of this response. If no change is detected, peripheral effects of iron overload on locomotor activity can also be examined (e.g., liver or mitochondrial function).

To summarise, iron exposure gave rise to hypoactive swimming patterns in larval zebrafish, characterized by increased periods of immobility, decreased distance swam, and slower swimming speeds, irrespective of changes to photic stimuli. This has serious ecological implications: this impaired locomotor function may prevent developing fish in iron-contaminated freshwaters from successfully escaping adverse conditions (e.g., predation), or from effectively foraging for food or shelter, potentially leading to decreased viability during development.

4.6.2 Touch-Evoked Escape Response

Interestingly, iron overload may also have caused impairments in sensory-motor function, as our iron-exposed larvae exhibited delayed responses to tactile stimuli, requiring numerous taps before execution of movement occurs. Under normal conditions, larval zebrafish display a stereotyped escape response, consisting of an increased bout of swimming activity oriented away from a tactile stimulus. This can also be called a startle response and can be elicited in larval zebrafish using water flow (at 3-4 dpf), abrupt auditory/vibrational stimuli (at 5 dpf) or light stimuli (i.e. sudden and rapid changes in light;

from 3-6 dpf)[209,334,335]. Zebrafish larvae develop the ability to respond to tactile stimuli around 24-27 hpf and this response can be elicited by applying the stimulus to either the head or the tail. The extent and type of response varies depending on the developmental age, with a twitch in pre-swimming larvae (e.g., 1 dpf), tail flip in 48 hpf larvae, and an escape response in older larvae (e.g., 3 dpf)[201,336,337]. Depending on where the stimulus is applied, the resulting response differs. Touch response elicited by applying stimuli to the head gives rise to tail coils and occasional bouts of swimming, or 180 degree turns away from stimulus, while tail/trunk stimuli induces a c-start (i.e., coiling of tail into a 'c' shape followed by rapid forward burst swimming)[338,339].

This startle response has been extensively studied and, in older larvae/adults, consists of Mauthner neurons, or other reticulospinal neurons, which relay the sensory input from dorsal root ganglions to contralateral motor neurons located in the spinal cord, initiating the rapid escape response[340]. In younger embryos (1-3 dpf), Mauthner involvement is still debated, while the mechanosensory Rohon-Beard (RB) cell and the ascending primary commissural interneuron (CoPA) possess critical roles in the touch-evoked escape response[336].

RB cells are mechanosensitive, with stretch sensitive ion channels on their nerve endings that can respond to light touch. The mechanisms involved behind this mechanosensory response are still being studied[269,341]. Their cell body is bilaterally localized in the dorsal spinal cord with projecting central ascending and descending axons, as well as peripheral processes. The central axon projects to the hindbrain, and another within the spinal cord (caudally). The peripheral axon extends from the spinal cord dorsolaterally and innervates the skin with free nerve endings, forming a close

association with the periderm of the larval zebrafish skin, the outermost skin layer[341,342].The peripheral axons of the RB cell are not restricted to a single segment but can be found branched out, extended over numerous myotomes on one side of the larva, but do not extend past the midline to the other side [342]. RB cells are progressively replaced by dorsal root ganglion (DRG) neurons, which mediate the sensory function, beginning around 60 hpf. After 120 hpf, RB cells are absent and the DRG and the lateral line system are the main pathways utilized to detect mechanosensory stimuli[336,343,344].

Following tactile stimulus to the tail in 3 dpf larval zebrafish, these mechanosensitive RB cells are activated, and Ca^{2+} signalling stimulates the release of glutamate from the RB cell, synapsing and activating the CoPA interneurons[345]. CoPA also display glutaminergic activity, synapsing to descending interneurons, which subsequently activate motor neurons on the contralateral side of the spinal cord [337]. Motor neurons are segmentally restricted, found dorsal to the RB cell in the trunk spinal cord[342]. Motor neurons activate skeletal muscle via cholinergic neurotransmission (acetylcholine), initiating the stereotyped escape response. These axial skeletal muscles consist of a layer of slow twitch muscle fibres and many layers of fast-twitch fibres localized medially[177,346]. Motor neurons and CoPA interneurons show spontaneous activity, displaying large currents and dynamic membrane potentials, with passive control from descending interneurons displaying smaller currents and controlled membrane potentials[337].

Conflicting information exists regarding hindbrain (i.e., Mauthner cell) involvement in embryonic/larval zebrafish touch-evoked escape response following stimulus to the tail[337,347]. However, certain studies have revealed that Mauthner and other reticulospinal neurons displayed increased electrical activity and Ca^{2+} currents following tactile stimuli

to the tail in 2-4, 3, and 12 dpf larvae and thus may be involved in coordinating the escape behaviour [339,348,349]. When Mauthner neurons were ablated in another study, the larvae were still able to elicit an escape response, but with increased response latencies after caudal stimuli, and a weaker c-turn[348]. In fact, descending neurons from the reticulospinal system to the spinal cord have been suggested to be involved in relaying escape-related information (which are dopaminergic) to the motor neurons[311]. It seems that sensory information is relayed to supraspinal neurons via the CoPA interneurons, while the escape response is triggered by the intraspinal circuits via RB activation[350]. Several neurotransmitters are involved in modulating the escape response, including dopamine, glutamate, glycine, serotonin, and GABA[204].

Since numerous pathways, neurotransmitters, and cell types are involved in eliciting the response, the challenge is attempting to determine how and where iron exposure could have affected this reflex response.

Like locomotor activity, studies examining larval touch-evoked escape responses following iron exposure do not currently exist. A fieldwork-based study mentioned in passing that escape responses of carp living in water contaminated with iron and aluminum (Al) were absent. However, these fish were exposed to ferrous iron (0.65-0.8 mg/L) in acidic conditions (pH 5.8), in addition to Al, so it does not convey which factor specifically induced this lack of response[10]. However, studies examining the effects of environmental toxicants noted decreased response to touch, suggesting effects on axonal growth and muscle development, or ROS mediated necrosis and apoptotic cell death[179,351–353]. Exposure to Co, Cu, and Cd all gave rise to a concentration-dependent delayed response to touch that was correlated with motor neuron (primary and

secondary) damage and thus impaired tail muscle innervation in 3 dpf larvae[354]. Larval zebrafish (7 dpf) also displayed delayed response to tactile stimuli (e.g., increased latency to swim and decreased swim escape speed) following sublethal exposure to lead (Pb), which they hypothetically suggest may be due impairments in Ca^{2+} currents and muscle fibre activity, or increased sensory threshold since Pb can damage the lateral line neuromasts[355]. It is clear the pathways by which touch response is attenuated will therefore differ depending on the metal's means of toxicity in the larval zebrafish. For example, iron is likely less toxic than the above listed environmental toxicants and may be affecting behaviour via ROS-mediated damage to cellular components. Exposing developing zebrafish to low level of toxicants, either time or concentration-wise, (like in our case) may not yield detectable changes in gross anatomy or external morphological development that we can thus associate to the changes in behaviour witnessed. Any subtle changes in behaviour, therefore, can potentially be attributed to changes in neuronal connectivity, electrical activity, neurotransmitter release, or muscle activation[338].

Nevertheless, iron can affect electrical activity of electrical based cells through its effect on Ca^{2+} channel activity. During periods of iron overload, iron has been shown to enter neuronal cells via VGCC, as mentioned earlier, but whether that can cause delays in neuronal signalling (i.e., neurotransmitter release) remains to be seen[262,356,357]. Additionally, iron has been shown to inhibit the activity of Ca^{2+}-ATPases during periods of iron overload by direct iron-mediated ROS attack, resulting in Ca^{2+} accumulation in neuronal cells and muscle fibres, which may delay signalling and potentially lead to apoptosis. Iron-produced ROS can also induce lipid peroxidation of the plasma membrane, which can reduce the membrane potential in these cells or lead to damage

to other cellular components[247]. Models of systemic iron overload in mice do display decreased transcript levels of proteins involved in Ca^{2+} homeostasis and signalling (e.g. *Cacna1a*, P/Q type voltage gated calcium channel alpha 1A subunit; *Camk2a*, Calcium/calmodulin-dependent protein kinase IIα) and the importance of VGCC activity (specifically P/Q type) in the fast synaptic transmission required during touch-evoked escape responses in zebrafish larvae has been emphasized[164,346]. CaM kinase IIα involvement has also been shown to be involved in the sensorimotor circuit (as part of CoPA)[345]. Furthermore, we also observed increased whole body Ca^{2+} levels in 3 dpf iron-exposed larvae, which lends credence to possible alteration of Ca^{2+} homeostasis in these larvae.

However, whether this does occur in fish, and whether iron-mediated impaired Ca^{2+} signalling plays a role in the delayed escape response exhibited by our iron-exposed larvae remain to be seen. Further investigations are required to address this.

To conclude, our results demonstrate that developing fish in iron-contaminated freshwater systems may exhibit delayed responses to tactile stimuli, which can render them vulnerable to predation or other averse environmental cues that require immediate escape from the stimulus. While a subset of the iron-exposed larvae did respond to the tactile stimuli, examining the acceleration of their burst escape response may yield additional noteworthy information regarding their muscle function. Since peak acceleration occurs within the first 0.2 sec, the larvae would need to remain in the field of view (FOV) to measure changes in acceleration[358]. Since our FOV was relatively smaller (e.g., control larvae were out of the FOV in less than 0.14 s), measuring such parameters were not feasible, but can be something we can certainly optimize in future studies.

4.6.3 Thigmotactic Response

We also decided to determine whether iron overload resulted in altered anxiety responses in zebrafish, by measuring their thigmotactic response. In response to an external stressor, larval zebrafish will avoid the centre of a novel environment and move or stay still near the boundary of that environment (i.e., walls of a well). Analysis of thigmotactic response in larval zebrafish is typically examined in the dark, as sudden darkness elicits a visual-motor response (VMR) in the larvae. VMR is characterized by a robust increase in activity that slowly decays over time as the larval zebrafish habituates to its environment[206,334]. Zebrafish have an innate tendency to avoid dark or open spaces and these responses are related, and important for, predator avoidance or seeking shelter[296]. Many fish species, including zebrafish, are diurnal in nature and a change to darkness (i.e., sunset) triggers a sudden hyperactivity correlated with an attempt to find shelter before it turns dark. Also, changes that suddenly cause darkness (presence of predator, falling debris) will also result in hyperactivity, as the fish may be trying to rapidly navigate itself back to illuminated regions where it is safer[206,359]. They rely on vision and thus a lit environment[195]. Eliciting VMR in the larvae forces them to explore the whole well, which would consequently give a more accurate readout in terms of whether they truly display differences in thigmotactic behaviour based on the treatment[206]. The neural pathway underlying this response is still being studied, though the involvement of dopamine, serotonin, GABA, and histamine have been suggested[204].

However, our thigmotaxis results, unfortunately, were inconclusive at best. Thigmotactic behaviour can be measured as % time spent per zone and percent distance moved per zone (time- or distance- related parameters)[360,361]. In our case, percent

duration in outer zone of iron-exposed larvae was lower than control, potentially indicating decreased thigmotaxic response, and consequently iron-induced changes in anxiety. However, percent distance traveled in outer zone, between control and iron-exposed larvae, were not statistically significant, meaning iron did not alter anxiety responses.

As mentioned previously, thigmotaxis is measured in the dark, as a sudden change to darkness elicits increased locomotor activity and exploratory behaviour. However, in our case, the change from light to dark, while increasing activity level of iron-exposed larvae, did not do so to the level of control larvae. Since they are not showing a robust locomotor activity in the dark (as it was marked with multiple periods of immobility), that creates a challenge as we cannot confidently make a definite conclusion as to whether they do show altered anxiety response. In support of this conclusion, Bouwknecht and Paylor (2008) and Shnorr et al., (2012) have stated that since thigmotaxis is an assay that falls under the category of *exploratory-driven anxiety model*, locomotion can consequently influence our assessment of anxiety behaviour. This model requires that the organism actively explores all zones present throughout the duration of the test. This means that if we have larvae that show natural hypoactive tendencies, they may remain immobile in one zone over the other, which could lead to a conclusion that the organism showed high (or low) thigmotactic response. This may not actually indicate an anxiety-driven preference for a specific zone[206,362]. In fact, our preliminary results indicated that our FAC-exposed larvae spent more time immobile rather than actively swimming while in the inner zone when compared to control, supporting this idea. Further analysis of the dataset, however, will be required to better understand the behavioural pattern exhibited. Nevertheless, this idea is also in accordance to a study examining changes in emotional

behaviour and anxiety responses in rodents following a 5-day exposure to iron sulphate. While they saw behaviours that could be interpreted as anxious (e.g., spending more time in the closed arms of the elevated plus maze rather than in the anxiogenic open arms) they also noticed that their activity in the maze and number of closed-arm entries were reduced compared to other treatments (control and moderate iron levels) which may also indicate reduced activity and exploratory drive (which are more motor function-related)[172]. They have suggested that using models of anxiety that do not depend as much on exploratory drive or activity may help delineate the root cause of the altered behaviour.

Another cause may be that the larval zebrafish often crosses the inner zone to reach the other side of the well, which would increase the time spent in the inner zone. In fact, while not a metal, larval zebrafish exposed to an herbicide displayed the same pattern of results. They would actively cross the inner zone increasing the time spent in that zone relative to control, while percent distance moved was the same between control. However, these larvae were slightly hyperactive compared to control[363]. Additionally, injection of dopaminergic neurotoxins have shown to alter thigmotactic response in adult zebrafish, where they would often cross the centre zone of the tank, rather than swim along the tank walls, while also exhibiting hypoactivity; however they also saw considerable variability with respect to this behaviour among fish[319].

5 Conclusions

There are numerous conclusions that can be made from our results. Figure 24 contains a brief overview of the main findings. First, we saw that developing zebrafish exhibited delayed regulation of iron uptake, resulting in whole-body iron loading, 6 times higher than control, by the time they were 5 dpf. While they tried to mount an oxidative stress-response against the increase iron and iron-mediated ROS production, levels were still high at 5 dpf, and that was correlated with a downregulation of key phase I antioxidases that are uniquely involved in ROS scavenging (SOD1, SOD2, CAT). However, the larvae did activate the phase II antioxidant system as shown by elevated *gstp1* levels at 5 dpf, indicating that the larvae were trying to mitigate the potential damage produced. Furthermore, while exposure to 50 mg/L FAC was not fatal, nor did it cause morphological deformities, it did give rise to altered physiological and behavioural phenotypes. They displayed a bradykinetic heart rate, hypokinetic locomotor activity, and delayed touch-evoked responses. This demonstrates that larval zebrafish fitness can be affected by elevated ferric iron exposure, which may potentially impact its survival long term. Further studies can be done to elucidate the type of effects iron had on fish neurophysiology, as we cannot at this point conclude that the altered behavioural functions were a result of increased ROS production in the CNS.

To conclude, this is the first study that has examined neurophysiological effects of iron overload on fish, demonstrating that iron contamination of freshwater systems should be addressed as an environmental concern as while not lethal, both fish physiological

and neurophysiological functions were detrimentally affected, following exposure to 50 mg/L FAC (measured [Fe]: 12.1 mg/L), an environmentally relevant iron concentration.

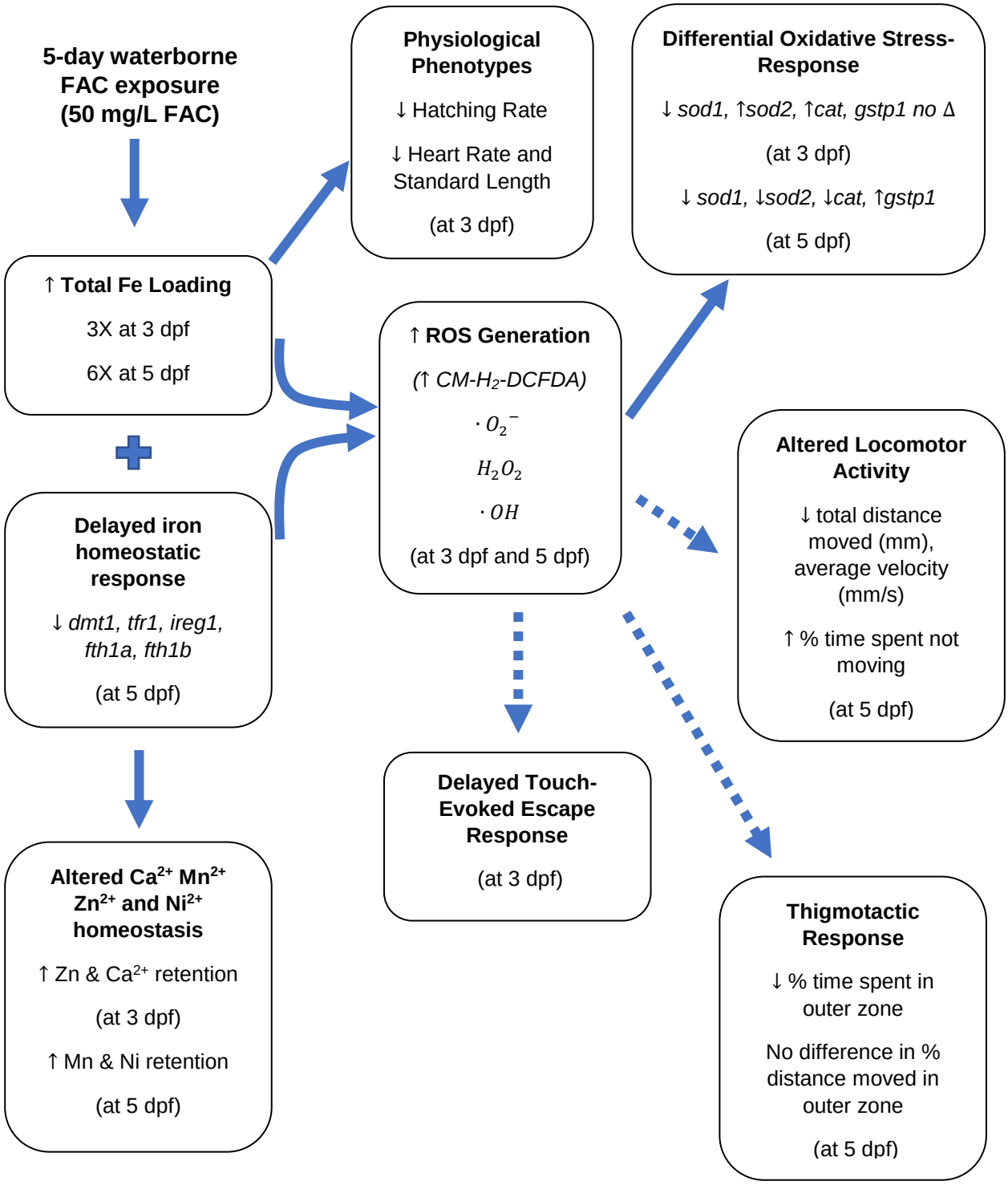

Figure 24. Summary of Main Findings.

6 Future Directions

This research has revealed that waterborne ferric iron exposure can lead to (i) increased whole body iron burden, (ii) ROS production, (iii) activation (and attenuation) of an oxidative-stress response, and (iv) altered neurophysiological functioning in developing zebrafish. To further our understanding behind the mechanisms implicated in these altered responses, further investigations need to be carried out.

First, while ddPCR provided us with a detailed dataset regarding the mRNA expression of key iron homeostasis and oxidative stress-response proteins, this does not convey what may be occurring at individual tissue levels (e.g., brain vs. heart expression levels, for example). Utilizing in situ hybridization to check for tissue specific expression patterns may provide a more complete picture of how individual tissues respond to elevated iron levels and the type of oxidative-stress response they mount.

Furthermore, investigating other key genes involved in both pathways will be beneficial. Additional iron homeostatic genes to consider are hepcidin (*hamp1, hamp2*) and TfR2 (*tfr2*). We can try to examine if there are correlations between changes in hepcidin mRNA expression with that of IREG1 to ascertain whether their expression levels mirror (e.g., either both increase or decrease at specific time points) to lend credence to the hypothesis that the decreased *ireg1* expression witnessed was associated with increased hepcidin activity. Additionally, TfR2 does not possess an IRE, as it is sensitive to systemic levels of iron, which may shed light on how the developing zebrafish (specifically its liver, where TfR2 is expressed) respond to iron exposure at the systemic level. We can also examine the expression of the zebrafish ferric chelate

reductase (*frrs1)* which reduces ferric iron to ferrous iron. It has shown to be expressed in the gut of larval zebrafish via in situ hybridization, and may disclose whether there were any changes it its expression following elevated ferric iron exposure[91].

Furthermore, we can expand the expression profile of genes involved in the Phase II and III detoxification system of the oxidative stress response, as we only examined GSTP. We may thus uncover additional, and much needed, biomarkers for iron toxicity in fish. Peroxiredoxin 1 (*prdx1*), an antioxidase, and glutamate-cysteine ligase catalytic subunit (*gclc*), involved in GSH synthesis, are both key examples of highly expressed Nrf2-regulated genes in developing zebrafish that can respond to toxicants such as arsenic and Cd, and to iron overload in rodents[91,276,364,365]. They are typically co-studied with *gstp1*. In fact, *prxd1* is involved in regulating heme degradation, and *gclc* is a biomarker for ferroptosis in humans, indicating that these genes are linked to both iron homeostasis and oxidative stress[366,367].

Additionally, glutathione peroxidase (GPX), while not a Phase II or III antioxidant, is also another key biomarker for environmental toxicity in fish, including zebrafish[103]. It shares a similar role to CAT, and is involved in catalyzing both H_2O_2 (*gpx1a*) and lipid peroxides (*gpx4*) utilizing GSH as a substrate[368]. This will provide us with additional key information. Examining GPX will inform us of the state of peroxidase activity in the mitochondria and the cytosol, where it is typically active[105]. Furthermore, an increase in *gpx4* expression, may indicate increased lipid peroxidation, which is advantageous to know as well[368]. GPX is also linked to the Phase II detoxification system as it utilizes GSH, an antioxidant required by GST. Any change in GSH levels may affect GPX activity[368].

However, measuring mRNA expression of antioxidant enzymes does not inform us of the efficacy or functionality of their corresponding enzymatic activities, for instance, whether the antioxidant enzyme was inactivated following elevated iron exposure and subsequent ROS production. Therefore, conducting kinetic-based experiments, such as enzyme assays (which measure activity levels of key antioxidant enzymes such as SOD, CAT, GPX, and GST), will give rise to a better understanding of their antioxidant capacities under iron overload conditions.

Even more valuable would be measuring cellular impairment as a result of iron-mediated ROS attack, to identify the impact of iron exposure on cellular integrity and function in developing fish. We can thus utilize lipid peroxidation assays to measure the amount of the breakdown product MDA in larval zebrafish (i.e., TBARS assay)[103]. Any increase in lipid peroxidation signifies that membrane permeability could have been altered, and therefore membrane receptors and transporters, which could affect cellular signalling[103]. Moreover, ferroptosis, an Fe^{2+}-dependent form of cell death, is induced by lipid peroxidation[12]. This can thus be another parameter we can examine[149]. Assays for measuring levels of carbonyls (i.e., oxidation of proteins) and DNA damage should also be done. DNA damage is a typically employed parameter to examine the effects of environmental toxicants[103,179]. Furthermore, since numerous enzymes utilize GSH as part of the oxidative stress response, GSH depletion can be measured[31,96].

Most importantly, the mechanisms (or potential pathways) implicated in the behavioural changes observed in the iron-exposed larvae must be elucidated. For example, we cannot be certain if the iron overload-induced delay in escape response we saw is due to (1) impaired detection (sensory neurons; sensory perception or processing),

(2) integration (Mauthner/reticulospinal cells), or (3) response (interneurons or neuromuscular junctions; neuromuscular activation), without carrying out additional tests. For instance, we can measure axonal growth of motor, reticulospinal, or mechanosensory neurons (RB cells), examine mRNA expression of genes involved in axonal development such as *gap43* and *a1-tubulin* (known markers for neuronal impairment), or stain for nAChR (acetylcholine receptors)[294,369]. As iron overload may affect Ca^{2+} homeostasis, examining different aspects of Ca^{2+} regulation (including Ca^{2+} channel expression and cellular Ca^{2+} flux) is another possibility[164]. Performing other forms of larval zebrafish startle response tests, like auditory/vibrational startle (via activation of larval auditory hair cells), can also help determine whether sensory pathways in general were affected by iron exposure, since they all utilize the same motor unit to initiate the reflex (via Mauthner involvement)[370]. Interestingly, delayed reflex startle response following auditory stimuli was displayed in weanling rats fed a high iron diet, in conjunction with decreased locomotor activity[166].

With regards to the decreased locomotor activity witnessed with our iron-exposed larvae, examining dopamine content and expression of key dopaminergic genes can be a place to start, as rodent studies of iron overload have shown that iron-mediated oxidation of dopamine can occur. Furthermore, elevated ROS levels were detected in larval zebrafish brains which lends support to a potential impairment in neuronal function. In fact, there is a known link between exposure to heavy metals (and other environmental toxicants) and dopaminergic dysfunction in humans[330]. Conversely, other neurotransmitter levels should be examined, such as serotonin or noradrenaline, to rule out their potential involvement, as they can also modulate different forms of motor

responses[371]. For example, serotonin controls arousal, with decreased arousal manifesting as hypolocomotion. We also detected elevated ROS in the midbrain and hindbrain regions of the larval zebrafish, where serotonergic populations are nestled[372]. Furthermore, decreased serotonin levels in brains of rodents fed a high iron diet has been demonstrated[4]. However, it may also be advantageous to measure liver enzyme activity (GPase, phosphorylase *a*), as hepatotoxicity may affect other physiological functions (and the liver did display very elevated ROS levels), or mitochondrial function (basal respiration and ATP production)[124,164,265,325]. These may have given rise to the overall slower movements and lower heart rates that were detected. Lastly, a study examining the effects of deferoxamine (DFO) on FAC-exposed larvae showed that this iron-chelator can both reduce whole-body iron and ROS levels in larvae, following iron treatment[184]. Using DFO can allow us to determine whether decreasing iron-loading post exposure period can rescue the neurophysiological phenotypes, or whether the effects of iron loading are permanent.

Together, these additional investigations will aid in forming a better understanding of the neuropathophysiological effects of iron overload and shed light on the diverse consequences that iron contaminated freshwater ecosystems have on developing fish. Next steps would involve examining the effects of chronic iron exposure (i.e., extending past 5 dpf) and verify whether neurophysiological impairments are lifelong, considering adult zebrafish have a marked capacity for neurogenesis[190,373].

7 References

1. Dev, S. & Babitt, J. L. Overview of iron metabolism in health and disease. *Hemodial. Int.* **21**, S6–S20 (2017).

2. Hare, D., Ayton, S., Bush, A. & Lei, P. A delicate balance: Iron metabolism and diseases of the brain. *Front. Aging Neurosci.* **5**, 1–19 (2013).

3. Benarroch, E. E. Brain iron homeostasis and neurodegenerative disease. *Neurology* **72**, 1436–1440 (2009).

4. Elseweidy, M. M. & El-Baky, A. E. A. Effect of dietary iron overload in rat brain: Oxidative stress, neurotransmitter level and serum metal ion in relation to neurodegenerative disorders. *Indian J. Exp. Biol.* **46**, 855–858 (2008).

5. Ganz, T. & Nemeth, E. Iron homeostasis in host defence and inflammation. *Nat. Rev. Immunol* **15**, (2015).

6. SkjÃ¸rringe, T., Burkhart, A., Johnsen, K. B. & Moos, T. Divalent metal transporter 1 (DMT1) in the brain: implications for a role in iron transport at the blood-brain barrier, and neuronal and glial pathology. *Front. Mol. Neurosci.* **8**, 1–13 (2015).

7. Silva, B. & Faustino, P. An overview of molecular basis of iron metabolism regulation and the associated pathologies. *Biochim. Biophys. Acta.* **1852**, 1347–59 (2015).

8. Garton, T., Keep, R. F., Hua, Y. & Xi, G. Brain iron overload following intracranial haemorrhage. *Bmj* **1**, 172–184 (2016).

9. Imam, M. U., Zhang, S., Ma, J., Wang, H. & Wang, F. Antioxidants mediate both iron homeostasis and oxidative stress. *Nutrients* **9**, 1–19 (2017).

10. Slaninova, A., Machova, J. & Svobodova, Z. Fish kill caused by aluminium and iron contamination in a natural pond used for fish rearing: A case report. *Vet. Med. (Praha).* **59**, 573–581 (2014).

11. Vuori, K.-M. Direct and indirect effects of iron on river ecosystems. *Ann. Zool. Fenn.* **32**, 317–329 (1995).

12. Cobley, J. N., Fiorello, M. L. & Bailey, D. M. 13 reasons why the brain is susceptible to oxidative stress. *Redox Biol.* **15**, 490–503 (2018).

13. Anderson, G. J. & Frazer, D. M. Current understanding of iron homeostasis. in *Am. J. Clin. Nutr.* **106**, 1559S-1566S (2017).

14. Gozzelino, R. & Arosio, P. Iron homeostasis in health and disease. *Int. J. Mol. Sci.* **17**, 2–14 (2016).

15. Kaplan, J., Ward, D. M. & De Domenico, I. The molecular basis of iron overload disorders and iron-linked anemias. *Int. J. Hematol.* **93**, 14–20 (2011).

16. Cottet, M., Descloux, S., Guédant, P., Godon, A., Cerdan, P & Vigouroux, R. Total iron concentrations in waters and fish tissues in the Nam Theun 2 Reservoir area (Lao PDR). *Environ. Monit. Assess.* **187**, 529 (2015).

17. Payne, J. F., Malins, D. C., Gunselman, S., Rahimtula, A. & Yeats, P. A. DNA oxidative

damage and vitamin A reduction in fish from a large lake system in Labrador, Newfoundland, contaminated with iron-ore mine tailings. in *Mar. Environ. Res.* **46**, 289–294 (1998).

18. Authman, M. M. Use of Fish as Bio-indicator of the Effects of Heavy Metals Pollution. *J. Aquac. Res. Dev.* **06**, 1-13 (2015).

19. Cadmus, P., Brinkman, S. F. & May, M. K. Chronic Toxicity of Ferric Iron for North American Aquatic Organisms: Derivation of a Chronic Water Quality Criterion Using Single Species and Mesocosm Data. *Arch. Environ. Contam. Toxicol.* **74**, 605–615 (2018).

20. Su, C., Lu, Y., Johnson, A. C., Shi, Y., Zhang, M., Zhang, Y., Juergens, M. D. & Jin, X. Which metal represents the greatest risk to freshwater ecosystem in bohai region of china? *Ecosyst. Heal. Sustain.* **3**, e01260 (2017).

21. Lappivaara, J., Kiviniemi, A. & Oikari, A. Bioaccumulation and subchronic physiological effects of waterborne iron overload on whitefish exposed in humic and nonhumic water. *Arch. Environ. Contam. Toxicol.* **37**, 196–204 (1999).

22. Brenner, F. J. & Cooper, W. L. Effect of Suspended Iron Hydroxide on the Hatchability and Embryonic Development of the Coho Salmon. *Ohio J. Sci.* **78**, 34–38 (1978).

23. Phippen, B., Horvath, C., Nordin, R. & Nagpal, N. *Ambient Water Quality Guidelines for Iron*. B.C. Ministry of Environment (2008).

24. Craig, P. M., Galus, M., Wood, C. M. & McClelland, G. B. Dietary iron alters waterborne copper-induced gene expression in soft water acclimated zebrafish (Danio rerio). *AJP Regul. Integr. Comp. Physiol.* **296**, R362–R373 (2008).

25. Weber, P., Behr, E. R. , Knorr, C. D. L., Vendruscolo, D. S., Flores, E. M. M., Dressler, V. L. & Baldisserotto, B. Metals in the water, sediment, and tissues of two fish species from different trophic levels in a subtropical Brazilian river. *Microchem. J.* **106**, 61–66 (2013).

26. Jabeen, F. & Chaudhry, A. S. Environmental impacts of anthropogenic activities on the mineral uptake in Oreochromis mossambicus from Indus River in Pakistan. *Environ. Monit. Assess.* **166**, 641–651 (2010).

27. Bakker, E. S., Van Donk, E. & Immers, A. K. Lake restoration by in-lake iron addition: a synopsis of iron impact on aquatic organisms and shallow lake ecosystems. *Aquat. Ecol.* **50**, 121–135 (2016).

28. Michiels, E., Vergauwen, L., Hagenaars, A., Fransen, E., Van Dongen, S., Van Cruchten, S. J., Bervoets, L. & Knapen, D. Evaluating Complex Mixtures in the Zebrafish Embryo by Reconstituting Field Water Samples: A Metal Pollution Case Study. *Int. J. Mol. Sci.* **18**, 539 (2017).

29. Mizuno, S., Sasaki, Y., Omoto, N. & Imada, K. Elimination of adhesiveness in the eggs of shishamo smelt Spirinchus lanceolatus using kaolin treatment to achieve high hatching rate in an environment with a high iron concentration. *Aquaculture* **242**, 713–726 (2004).

30. Gorchev, H. G. & Ozolins, G. WHO guidelines for drinking-water quality. *WHO Chron.* **38**, 104–8 (1984).

31. Ruas, C. B. G., Carvalho, C. dos S., de Araújo, H. S. S., Espíndola, E. L. G. & Fernandes, M. N. Oxidative stress biomarkers of exposure in the blood of cichlid species

from a metal-contaminated river. *Ecotoxicol. Environ. Saf.* **71**, 86–93 (2008).

32. Payne, J. F., French, B., Hamoutene, D., Yeats, P., Rahimtula, A., Scruton, D. & Andrews, C. Are metal mining effluent regulations adequate: Identification of a novel bleached fish syndrome in association with iron-ore mining effluents in Labrador, Newfoundland. *Aquat. Toxicol.* **52**, 311–317 (2001).

33. Schaider, L. A., Senn, D. B., Estes, E. R., Brabander, D. J. & Shine, J. P. Sources and fates of heavy metals in a mining-impacted stream: Temporal variability and the role of iron oxides. *Sci. Total Environ.* **490**, 456–466 (2014).

34. Mayes, W. M., Gozzard, E., Potter, H. A. B. & Jarvis, A. P. Quantifying the importance of diffuse minewater pollution in a historically heavily coal mined catchment. *Environ. Pollut.* **151**, 165–175 (2008).

35. Boult, S., Collins, D. N., White, K. N. & Curtis, C. D. Metal transport in a stream polluted by acid mine drainage-The Afon Goch, Anglesey, UK. *Environ. Pollut.* **84**, 279–284 (1994).

36. Gemici, Ü. Evaluation of the water quality related to the acid mine drainage of an abandoned mercury mine (Alaşehir, Turkey). *Environ. Monit. Assess.* **147**, 93–106 (2008).

37. Vuorinen, P. J., Keinänen, M., Peuranen, S. & Tigerstedt, C. Effects of iron, aluminium, dissolved humic material and acidity on grayling (Thymallus thymallus) in laboratory exposures, and a comparison of sensitivity with brown trout (Salmo trutta). *Boreal Environ. Res.* **3**, 405–419 (1998).

38. Cadmus, P., Guasch, H., Herdrich, A. T., Bonet, B., Urrea, G. & Clements, W. H. Structural and functional responses of periphyton and macroinvertebrate communities to ferric Fe, Cu, and Zn in stream mesocosms. *Environ. Toxicol. Chem.* **37**, 1320–1329 (2018).

39. Linton, T. K., Pacheco, M. A. W., McIntyre, D. O., Clement, W. H. & Goodrich-Mahoney, J. Development of bioassessment-based benchmarks for iron. *Environ. Toxicol. Chem.* **26**, 1291–1298 (2007).

40. Shuhaimi-Othman, M., Nadzifah, Y., Nur-Amalina, R. & Umirah, N. S. Deriving freshwater quality criteria for iron, lead, nickel, and zinc for protection of aquatic life in malaysia. *Sci. World J.* **2012**, 1-7 (2012).

41. Teien, H. C., Garmo, Ø. A., Åtland, Å.˚& Salbu, B. Transformation of iron species in mixing zones and accumulation on fish gills. *Environ. Sci. Technol.* **42**, 1780–1786 (2008).

42. Mcknight, D. M. & Feder, G. L. The ecological effect of acid conditions and precipitation of hydrous metal oxides in a Rocky Mountain stream. *Hydrobiol* **119**, 129–138 (1985).

43. Zhu, X., Tian, S. & Cai, Z. Toxicity Assessment of Iron Oxide Nanoparticles in Zebrafish (Danio rerio) Early Life Stages. *PLoS One* **7**, e46286 (2012).

44. Lehtinen, K. J. & Klingstedt, G. X-ray microanalysis in the scanning electron microscope on fish gills affected by acidic, heavy metal containing industrial effluents. *Aquat. Toxicol.* **3**, 93–102 (1983).

45. Liang, H. C. & Thomson, B. M. Minerals and Mine Drainage. *Source Water Environ. Res.*

81, 1615–1663 (2009).

46. Rozon-Ramilo, L. D., Dubé, M. G., Squires, A. J. & Niyogi, S. Examining waterborne and dietborne routes of exposure and their contribution to biological response patterns in fathead minnow (Pimephales promelas). *Aquat. Toxicol.* **105**, 466–481 (2011).

47. Kwong, R. W. M., Kumai, Y. & Perry, S. F. The Role of Aquaporin and Tight Junction Proteins in the Regulation of Water Movement in Larval Zebrafish (Danio rerio). *PLoS One* **8**, 70764 (2013).

48. Lin, L., Weng, C. & Hwang, P. Effects of Cortisol and Salinity Challenge on Water Balance in Developing Larvae of Tilapia (Oreochromis mossambicus). *Physiol. Biochem. Zool.* **73**, 283–289 (2002).

49. Singh, M., Sundar Barman, A., Devi, A. L., Devi, G. & Pandey, K. Iron mediated hematological, oxidative and histological alterations in freshwater fish Labeo rohita. *Ecotoxicol. Environ. Saf.* **170**, 87–97 (2019).

50. Van Anholt, R. D., Spanings, F. A. T., Knol, A. H., Van der Velden, J. A. & Wendelaar Bonga, S. E. Effects of iron sulfate dosage on the water flea (Daphnia magna Straus) and early development of carp (Cyprinus carpio L.). *Arch. Environ. Contam. Toxicol.* **42**, 182–192 (2002).

51. Andersen, Ø. Accumulation of waterborne iron and expression of ferritin and transferrin in early developmental stages of brown trout (Salmo trutta). *Fish Physiol. Biochem.* **16**, 223–231 (1997).

52. Dalzell, D. The toxicity of iron to brown trout and effects on the gills: a comparison of two grades of iron sulphate. *J. Fish Biol.* **55**, 301–315 (2002).

53. Milam, C. D. & Farris, J. L. Risk identification associated with iron-dominated mine discharges and their effect upon freshwater bivalves. *Environ. Toxicol. Chem.* **17**, 1611 (1998).

54. American Electric Power Service Corporation. *Reappraisal of the appropriateness of the iron water quality criterion in West Virginia.* (1983).

55. Dave, G. The influence of pH on the toxicity of aluminum, cadmium, and iron to eggs and larvae of the zebrafish, Brachydanio rerio. *Ecotoxicol. Environ. Saf.* **10**, 253–267 (1985).

56. Kremastinos, D. T. & Farmakis, D. Iron overload cardiomyopathy in clinical practice. *Circulation* **124**, 2253–2263 (2011).

57. Peuranen, S., Vuorinen, P. J., Vuorinen, M. & Hollender, A. The effects of iron, humic acids and low pH on the gills and physiology of Brown Trout (Salmo trutta). *Ann. Zool. Fenn.* **31**, 389–396 (1994).

58. Gonzalez, R. J., Grippo, R. S. & Dunson, W. A. The disruption of sodium balance in brook charr, Salvelinus fontinalis (Mitchill), by manganese and iron. *J. Fish Biol.* **37**, 765–774 (1990).

59. Dalzell, D. J. B. & MacFarlane, N. A. A. The toxicity of iron to brown trout and effects on the gills: A comparison of two grades of iron sulphate. *J. Fish Biol.* **55**, 301–315 (1999).

60. Grobler-Van Heerden, E., Van Vuren, J. H. J. & Du Preez, H. H. Bioconcentration of atrazine, zinc and iron in the blood of Tilapia sparrmanii (cichlidae). *Biochem. Physiot*

IOOC, 629–633 (1991).

61. Sykora, J. L., Smith, E. J., Synak, M. & Shapiro, M. A. Some observations on spawning of brook trout (Salvelinus Fontinalis, mitchill) in lime neutralized iron hydroxide suspensions. *Water Res.* **9**, 451–458 (1975).

62. Sykora, J. L., Smith, E. J. & Synak, M. Effect of lime neutralized iron hydroxide suspensions on juvenile brook trout (salvelinus fontinalis, mitchill). *Water Res.* **6**, 935–950 (1972).

63. Sinha, S., Gupta, M. & Chandra, P. Oxidative stress induced by iron in Hydrilla verticillata (l.f.) Royle: Response of antioxidants. *Ecotoxicol. Environ. Saf.* **38**, 286–291 (1997).

64. Aboul-Ela, H. M., Saad, A. A., El-Sikaily, A. M. A. & Zaghloul, T. I. Oxidative stress and DNA damage in relation to transition metals overload in Abu-Qir Bay, Egypt. *J. Genet. Eng. Biotechnol.* **9**, 51–58 (2011).

65. Sfakianakis, D. G., Renieri, E., Kentouri, M. & Tsatsakis, A. M. Effect of heavy metals on fish larvae deformities: A review. *Environ. Res.* **137**, 246–255 (2015).

66. van der Vorm, L. N. & Paw, B. H. Studying disorders of vertebrate iron and heme metabolism using zebrafish. *Methods Cell Biol.* **138**, 193–220 (2017).

67. Loréal, O., Cavey, T., Bardou-Jacquet, E., Guggenbuhl, P., Ropert, M. & Brissot, P. Iron, hepcidin, and the metal connection. *Front. Pharmacol.* **5**, 1–10 (2014).

68. Standat, H., Rorvik, K.-A. & Lien, H. Effects of Acute Iron Overload on Atlantic Salmon (Salmo salar) and Rainbow Trout. *Biol. Trace. Elem. Res.* **59**, 13–22 (1998).

69. Rouault, T. A. Iron metabolism in the CNS: Implications for neurodegenerative diseases. *Nat. Rev. Neurosci.* **14**, 551–564 (2013).

70. Aisen, P., Enns, C. & Wessling-Resnick, M. Chemistry and biology of eukaryotic iron metabolism. *Int. J. Biochem. Cell Biol.* **33**, 940–959 (2001).

71. Daher, R. & Karim, Z. Iron metabolism: State of the art Métabolisme du fer : état de l'art. *Transfus. Clin. Biol.* **24**, 115–119 (2017).

72. Biasiotto, G., Di Lorenzo, D., Archetti, S. & Zanella, I. Iron and Neurodegeneration: Is Ferritinophagy the Link? *Mol. Neurobiol.* **53**, 5542–5574 (2016).

73. Bresgen, N. & Eckl, P. M. Oxidative stress and the homeodynamics of iron metabolism. *Biomolecules* **5**, 808–847 (2015).

74. Bury, N. R. & Grosell, M. Waterborne iron acquisition by a freshwater teleost fish, zebrafish Danio rerio. *J. Exp. Biol.* **206**, 3529–3535 (2003).

75. Duck, K. A. & Connor, J. R. Iron uptake and transport across physiological barriers. *BioMetals* **29**, 573–591 (2016).

76. Moos, T. & Morgan, E. H. The metabolism of neuronal iron and its pathogenic role in neurological disease review. *Ann. NY. Acad. Sci.* **1012**, 14–26 (2004).

77. Morris, C. M., Candy, J. M., Keith, A. B., Oakley, A. E., Taylor, G. A., Pullen, R. G. L., Bloxhan, C. A., Gocht, A. & Edwardson, J. A. Brain iron homeostasis. *J. Inorg. Biochem.* **47**, 257–265 (1992).

78. Abbaspour, N., Hurrell, R. & Kelishadi, R. Review on iron and its importance for human health Review on iron and its importance for human health. *J. Res. Med. Sci.* **19**, 1–9 (2015).

79. Andrews, N. C. Molecular control of iron metabolism. *Best. Pract. Res. Clin. Haematol.* **18**, 159–169 (2005).

80. Wilkinson, N. & Pantopoulos, K. The IRP/IRE system in vivo: Insights from mouse models. *Front. Pharmacol.* **5**, 1–15 (2014).

81. Pantopoulos, K. Iron metabolism and the IRE/IRP regulatory system: an update. *Ann. N. Y. Acad. Sci.* **1012**, 1–13 (2004).

82. Bury, N. Iron acquisition by teleost fish. *Comp. Biochem. Physiol. Part C* **135**, 97–105 (2003).

83. Howe, D. ZFIN, the Zebrafish Model Organism Database: increased support for mutants and transgenics. *Nucleic Acids Res* (2013). Available at: https://wiki.zfin.org/display/general/ZFIN+db+information.

84. Donovan, A., Brownlie, A., Dorschner, M. O., Zhou, Y., Pratt, S. J., Paw, B. H., Phillips, R. B., Thisse, C., Thisse, B. & Zon, L. I. The zebrafish mutant gene chardonnay (cdy) encodes divalent metal transporter 1 (DMT1). *Blood* **100**, 4655–4659 (2002).

85. Zhao, L., Xia, Z. & Wang, F. Zebrafish in the sea of mineral (iron, zinc, and copper) metabolism. *Front. Pharmacol.* **5**, 1–23 (2014).

86. Donovan, A., Brownlie, A., Zhou, Y. & Shepard, J. Positional cloning of zebrafish ferroportin1 identiefies a conserved vertrebrate iron exporter. *Nature* **403**, 776–781 (2000).

87. Wingert, R. A., Brownlie, A., Galloway, J. L., Dooley, K., Fraenkel, P., Axe, J. L., Davidson, A. J., Barut, B., Noriega, L., Sheng, X., Zhou, Y. & Zon, L. I. The chianti zebrafish mutant provides a model for erythroid-specific disruption of transferrin receptor 1. *Development* **131**, 6225–6235 (2004).

88. Fraenkel, P. G., Gibert, Y., Holzheimer, J. L., Lattanzi, V. J., Burnett, S. F., Dooley, K. A., Wingert, R. A. & Zon, L. I. Transferrin-a modulates hepcidin expression in zebrafish embryos. *Blood* **113**, 2843–2850 (2009).

89. Scudiero, R., Trinchella, F., Riggio, M. & Parisi, E. Structure and expression of genes involved in transport and storage of iron in red-blooded and hemoglobin-less antarctic notothenioids. *Gene* **397**, 1–11 (2007).

90. Cooper, C. A., Handy, R. D. & Bury, N. R. The effects of dietary iron concentration on gastrointestinal and branchial assimilation of both iron and cadmium in zebrafish (Danio rerio). *Aquat. Toxicol.* **79**, 167–175 (2006).

91. Nakajima, H., Nakajima-Takaji, Y., Tsujita, T., Akiyama, S., Wakasa, T., Mukaigasa, K., Kaneko, H., Tamaru, Y., Yamamoto, M. & Kobayashi, M. Tissue-restricted expression of Nrf2 and its target genes in zebrafish with gene-specific variations in the induction profiles. *PLoS One* **6**, e26884 (2011).

92. Kwong, R. W. M., Hamilton, C. D. & Niyogi, S. Effects of elevated dietary iron on the gastrointestinal expression of Nramp genes and iron homeostasis in rainbow trout (Oncorhynchus mykiss). *Fish Physiol. Biochem.* **39**, 363–372 (2013).

93. Cooper, C. A. & Bury, N. R. The gills as an important uptake route for the essential nutrient iron in freshwater rainbow trout Oncorhynchus mykiss. *J. Fish Biol.* **71**, 115–128 (2007).

94. Munoz, M., Garcia-Erce, J. A. & Remacha, A. F. Disorders of iron metabolism. Part II: iron deficiency and iron overload. *J. Clin. Pathol.* **64**, 287–296 (2011).

95. Jomova, K. & Valko, M. Advances in metal-induced oxidative stress and human disease. *Toxicology* **283**, 65–87 (2011).

96. Espinosa-Diez, C., Miguel, V., Mennerich, D., Kietzmann, T., Sanchez-Perez, P., Cadenas, S. & Lamas, S. Antioxidant responses and cellular adjustments to oxidative stress. *Redox. Biol.* **6**, 183–197 (2015).

97. Rodriguez, C., Mayo, J. C., Sainz, R. M., Antolin, I., Herrera, F., Martin, V. & Reiter, R. J. Regulation of antioxidant enzymes: A significant role for melatonin. *J. Pineal. Res.* **36**, 1–9 (2004).

98. Livingstone, D. R. Contaminant-stimulated Reactive Oxygen Species Production and Oxidative Damage in Aquatic Organisms. *Mar. Pollut. Bull.* **42**, 656–666 (2001).

99. Andersen, H. H., Johnsen, K. B. & Moos, T. Iron deposits in the chronically inflamed central nervous system and contributes to neurodegeneration. *Cell. Mol. Life Sci.* **71**, 1607–1622 (2014).

100. Pisoschi, A. M. & Pop, A. The role of antioxidants in the chemistry of oxidative stress: A review. *Eur. J. Med. Chem.* **97**, 55–74 (2015).

101. Schieber, M. & Chandel, N. S. ROS function in redox signaling and oxidative stress. *Curr. Biol.* **24**, 453–462 (2014).

102. Wang, Y., Branicky, R., Noë, A. & Hekimi, S. Superoxide dismutases: Dual roles in controlling ROS damage and regulating ROS signaling. *J. Cell Biol.* **217**, 1915–1928 (2018).

103. Valavanidis, A., Vlahogianni, T., Dassenakis, M. & Scoullos, M. Molecular biomarkers of oxidative stress in aquatic organisms in relation to toxic environmental pollutants. *Ecotoxicol. Environ. Saf.* **64**, 178–189 (2006).

104. Stohs, S. J. & Bagchi, D. Oxidative mechanisms in the toxicity of metal ions. *Free. Radic. Biol. Med.* **18**, 321-336 (1995).

105. Ighodaro, O. M. & Akinloye, O. A. First line defence antioxidants-superoxide dismutase (SOD), catalase (CAT) and glutathione peroxidase (GPX): Their fundamental role in the entire antioxidant defence grid. *Alexandria J. Med.* **54**, 287–293 (2017).

106. Chiueh, C. C. Iron overload, oxidative stress, and axonal dystrophy in brain disorders. *Pediatr. Neurol.* **25**, 138–147 (2001).

107. Birben, E., Sahiner, U. M., Sackesen, C., Erzurum, S. & Kalayci, O. Oxidative stress and antioxidant defense. *World Allergy Organ. J.* **5**, 9–19 (2012).

108. Daniel, V. Glutathione s-transferases: Gene structure and regulation of expression. *Crit. Rev. Biochem. Mol. Biol.* **28**, 173–207 (1993).

109. Nguyen, T., Nioi, P. & Pickett, C. B. The Nrf2-antioxidant response element signaling pathway and its activation by oxidative stress. *J. Biol. Chem.* **284**, 13291–13295 (2009).

110. Hayes, J. D. & Dinkova-Kostova, A. T. The Nrf2 regulatory network provides an interface between redox and intermediary metabolism. *Trends Biochem. Sci.* **39**, 199–218 (2014).

111. Matés, J. M. Effects of antioxidant enzymes in the molecular control of reactive oxygen species toxicology. *Toxicology* **153**, 83-104 (2000).

112. Hauser-davis, R. A., Campos, R. C. De & Ziolli, R. L. Reviews of Environmental Contamination and Toxicology. **218**, 101–124 (2012).

113. Kim, G. H., Kim, J. E., Rhie, S. J. & Yoon, S. The Role of Oxidative Stress in Neurodegenerative Diseases. *Exp. Neurobiol.* **24**, 325–340 (2015).

114. Culotta, V. C., Yang, M. & O'Halloran, T. V. Activation of superoxide dismutases: Putting the metal to the pedal. *Biochim. Biophys. Acta.* **1763**, 747–758 (2006).

115. Glorieux, C., Zamocky, M., Sandoval, J. M., Verrax, J. & Calderon, P. B. Regulation of catalase expression in healthy and cancerous cells. *Free. Radic. Biol. Med.* **87**, 84–97 (2015).

116. Tonelli, C., Chio, I. I. C. & Tuveson, D. A. Transcriptional Regulation by Nrf2. *Antioxid. Redox Signal.* **29**, 1727–1745 (2017).

117. Sies, H. On the history of oxidative stress: Concept and some aspects of current development. *Curr. Opin. Toxicol.* **7**, 122–126 (2018).

118. Tjalkens, R. B., Valerio, L. G., Awasthi, Y. C. & Petersen, D. R. Association of glutathione S-transferase isozyme-specific induction and lipid peroxidation in two inbred strains of mice subjected to chronic dietary iron overload. *Toxicol. Appl. Pharmacol.* **151**, 174–181 (1998).

119. Glisic, B., Mihaljevic, I., Popovic, M., Zaja, R., Loncar, J., Fent, K., Kovacevic, R. & Smital, T. Characterization of glutathione-S-transferases in zebrafish (Danio rerio). *Aquat. Toxicol.* **158**, 50–62 (2015).

120. Padmini, E. & Rani, U. Evaluation of oxidative stress biomarkers in hepatocytes of grey mullet inhabiting natural and polluted estuaries. *Sci. Total Environ.* **407**, 4533–4541 (2009).

121. Carvalho, C. dos S., Bernusso, V. A., Araújo, H. S. S. de, Espíndola, E. L. G. & Fernandes, M. N. Biomarker responses as indication of contaminant effects in Oreochromis niloticus. *Chemosphere* **89**, 60–69 (2012).

122. Allocati, N., Masulli, M., Di Ilio, C. & Federici, L. Glutathione transferases: Substrates, inihibitors and pro-drugs in cancer and neurodegenerative diseases. *Oncogenesis* **7**, 8 (2018).

123. Marinho, H. S., Real, C., Cyrne, L., Soares, H. & Antunes, F. Hydrogen peroxide sensing, signaling and regulation of transcription factors. *Redox Biol.* **2**, 535–562 (2014).

124. Urrutia, P. J., Mena, N. P. & Núñez, M. T. The interplay between iron accumulation, mitochondrial dysfunction, and inflammation during the execution step of neurodegenerative disorders. *Front. Pharmacol.* **5**, 1–12 (2014).

125. Miao, L. & St. Clair, D. K. Regulation of superoxide dismutase genes: Implications in disease. *Free. Radic. Biol. Med.* **47**, 344–356 (2009).

126. Ma, Q. & He, X. Molecular Basis of Electrophilic and Oxidative Defense: Promises and

Perils of Nrf2. *Pharmacol. Rev.* **64**, 1055–1081 (2012).

127. Blaser, H., Dostert, C., Mak, T. W. & Brenner, D. TNF and ROS Crosstalk in Inflammation. *Trends Cell Biol.* **26**, 249–261 (2016).

128. Raghunath, A., Sundarraj, K., Nagarajan, R., Arfuso, F., Bian, J., Kumar, A. P., Sethi, G. & Perumal, E. Antioxidant response elements: Discovery, classes, regulation and potential applications. *Redox Biology* **17**, 297–314 (2018).

129. Hahn, M. E., Timme-Laragy, A. R., Karchner, S. I. & Stegeman, J. J. Nrf2 and Nrf2-related proteins in development and developmental toxicity: Insights from studies in zebrafish (Danio rerio). *Free. Radic. Biol. Med.* **88**, 275–289 (2015).

130. Suzuki, T., Takagi, Y., Osanai, H., Ll, L., Takeuchi, M., Katoh, Y., Kobayashi, M. & Yamamoto, M. Pi class glutathione S-transferase genes are regulated by Nrf 2 through an evolutionarily conserved regulatory element in zebrafish. *Biochem. J.* **388**, 65–73 (2005).

131. Rageb, A. & Matkovics, B. Effects of metal ions on the antioxidant enzyme activities, protein contents and lipid peroxidation of carp tissues. Comp. *Biochem. Physiol* **9**, 69–72 (1988).

132. Olivari, F. A., Hernández, P. P. & Allende, M. L. Acute copper exposure induces oxidative stress and cell death in lateral line hair cells of zebrafish larvae. *Brain Res.* **1244**, 1–12 (2008).

133. Fitsanakis, V. A., Zhang, N., Garcia, S. & Aschner, M. Manganese (Mn) and iron (Fe): Interdependency of transport and regulation. *Neurotox. Res.* **18**, 124–131 (2010).

134. Gunshin, H., Mackenzie, B., Berger, U. V., Gunshin, Y., Boron, W. F., Nussberger, S., Gollan, J. L. & Hediger, M. A. Cloning and characterization of a mammalian proton-coupled metal-ion transporter. *Nature* **388**, 482–488 (1997).

135. Kwong, R. W. M. & Niyogi, S. The interactions of iron with other divalent metals in the intestinal tract of a freshwater teleost, rainbow trout (Oncorhynchus mykiss). *Comp. Biochem. Physiol. Part C* **150**, 442–449 (2009).

136. Ye, Q., Park, J. E., Gugnani, K., Betharia, S., Pino-Figueroa, A. & Kim, J. Influence of iron metabolism on manganese transport and toxicity. *Metallomics* **9**, 1028–1046 (2017).

137. Troadec, M. B., Ward, D. M., Lo, E., Kaplan, J. & De Domenico, I. Induction of FPN1 transcription by MTF-1 reveals a role for ferroportin in transition metal efflux. *Blood* **116**, 4657–4664 (2010).

138. Yin, Z., Jiang, H., Lee, E-S.Y., Ni, M., Erikson, K. M., Milatovic, D., Bowman, A. B. & Aschner, M. Ferroportin is a manganese-responsive protein that decreases manganese cytotoxicity and accumulation. *J. Neurochem.* **6**, 1249–1254 (2009).

139. Mitchell, C. J., Shawki, A., Ganz, T., Nemeth, E. & Mackenzie, B. Functional properties of human ferroportin, a cellular iron exporter reactive also with cobalt and zinc. *Am. J. Physiol. Cell. Physiol.* **306**, C450–C459 (2014).

140. Chung, J., Haile, D. J. & Wessling-Resnick, M. Copper-induced ferroportin-1 expression in J774 macrophages is associated with increased iron efflux. *Proc. Natl. Acad. Sci.* **101**, 2700–2705 (2004).

141. Wang, X., Miller, D. S. & Zheng, W. Intracellular localization and subsequent redistribution of metal transporters in a rat choroid plexus model following exposure to manganese or iron. *Toxicol. Appl. Pharmacol.* **230**, 167–174 (2008).

142. Tipping, E., Rey-Castro, C., Bryan, S. E. & Hamilton-Taylor, J. Al(III) and Fe(III) binding by humic substances in freshwaters, and implications for trace metal speciation. *Geochim. Cosmochim. Acta* **66**, 3211–3224 (2002).

143. Kwong, R. W. M. & Niyogi, S. An in vitro examination of intestinal iron absorption in a freshwater teleost, rainbow trout (Oncorhynchus mykiss). *J. Comp. Physiol. B Biochem. Syst. Environ. Physiol.* **178**, 963–975 (2008).

144. Wepener, V., Vuren, J. H. J. Van & Preez, H. H. Du. Effect of Manganese and Iron at a Neutral and Acidic pH (Tilapia sparrmanii). *Environ. Contam. Toxicol.* **49**, 613–619 (1992).

145. Subhash Peter, M. C., Leji, J., Rejitha, V., Ignatius, J. & Peter, V. S. Physiological responses of African catfish (Clarias gariepinus) to water-borne ferric iron: Effects on thyroidal, metabolic and hydromineral regulations. *J Endocrinol Reprod* **12**, 24–30 (2008).

146. Lappivaara, J. & Marttinen, S. Effects of waterborne iron overload and simulated winter conditions on acute physiological stress response of whitefish, Coregonus lavaretus. *Ecotoxicol. Environ. Saf.* **60**, 157–168 (2005).

147. Li, H., Zou, Q., Wu, Y., Fu., J., Wang, T. & Jiang, G. Effects of waterborne nano-iron on medaka (Oryzias latipes): Antioxidant enzymatic activity, lipid peroxidation and histopathology. *Ecotoxicol. Environ. Saf.* **72**, 684–692 (2009).

148. Núñez, M. T. & Hidalgo, C. Noxious iron–calcium connections in neurodegeneration. *Front. Neurosci.* **13**, 1-18 (2019).

149. Jia, F., Song, N., Wang, W., Du, X., Chi, Y. & Jiang, H. High dietary iron supplement induces the nigrostriatal dopaminergic neurons lesion in transgenic mice expressing mutant A53T human alpha-synuclein. *Front. Aging Neurosci.* **10**, 1–9 (2018).

150. Dias, V., Junn, E. & Mouradian, M. M. The role of oxidative stress in Parkinson's disease. *J. Parkinsons. Dis.* **3**, 461–91 (2013).

151. Kim, J. & Wessling-Resnick, M. Iron and mechanisms of emotional behavior. *J. Nutr. Biochem.* **25**, 1101–1107 (2014).

152. Sipe, J. C., Lee, P. & Beutler, E. Brain iron metabolism and neurodegenerative disorders. *Dev. Neurosci.* **24**, 188–196 (2002).

153. Guo, J., Zhao, X., Li, Y., Li, G. & Liu, X. Damage to dopaminergic neurons by oxidative stress in Parkinson's disease (Review). *Int. J. Mol. Med.* **41**, 1817–1825 (2018).

154. Carocci, A., Catalano, A., Sinicropi, M. S. & Genchi, G. Oxidative stress and neurodegeneration: the involvement of iron. *BioMetals* **31**, 715–735 (2018).

155. Benarroch, E. E. Brain iron homeostasis and neurodegenerative disease. *Am. Acad. Neurol.* **72**, 1436–1440 (2009).

156. Hare, D. J., Arora, M., Jenkins, N. L., Finkelstein, D. I., Doble, P. A. & Bush, A. I. Is early-life iron exposure critical in neurodegeneration? *Nat. Rev. Neurol.* **11**, 536–544 (2015).

157. Kaur, D., Peng, J., Chinta, S. J., Rajagopalan, S., Di Monte, D. A., Cherney, R. A. &

Andersen, J. K. Increased murine neonatal iron intake results in Parkinson-like neurodegeneration with age. *Neurobiol. Aging* **28**, 907–913 (2007).

158. De Lima, M. N. M., Polydoro, M., Laranja, D. C., Bonatto, F., Bromberg, E., Moreira, J. C. F., Dal-Pizzol, F. & Schroder, N. Recognition memory impairment and brain oxidative stress induced by postnatal iron administration. *Eur. J. Neurosci.* **21**, 2521–2528 (2005).

159. Moos, T. & Morgan, E. H. The metabolism of neuronal iron and its pathogenic role in neurological disease review. *Ann. NY. Acad. Sci.* **1012**, 14–26 (2004).

160. Saunders, N. R., Liddelow, S. A. & Dziegielewska, K. M. Barrier mechanisms in the developing brain. *Front. Pharmacol.* **3 MAR**, 1–18 (2012).

161. Siddappa, A. J. M., Rao, R. B., Wobken, J. D., Leibold, E. A., Connoer, J. R. & Georgieff, M. K. Developmental changes in the expression of iron regulatory proteins and iron transport proteins in the perinatal rat brain. *J. Neurosci. Res.* **68**, 761–775 (2002).

162. Baxter, P. S. & Hardingham, G. E. Adaptive regulation of the brain's antioxidant defences by neurons and astrocytes. *Free Radic. Biol. Med.* **100**, 147–152 (2016).

163. Piloni, N. E., Perazzo, J. C., Fernandez, V., Videla, L. A. & Puntarulo, S. Sub-chronic iron overload triggers oxidative stress development in rat brain: Implications for cell protection. *BioMetals* **29**, 119–130 (2016).

164. Acikyol, B., Graham, R. M., Trinder, D., House, M. J., Olynyk, J. K., Scoett, R. J., Milward, E. A. & Johnstone, D. M. Brain transcriptome perturbations in the transferrin receptor 2 mutant mouse support the case for brain changes in iron loading disorders, including effects relating to long-term depression and long-term potentiation. *Neuroscience* **235**, 119–128 (2013).

165. Piñero, D. J., Li, N.-Q., Connor, J. R. & Beard, J. L. Variations in Dietary Iron Alter Brain Iron Metabolism in Developing Rats. *J. Nutr.* **130**, 254–263 (2018).

166. Sobotka, T. J., Whitaker, P., Sobotka, J. M., Brodie, R. E., Quander, D. Y., Robi, M., Bryant., M. & Barton, C. N. Neurobehavioral Dysfunctions Associated With Dietary Iron Overload. *Physiol. Behav.* **59**, 213–219 (1996).

167. Fredriksson, A., Eriksson, P. & Archer, T. Postnatal iron-induced motor behaviour alterations following chronic neuroleptic administration in mice. *J. Neural Transm.* **113**, 137–150 (2005).

168. Du, F., Qian, Z. M., Luo, Q., Yung, W. H. & Ke, Y. Hepcidin Suppresses Brain Iron Accumulation by Downregulating Iron Transport Proteins in Iron-Overloaded Rats. *Mol. Neurobiol.* **52**, 101–114 (2015).

169. Nandar, W. & Connor, J. R. HFE Gene Variants Affect Iron in the Brain. *J. Nutr.* **141**, 729S-739S (2011).

170. Dornelles, A. S., Garcia, V. A., de Lima, M. N. M., Vedana, G., Alcade, L. A., Bogo, M. R. & Schroder, N. mRNA expression of proteins involved in iron homeostasis in brain regions is altered by age and by iron overloading in the neonatal period. *Neurochem. Res.* **35**, 564–571 (2010).

171. Erikson, K. M., Pinero, D. J., Connor, J. R. & Beard, J. L. Regional Brain Iron, Ferritin and Transferrin Concentrations during Iron Deficiency and Iron Repletion in Developing Rats. *J. Nutr.* **127**, 2030–2038 (2018).

172. Maaroufi, K., Ammari, M., Jeljeli, M., Roy, V., Sakly, M. & Abdelmalek, H. Impairment of emotional behavior and spatial learning in adult Wistar rats by ferrous sulfate. *Physiol. Behav.* **96**, 343–349 (2009).

173. Fredriksson, A., Schröder, N., Eriksson, P., Izquierdo, I. & Archer, T. Maze learning and motor activity deficits in adult mice induced by iron exposure during a critical postnatal period. *Dev. Brain Res.* **119**, 65–74 (2000).

174. Lozoff, B., Castillo, M., Clark, K. M. & Smith, J. B. Iron-fortified vs low-iron infant formula: Developmental outcome at 10 years. *Arch. Pediatr. Adolesc. Med.* **166**, 208–215 (2012).

175. Babić, S., Barišić, J., Višić., H., Sauerborn Klobučar, R., Topić Popović, N., Strunjak-Perović, I., Čož-Rakovac, R. & Klobučar, G. Embryotoxic and genotoxic effects of sewage effluents in zebrafish embryo using multiple endpoint testing. *Water Res.* **115**, 9–21 (2017).

176. Li, C., Chen, Q., Zhang, X., Snyder, S. A., Gong, Z. & Lam, S. H. An integrated approach with the zebrafish model for biomonitoring of municipal wastewater effluent and receiving waters. *Water Res.* **131**, 33–44 (2018).

177. Dubińska-Magiera, M., Daczewska, M., Lewicka, A., Migocka-Patrzalek, M., Niedbalska-Tarnowska, J. & Jalga, K. Zebrafish: A model for the study of toxicants affecting muscle development and function. *Int. J. Mol. Sci.* **17**, 1-22 (2016).

178. Bambino, K. & Chu, J. Zebrafish in Toxicology and Environmental Health. in *Curr. Top. Dev. Biol.* **124**, 331–367 (2017).

179. Wang, X., DOng, Q., Chen, Y., Jiang, H., Xiao, Q., Wang, Y., Li, W., Bai, C., Huang, C. & Yang, D. Bisphenol A affects axonal growth, musculature and motor behavior in developing zebrafish. *Aquat. Toxicol.* **142**–**143**, 104–113 (2013).

180. Lee, J. & Freeman, J. Zebrafish as a Model for Developmental Neurotoxicity Assessment: The Application of the Zebrafish in Defining the Effects of Arsenic, Methylmercury, or Lead on Early Neurodevelopment. *Toxics* **2**, 464–495 (2014).

181. De Esch, C., Slieker, R., Wolterbeek, A., Woutersen, R. & de Groot, D. Zebrafish as potential model for developmental neurotoxicity testing. A mini review. *Neurotoxicol. Teratol.* **34**, 545–553 (2012).

182. Zhang, W., Xu., J., Qiu, J., Xing, C., Li, X., Leng, B., Su, Y., Lin, J., Lin, J., Mei, X., Huang., Y., Pan, Y. & Xue, Y. Novel and rapid osteoporosis model established in zebrafish using high iron stress. *Biochem. Biophys. Res. Commun.* **496**, 654–660 (2018).

183. Nasrallah, G. K., Younes, N. N., Baji, M. H., Shraim, A. M. & Mustafa, I. Zebrafish larvae as a model to demonstrate secondary iron overload. *Eur. J. Haematol.* 1–8 (2018). doi:10.1111/ejh.13035

184. Chen, B., Yuan, Y-L., Liu, C., Bo, L., Li, G-F., Wang, H. & Xu, Y-J. Therapeutic effect of deferoxamine on iron overload-induced inhibition of osteogenesis in a zebrafish model. *Calcif. Tissue Int.* **94**, 353–360 (2014).

185. Sant'Anna, M. C. B., Soares, V. D. M., Seibt, K. J., Ghisleni, G., Rico, E. P., Rosemberg, D. B., de Oliveira, J. R., Schroder, N., Bonan, C. D. & Bogo, M. R. Iron exposure modifies acetylcholinesterase activity in zebrafish (Danio rerio) tissues: Distinct susceptibility of tissues to iron overload. *Fish Physiol. Biochem.* **37**, 573–581 (2011).

186. De Domenico, I., Vaughn, M. B., Yoon, D., Kushner, J. P., Ward, D. M, & Kaplan, J. Zebrafish as a model for defining the functional impact of mammalian ferroportin mutations. *Blood* **110**, 3780–3783 (2007).

187. Lumsden, A. L., Henshall, T. L., Dayan, S., Lardelli, M. T. & Richards, R. I. Huntingtin-deficient zebrafish exhibit defects in iron utilization and development. *Hum. Mol. Genet.* **16**, 1905–1920 (2007).

188. Legradi, J., el Abdellaoui, N., van Pomeren, M. & Legler, J. Comparability of behavioural assays using zebrafish larvae to assess neurotoxicity. *Environ. Sci. Pollut. Res.* **22**, 16277–16289 (2014).

189. Garcia, G. R., Noyes, P. D. & Tanguay, R. L. Advancements in zebrafish applications for 21st century toxicology. *Pharmacol. Ther.* **161**, 11–21 (2016).

190. Kizil, C., Kaslin, J., Kroehne, V. & Brand, M. Adult neurogenesis and brain regeneration in zebrafish. *Dev. Neurobiol.* **72**, 429–461 (2012).

191. Gujja, P., Rosing, D. R., Tripodi, D. J. & Shizukuda, Y. Iron overload cardiomyopathy: better understanding of an increasing disorder. *J. Am. Coll. Cardiol.* **56**, 1001–12 (2010).

192. Fleming, A., Diekmann, H. & Goldsmith, P. Functional Characterisation of the Maturation of the Blood-Brain Barrier in Larval Zebrafish. *PLoS One* **8**, e77548 (2013).

193. Jeong, J.-Y., Kwon, H.-B, Ahn, J.-C., Kang, D., Kwon, S.-H., Park, J.-A. & Kim, K. W. Functional and developmental analysis of the blood-brain barrier in zebrafish. *Brain Res. Bull.* **75**, 619–628 (2008).

194. Vargas, R. & Ponce-Canchihuamán, J. Emerging various environmental threats to brain and overview of surveillance system with zebrafish model. *Toxicol. Reports* **4**, 467–473 (2017).

195. Ali, S., Champagne, D. L., Spaink, H. P. & Richardson, M. K. Zebrafish embryos and larvae: A new generation of disease models and drug screens. *Birth Defects. Res. C. Embryo. Today.* **93**, 115–133 (2011).

196. He, J. H., Gao, J. M., Huang, C. J. & Li, C. Q. Zebrafish models for assessing developmental and reproductive toxicity. *Neurotoxicol. Teratol.* **42**, 35–42 (2014).

197. Yin, J., Wang, A.-P., Li, W.-F., Shi, R., Jin, H.-T. & Wei, J.-F. Time-response characteristic and potential biomarker identification of heavy metal induced toxicity in zebrafish. *Fish Shellfish Immunol.* **72**, 309–317 (2018).

198. Kwong, R. W. M., Kumai, Y. & Perry, S. F. The physiology of fish at low pH: the zebrafish as a model system. *J. Exp. Biol.* **217**, 651-662 (2014).

199. Norton, W. H. J. Measuring Larval Zebrafish Behavior: Locomotion, Thigmotaxis, and Startle. in 3–20 (Humana Press, Totowa, NJ, 2012). doi:10.1007/978-1-61779-597-8_1

200. Ingebretson, J. J. & Masino, M. A. Quantification of locomotor activity in larval zebrafish: considerations for the design of high-throughput behavioral studies. *Front. Neural Circuits* **7**, 1–9 (2013).

201. Colwill, R. M. & Creton, R. Locomotor behaviors in zebrafish (Danio rerio) larvae. *Behav. Processes* **86**, 222–229 (2011).

202. Padilla, S., Hunter, D. L., Padnos, B., Frady, S. & MacPhail, R. C. Assessing locomotor

activity in larval zebrafish: Influence of extrinsic and intrinsic variables. *Neurotoxicol. Teratol.* **33**, 624–630 (2011).

203. Farrell, T. C., Cario, C. L., Milanese, C., Vogt, A., Jeong, J.-H. & Burton, E. A. Evaluation of spontaneous propulsive movement as a screening tool to detect rescue of Parkinsonism phenotypes in zebrafish models. *Neurobiol. Dis.* **44**, 9–18 (2011).

204. Walz, W. *Zebrafish Protocols for Neurobehavioral Research*. (Humana Press, Totowa, NJ, 2012).

205. MacPhail, R. C., Brooks, J., Hunter, D. L., Padnos, B., Irons, T. D. & Padilla, S. Locomotion in larval zebrafish: Influence of time of day, lighting and ethanol. *Neurotoxicology* **30**, 52–58 (2009).

206. Schnörr, S. J., Steenbergen, P. J., Richardson, M. K. & Champagne, D. L. Measuring thigmotaxis in larval zebrafish. *Behav. Brain Res.* **228**, 367–374 (2012).

207. Mugoni, V., Camporeale, A. & Santoro, M. M. Analysis of Oxidative Stress in Zebrafish Embryos. *J. Vis. Exp.* 1–11 (2014). doi:10.3791/51328

208. Pelka, K. E., Henn, K., Keck, A., Sapel, B. & Braunbeck, T. Size does matter – Determination of the critical molecular size for the uptake of chemicals across the chorion of zebrafish (Danio rerio) embryos. *Aquat. Toxicol.* **185**, 1–10 (2017).

209. Van Den Bos, R., Mes, W., Galligani, P., Hell, A., Zethof, J., Flik, G. & Gorissen, M. Further characterisation of differences between TL and AB Zebrafish (Danio rerio): Gene expression, physiology and behaviour at day 5 of the larval stage. *PLoS One* **12**, e0175420 (2017).

210. Gellert, G. Effect of age on the susceptibility of zebrafish eggs to industrial wastewater. *Water Res.* **35**, 3754–3757 (2002).

211. Böhme, S., Baccaro, M., Schmidt, M., Potthoff, A., Stark, H-.J., Reemtsma, T. & Kuhnet, D. Metal uptake and distribution in the zebrafish (: Danio rerio) embryo: Differences between nanoparticles and metal ions. *Environ. Sci. Nano* **4**, 1005–1015 (2017).

212. Kim, K.-T. & Tanguay, R. L. The role of chorion on toxicity of silver nanoparticles in the embryonic zebrafish assay. *Environ. Health Toxicol.* **29**, e2014021 (2014).

213. Ozoh, P. T. E. Effects of Reversible Incubations of Zebrafish Eggs in Copper and Lead Ions with or without Shell Membranes. *Bull. Environm. Contain. Toxicol* **24**, 270–275 (1980).

214. Braunbeck, T., Bottcher, M., Hollert, H., Kosmehl, T., Lammer, E., Leist, E., Rudolf, M. & Seitz, N. Towards an alternative for the acute fish LC(50) test in chemical assessment: the fish embryo toxicity test goes multi-species -- an update. *ALTEX* **22**, 87–102 (2005).

215. Bray, R. T. & Fitobór, K. Sizes of iron hydroxide particles formed during ferric coagulation processes. in *Desalin. Water. Treat.* **64**, 419–424 (2017).

216. Garcia, G. R., Noyes, P. D. & Tanguay, R. L. Advancements in zebrafish applications for 21st century toxicology. *Pharmacol. Ther.* **161**, 11–21 (2016).

217. Kamel, M. & Ninov, N. Catching new targets in metabolic disease with a zebrafish. *Curr. Opin. Pharmacol.* **37**, 41–50 (2017).

218. Kimmel, C. B., Ballard, W. W., Kimmel, S. R., Ullmann, B. & Schilling, T. F. Stages of

embryonic development of the zebrafish. *Dev. Dyn.* **203**, 253–310 (1995).

219. Wallace, K. N., Akhter, S., Smith, E. M., Lorent, K. & Pack, M. Intestinal growth and differentiation in zebrafish. *Mech. Dev.* **122**, 157–173 (2005).

220. Wallace, K. N. & Pack, M. Unique and conserved aspects of gut development in zebrafish. *Dev. Biol.* **255**, 12–29 (2003).

221. Nishimura, Y., Inoue, A., Sasagawa, S., Koiwa, J., Kawaguchi, K., Kawase, R., Maruyama, T., Kim, S. & Tanaka, T. Using zebrafish in systems toxicology for developmental toxicity testing. *Congenit. Anom.* **56**, 18–27 (2016).

222. Garrick, M. D., Dolan, K. G., Horbinski, C., Ghio, A. J., Higgins, D., Porubcin, M., Moore, E. G., Hainsworth, L. N., Umbreit, J. N., Conrad, M. E., Feng, L., Lis, A., Roth, J. A., Singleton, S. & Garrick, L. M. DMT1: A mammalian transporter for multiple metals. *BioMetals* **16**, 41–54 (2003).

223. De Domenico, I., Ward, D. M. & Kaplan, J. Hepcidin and ferroportin: The new players in iron metabolism. *Semin. Liver Dis.* **31**, 272–279 (2011).

224. Neves, J. V., Ramos, M. F., Moreira, A. C., Silva, T., Gomes, M. S. & Rodrigues, P. N. S. Hamp1 but not Hamp2 regulates ferroportin in fish with two functionally distinct hepcidin types. *Sci. Rep.* **7**, 14793 (2017).

225. Drakesmith, H., Nemeth, E. & Ganz, T. Ironing out Ferroportin. *Cell Metab.* **22**, 777–787 (2015).

226. Chen, H., Su, T., Attieh, Z. K., Fox, T. C., McKie, A. T., Anderson, G. J. & Vulpe, C. D. Systemic regulation of Hephaestin and Ireg1 revealed in studies of genetic and nutritional iron deficiency. *Blood* **102**, 1893–1899 (2003).

227. Zhang, D.-L., Hughes, R. M., Ollivierre-Wilson, H., Ghosh, M. C. & Rouault, T. A. A ferroportin transcript that lacks an iron-responsive element enables duodenal and erythroid precursor cells to evade translational repression. *Cell Metab.* **9**, 461–473 (2009).

228. Ward, D. M. & Kaplan, J. Ferroportin-mediated iron transport: Expression and regulation. *Biochim. Biophys. Acta - Mol. Cell Res.* **1823**, 1426–1433 (2012).

229. Lee, P. L. & Beutler, E. Regulation of Hepcidin and Iron-Overload Disease. *Annu. Rev. Pathol. Mech. Dis.* **4**, 489–515 (2009).

230. Fraenkel, P. G., Traver, D., Donovan, A., Zahrieh, D. & Zon, L. I. Ferroportin1 is required for normal iron cycling in zebrafish. *J. Clin. Invest.* **115**, 1532–1541 (2005).

231. Kerins, M. J. & Ooi, A. The roles of NRF2 in modulating cellular iron homeostasis. *Antioxid. Redox Signal.* **29**, 1756-1773 (2017). doi:10.1089/ars.2017.7176

232. Torti, F. M. & Torti, S. V. Regulation of ferritin genes and protein. *World Health* **99**, 3505–3516 (2008).

233. Zahringer, J., Baliga, B. S. & Munro, H. N. Novel mechanism for translational control in regulation of ferritin synthesis by iron. *Proc. Natl. Acad. Sci.* **73**, 857–861 (2006).

234. Zecca, L., Stroppolo, A., Gatti, A., Tampellini, D., Toscani, M., Gallorini, M., Giaveri, G., Arosio, P., Santambrogio, P., Fariello, R. G., Karatekin, E., Kleinman, M. H., Turro, N., Hornykiewicz, O. & Zucca, F. A. The role of iron and copper molecules in the neuronal

vulnerability of locus coeruleus and substantia nigra during aging. *Proc. Natl. Acad. Sci.* **101**, 9843–9848 (2004).

235. Piloni, N. E., Reiteri, M., Hernando, M. P., Cervino, C. O. & Puntarulo, S. Differential Effect of Acute Iron Overload on Oxidative Status and Antioxidant Content in Regions of Rat Brain. *Toxicol. Pathol.* **45**, 1067–1076 (2017).

236. Franklin, N. M., Glover, C. N., Nicol, J. A. & Wood, C. M. Calcium/cadmium interactions at uptake surfaces in rainbow trout: Waterborne versus dietary routes of exposure. *Environ. Toxicol. Chem.* **24**, 2954–2964 (2005).

237. Loro, V. L., Nogueira, L., Nadella, S. R. & Wood, C. M. Zinc bioaccumulation and ionoregulatory impacts in Fundulus heteroclitus exposed to sublethal waterborne zinc at different salinities. *Comp. Biochem. Physiol. Part - C Toxicol. Pharmacol.* **166**, 96–104 (2014).

238. Harley, R. Ion transport physiology and its interaction with trace element accumulation and toxicity in inanga (Galaxias maculatus). (2015).

239. Hwang, P. P. & Chou, M. Y. Zebrafish as an animal model to study ion homeostasis. *Pflugers Arch. Eur. J. Physiol.* **465**, 1233–1247 (2013).

240. Chen, P., Chakraborty, S., Mukopadhyay, S., Lee, E., Paoliello, M. M. B., Bowman, A. B. & Aschner, M. Manganese Homeostasis in the Nervous System. *J. Neurochem.* **17**, 1310–1314 (2012).

241. Choi, E. K., Nguyen, T. T., Iwase, S. & Seo, Y. A. Ferroportin disease mutations influence manganese accumulation and cytotoxicity. *FASEB J.* **33**, 2228–2240 (2019).

242. Seo, Y. A. & Wessling-Resnick, M. Ferroportin deficiency impairs manganese metabolism in flatiron mice. *FASEB J.* **29**, 2726–33 (2015).

243. Jin, L., Frazer, D. M., Lu, Y., Wilkins, S. J., Ayton, S., Bush, A. & Anderson, G. J. Mice overexpressing hepcidin suggest ferroportin does not play a major role in Mn homeostasis. *Metallomics* 1–9 (2019). doi:10.1039/c8mt00370j

244. Mitchell, C. J., Shawki, A., Ganz, T., Nemeth, E. & Mackenzie, B. Functional properties of human ferroportin, a cellular iron exporter reactive also with cobalt and zinc. *Am. J. Physiol. Cell. Physiol.* **306**, C450–C459 (2013).

245. Xia, Z., Wei, J., Li, Y., Wang, J., Li, W., Wang, K., Hong, X., Zhao, L., Chen, C., Min, J. & Wang, F. Zebrafish slc30a10 deficiency revealed a novel compensatory mechanism of Atp2c1 in maintaining manganese homeostasis. *PLoS Genet.* **13**, 1–29 (2017).

246. Vayenas, D. V, Repanti, M., Vassilopoulos, A. & Papanastasiou, D. A. Influence of iron overload on manganese, zinc, and copper concentration in rat tissues in vivo: study of liver, spleen, and brain. *Int J Clin Lab Res* **28**, 183–186 (1998).

247. Sousa, L., Pessoa, M. T. C., Costa, T. G. F., Cortes, V. F., Santos, H. L. & Barbosa, L. A. Iron overload impact on P-ATPases. *Ann. Hematol.* **97**, 377–385 (2018).

248. Khamseekaew, J., Kumfu, S., Chattipakorn, S. C. & Chattipakorn, N. Effects of Iron Overload on Cardiac Calcium Regulation: Translational Insights Into Mechanisms and Management of a Global Epidemic. *Can. J. Cardiol.* **32**, 1009–1016 (2016).

249. Liu, R., Lin, S., Rallo, R., Zhao, Y., Damoiseaux, R., Xia, T., Lin, S., Nel, A. & Cohen, Y.

Automated phenotype recognition for zebrafish embryo based in vivo high throughput toxicity screening of engineered nano-materials. *PLoS One* **7**, e35014 (2012).

250. Hill, A. J., Teraoka, H., Heideman, W. & Peterson, R. E. Zebrafish as a model vertebrate for investigating chemical toxicity. *Toxicol. Sci.* **86**, 6–19 (2005).

251. Jezierska, B., Ługowska, K. & Witeska, M. The effects of heavy metals on embryonic development of fish (a review). *Fish Physiol. Biochem.* **35**, 625–640 (2009).

252. Fraysse, B., Mons, R. & Garric, J. Development of a zebrafish 4-day embryo-larval bioassay to assess toxicity of chemicals. *Ecotoxicol. Environ. Saf.* **63**, 253–267 (2006).

253. Jin, Y., Liu, Z., Liu, F., Ye, Y., Peng, Tao. & Fu. Z. Embryonic exposure to cadmium (II) and chromium (VI) induce behavioral alterations, oxidative stress and immunotoxicity in zebrafish (Danio rerio). *Neurotoxicol. Teratol.* **48**, 9–17 (2015).

254. Zhang, Q. F., Li, Y. W., Liu, Z. H. & Chen, Q. L. Exposure to mercuric chloride induces developmental damage, oxidative stress and immunotoxicity in zebrafish embryos-larvae. *Aquat. Toxicol.* **181**, 76–85 (2016).

255. Brown, D., Samsa, L., Qian, L. & Liu, J. Advances in the Study of Heart Development and Disease Using Zebrafish. *J. Cardiovasc. Dev. Dis.* **3**, 13 (2016).

256. Hu, N., Sedmera, D., Yost, H. J. & Clark, E. B. Developing Zebrafish Heart. *Anat. Rec.* **157**, 148–157 (2000).

257. Keßler, M., Just, S. & Rottbauer, W. Ion flux dependent and independent functions of ion channels in the vertebrate heart: Lessons learned from zebrafish. *Stem Cells Int.* **2012**, 1–9 (2012).

258. Grillitsch, S. The influence of environmental PO2 on hemoglobin oxygen saturation in developing zebrafish Danio rerio. *J. Exp. Biol.* **208**, 309–316 (2005).

259. Jin, Y., Liu, Z., Peng, T. & Fu, Z. The toxicity of chlorpyrifos on the early life stage of zebrafish: Asurvey on the endpoints at development, locomotor behavior, oxidative stress and immunotoxicity. *Fish Shellfish Immunol.* **43**, 405–414 (2015).

260. De Luca, E., Zaccaria, M., Hadhoud, M., Rizzo, G., Ponzini, R., Morbiducci, U. & Santoro, M. M. ZebraBeat : A flexible platform for the analysis of the cardiac rate in zebrafish embryos. *Sci. Rep.* **4**, 4898 (2014).

261. DeVere Riley, D. & Lederer, W. J. Acute effects of Lipopolysaccharide on L-type Ca^{2+} channel currents and Transient Outward K^{+} channel currents in Rat Ventricular Myocytes. *Biophys. J.* **96**, 259a (2009).

262. Rose, R. A., Sellan, M., Simpson, J. A., Izaddoustdar, F., Cifelli, C., Panama, B. K., Davis, M., Zhao, Dongling, Z., Markhani, M., Murphey, G. G., Striessnig, J., Liu, P. P., Heximer, S. P. & Backx, P. Iron-overload decreases Cav1.3-dependent L-type Ca^{2+} currents leading to bradycardia, altered electrical conduction and atrial fibrillation. *Circ. Arrhythm. Electrophysiol.* **4**, 733-742 (2011)

263. Wongjaikam, S., Kumfu, S., Khamseekaew, J., Chattipakorn, S. C. & Chattipakorn, N. Restoring the impaired cardiac calcium homeostasis and cardiac function in iron overload rats by the combined deferiprone and N-acetyl cysteine. *Sci. Rep.* **7**, 1–12 (2017).

264. Moon, S. N., Han, J. W., Hwang, H. S., Kim, M. J., Lee, J. S., Lee, J. Y., Oh, C. K. &

Jeong, D. C. Establishment of secondary iron overloaded mouse model: Evaluation of cardiac function and analysis according to iron concentration. *Pediatr. Cardiol.* **32**, 947–952 (2011).

265. Link, G., Saada, A., Pinson, A., Konijn, A. M. & Hershko, C. Mitochondrial respiratory enzymes are a major target of iron toxicity in rat heart cells. *J. Lab. Clin. Med.* **131**, 466–474 (1998).

266. Burkhard, S., van Eif, V., Garric, L., Christoffels, V. & Bakkers, J. On the Evolution of the Cardiac Pacemaker. *J. Cardiovasc. Dev. Dis.* **4**, 4 (2017).

267. Sarmah, S. & Marrs, J. A. Zebrafish as a vertebrate model system to evaluate effects of environmental toxicants on cardiac development and function. *International Journal of Molecular Sciences* **17**, 1–16 (2016).

268. Blake, T., Adya, N., Kim, C.-H., Oates, A. C., Zon, L., Chitnis, A., Weinstein, B. M. & Liu, P. P. Zebrafish homolog of the leukemia gene CBFB : its expression during embryogenesis and its relationship to scl and gata-1 in hematopoiesis. *Blood* **96**, 4178–4184 (2000).

269. Faucherre, A., Nargeot, J., Mangoni, M. E. & Jopling, C. piezo2b Regulates Vertebrate Light Touch Response. *J. Neurosci.* **33**, 17089–17094 (2013).

270. Quiñonez-Silvero, C., Hübner, K. & Herzog, W. Development of the brain vasculature and the blood-brain barrier in zebrafish. *Dev. Biol.* 1–10 (2019). doi:10.1016/j.ydbio.2019.03.005

271. Panula, P., Chen, Y.-C., Priyadarshini, M., Semenova, S., Sundvik, M. & Sallinen, V. The comparative neuroanatomy and neurochemistry of zebrafish CNS systems of relevance to human neuropsychiatric diseases. *Neurobiol. Dis.* **40**, 46–57 (2010).

272. Sallinen, V., Torkko, V., Sundvik, M., Reenila, I., Khrustalyov, D., Kaslin, J. & Panula, P. MPTP and MPP+ target specific aminergic cell populations in larval zebrafish. *J. Neurochem.* **108**, 719–731 (2009).

273. Severi, K. E., Portugues, R., Marques, J. C., O'Malley, D. M., Orger, M. B. & Engert, F. Neural Control and Modulation of Swimming Speed in the Larval Zebrafish. *Neuron* **83**, 692–707 (2014).

274. Grant Colburn Hildebrand, D., Cicconet, M., Torres, R. M., Choi, W., Quan, T. M., Moon, J., Wetzel, A. W., Champion, A. S., Graham, B. J., Randlett, O., PLummer, G. S., Portugues, R., Bianco, I. H., Saalfeld, S., Baden, A. D., Lillaney, K., Burns, R., Vogelstein, J. T., Schier, A. F., Lee, W.-C. A., Jeong, W.-K., Lichtman, J. W. & Engert, F. Whole-brain serial-section electron microscopy in larval zebrafish. *Nat. Publ. Gr.* **545**, 345–349 (2017).

275. Myhre, O., Andersen, J. M., Aarnes, H. & Fonnum, F. Evaluation of the probes 2′,7′-dichlorofluorescin diacetate, luminol, and lucigenin as indicators of reactive species formation. *Biochemi. Pharmacol.* **65**, 1575–1582 (2003).

276. Moon, M. S., McDevitt, E. I., Zhu, J., Stanley, B., Krzeminski, J., Amin, S., Aliaga, C., Miller, T. G. & Isom, H. C. Elevated hepatic iron activates NF-E2-related factor 2-regulated pathway in a dietary iron overload mouse model. *Toxicol. Sci.* **129**, 74–85 (2012).

277. Venkatesan, B., Mahimainathan, L., Das, F., Ghosh-Choudhury, N. & Choudhury, G. G.

Downregulation of catalase by reactive oxygen species via PI 3 kinase/Akt signaling in mesangial cells. *J. Cell. Physiol.* **211**, 457–467 (2007).

278. Chibber, S., Sangeet, A. & Ansari, S. A. Downregulation of catalase by CuO nanoparticles: Via hypermethylation of CpG island II on the catalase promoter. *Toxicol. Res. (Camb).* **6**, 305–311 (2017).

279. Min, J. Y., Lim, S. O. & Jung, G. Downregulation of catalase by reactive oxygen species via hypermethylation of CpG island II on the catalase promoter. *FEBS Lett.* **584**, 2427–2432 (2010).

280. Pandey, S., Parvez, S., Sayeed, I., Haque, R., Bin-Hafeez, B. & Raisuddin, S. Biomarkers of oxidative stress: a comparative study of river Yamuna fish Wallago attu. *Sci. Total Environ.* **309**, 105–115 (2003).

281. Costa-Silva, D. G., Nunes, M. E. M., Wallau, G. L., Martins, I. K., Zemolin, A. P. P., Cruz, L. C., Rodrigues, N. R., Lopes, A. R., Posser, T. & Franco, J. L. Oxidative stress markers in fish (Astyanax sp. and Danio rerio) exposed to urban and agricultural effluents in the Brazilian Pampa biome. *Environ. Sci. Pollut. Res.* **22**, 15526–15535 (2015).

282. Shao, B., Zhu, L., Dong, M., Wang, J., Wang, J., Xie, H., Zhang, Q., Du, Z. & Zhu, S. DNA damage and oxidative stress induced by endosulfan exposure in zebrafish (Danio rerio). *Ecotoxicology* **21**, 1533–1540 (2012).

283. Ge, W., Yan, S., Wang, J., Zhu, L., Chen, A. & Wang, J. Oxidative stress and DNA damage induced by imidacloprid in zebrafish (Danio rerio). *J. Agric. Food Chem.* **63**, 1856–1862 (2015).

284. K. Saliu, J. & A. Bawa-Allah, K. Toxicological Effects of Lead and Zinc on the Antioxidant Enzyme Activities of Post Juvenile Clarias gariepinus. *Resour. Environ.* **2**, 21–26 (2012).

285. Nakajima, S. & Kitamura, M. Bidirectional regulation of NF-κB by reactive oxygen species: A role of unfolded protein response. *Free Radic. Biol. Med.* **65**, 162–174 (2013).

286. Cai, G., Zhu, J., Shen, C., Cui, Y., Du, J. & Chen, X. The effects of cobalt on the development, oxidative stress, and apoptosis in zebrafish embryos. *Biol. Trace Elem. Res.* **150**, 200–207 (2012).

287. Pedrajas, J. R., Peinado, J. & López-Barea, J. Oxidative stress in fish exposed to model xenobiotics. Oxidatively modified forms of Cu,Zn-superoxide dismutase as potential biomarkers. *Chem. Biol. Interact.* **98**, 267–282 (1995).

288. Rojo, A. I. Regulation of Cu/Zn-Superoxide Dismutase Expression via the Phosphatidylinositol 3 Kinase/Akt Pathway and Nuclear Factor- B. *J. Neurosci.* **24**, 7324–7334 (2004).

289. Afonso, V., Santos, G., Collin, P., Khatib, A. M., Mitrovic, D. R., Lomri, N., Leitman, D. C. & Lomri, A. Tumor necrosis factor-α down-regulates human Cu/Zn superoxide dismutase 1 promoter via JNK/AP-1 signaling pathway. *Free Radic. Biol. Med.* **41**, 709–721 (2006).

290. Lijnen, P. J., Van Pelt, J. F. & Fagard, R. H. Downregulation of manganese superoxide dismutase by angiotensin II in cardiac fibroblasts of rats: Association with oxidative stress in myocardium. *Am. J. Hypertens.* **23**, 1128–1135 (2010).

291. De Esch, C., van der Linde, H., Slieker, R., Willemsen, R., Wolterbeek, A., Woutersen, R. & De Groot, D. Locomotor activity assay in zebrafish larvae: Influence of age, strain and

ethanol. *Neurotoxicol. Teratol.* **34**, 425–433 (2012).

292. García-Cambero, J. P., Catalá, M. & Valcárcel, Y. River waters induced neurotoxicity in an embryo-larval zebrafish model. *Ecotoxicol. Environ. Saf.* **84**, 84–91 (2012).

293. Nellore, J. & Nandita, P. Paraquat exposure induces behavioral deficits in larval zebrafish during the window of dopamine neurogenesis. *Toxicol. Reports* **2**, 950–956 (2015).

294. Chen, X., Huang, C., Wang, X., Chen, J., Bai, C., Chen, Y., Chen, K., Dong, Q. & Yang, D. BDE-47 disrupts axonal growth and motor behavior in developing zebrafish. *Aquat. Toxicol.* **120**–**121**, 35–44 (2012).

295. Zhao, J., Xu, T. & Yin, D. Q. Locomotor activity changes on zebrafish larvae with different 2,2',4,4'-tetrabromodiphenyl ether (PBDE-47) embryonic exposure modes. *Chemosphere* **94**, 53–61 (2014).

296. Abu Bakar, N., Sata, N. S. S. M., Ramlan, F. N., Ibrahim, W. N. W., Zulkifli, S. Z., Abdullah, C. A. C., Ahmad, S. & Amal, M. N. A. Evaluation of the neurotoxic effects of chronic embryonic exposure with inorganic mercury on motor and anxiety-like responses in zebrafish (Danio rerio) larvae. *Neurotoxicol. Teratol.* **59**, 53–61 (2017).

297. Ašmonaite, G., Boyer, S., de Souza, K. B., Wassmur, B. & Sturve, J. Behavioural toxicity assessment of silver ions and nanoparticles on zebrafish using a locomotion profiling approach. *Aquat. Toxicol.* **173**, 143–153 (2016).

298. Kienle, C., Köhler, H. R. & Gerhardt, A. Behavioural and developmental toxicity of chlorpyrifos and nickel chloride to zebrafish (Danio rerio) embryos and larvae. *Ecotoxicol. Environ. Saf.* **72**, 1740–1747 (2009).

299. Tierney, K. B. Behavioural assessments of neurotoxic effects and neurodegeneration in zebrafish. *Biochim. Biophys. Acta - Mol. Basis Dis.* **1812**, 381–389 (2011).

300. Schröder, N., Fredriksson, A., Vianna, M. R. M., Roesler, R., Izquierdo, I. & Archer, T. Memory deficits in adult rats following postnatal iron administration. *Behav. Brain Res.* **124**, 77–85 (2001).

301. Xu, H., Wang, Y., Song, N., Wang, J., Jiang, H. & Xie, J. New Progress on the Role of Glia in Iron Metabolism and Iron-Induced Degeneration of Dopamine Neurons in Parkinson's Disease. *Front. Mol. Neurosci.* **10**, 1-12 (2018).

302. Mills, E., Dong, X.-P., Wang, F. & Xu, H. Mechanisms of brain iron transport: insight into neurodegeneration and CNS disorders. *Future Med. Chem.* **2**, 51–64 (2010).

303. Fredriksson, A., Schröder, N., Eriksson, P., Izquierdo, I. & Archer, T. Neonatal iron exposure induces neurobehavioural dysfunctions in adult mice. *Toxicol. Appl. Pharmacol.* **159**, 25–30 (1999).

304. Piloni, N. E., Fermandez, V., Videla, L. A. & Puntarulo, S. Acute iron overload and oxidative stress in brain. *Toxicology* **314**, 174–182 (2013).

305. Rink, E. & Wullimann, M. F. Development of the catecholaminergic system in the early zebrafish brain: An immunohistochemical study. *Dev. Brain Res.* **137**, 89–100 (2002).

306. Rink, E. & Wullimann, M. F. The teleostean (zebrafish) dopaminergic system ascending to the subpallium (striatum) is located in the basal diencephalon (posterior tuberculum). *Brain Res.* **889**, 316–330 (2001).

307. Parker, M. O., Brock, A. J., Walton, R. T. & Brennan, C. H. The role of zebrafish (Danio rerio) in dissecting the genetics and neural circuits of executive function. *Front. Neural Circuits* **7**, 63 (2013).

308. Kastenhuber, E., Kratochwil, C. F., Ryu, S., Schweitzer, J. & Driever, W. Genetic dissection of dopaminergic and noradrenergic contributions to catecholaminergic tracts in early larval zebrafish. *J. Comp. Neurol.* **518**, 439–58 (2010).

309. Pasterkamp, R. J. Development and Engineering of Dopamine Neurons. *Adv. Exp. Med. Biol.* (2009). doi:10.1007/978-1-4419-0322-8

310. Du, Y., Guo, Q., Shan, M., Wu., Y., Huang, S., Zhao, H., Hong, H., Yang, M., Yang, X., Ren, L., Peng, J., Sun, J., Zhou, H., Li, S. & Su, B. Spatial and Temporal Distribution of Dopaminergic Neurons during Development in Zebrafish. *Front. Neuroanat.* **10**, 1–7 (2016).

311. Sallinen, V. *Zebrafish as a model of Parkinson's disease*. *Academic Dissertation* (2009). doi:10.1100/tsw.2009.68 [doi]

312. Tay, T. L., Ronneberger, O., Ryu, S., Nitschke, R. & Driever, W. Comprehensive catecholaminergic projectome analysis reveals single-neuron integration of zebrafish ascending and descending dopaminergic systems. *Nat Commun.* **2**, 171 (2011).

313. Palmér, T., Ek, F., Enqvist, O., Olsson, R., Astrom, K. & Petersson, P. Action sequencing in the spontaneous swimming behavior of zebrafish larvae - Implications for drug development. *Sci. Rep.* **7**, 1-13 (2017).

314. Jay, M., De Faveri, F. & McDearmid, J. R. Firing dynamics and modulatory actions of supraspinal dopaminergic neurons during zebrafish locomotor behavior. *Curr. Biol.* **25**, 435–444 (2015).

315. Haehnel-Taguchi, M., Fernandes, A. M., Bohler, M., Schmitt, I., Tittel, L. & Driever, W. Projections of the Diencephalospinal Dopaminergic System to Peripheral Sense Organs in Larval Zebrafish (Danio rerio). *Front. Neuroanat.* **12**, 1-21 (2018).

316. Reinig, S., Driever, W. & Arrenberg, A. B. The Descending Diencephalic Dopamine System Is Tuned to Sensory Stimuli. *Curr. Biol.* **27**, 318–333 (2017).

317. Boehmler, W., Carr, T., Thisse, C., Thisse, B., Canfield, V. A. & Levenson, R. D4 Dopamine receptor genes of zebrafish and effects of the antipsychotic clozapine on larval swimming behaviour. *Genes, Brain Behav.* **6**, 155–166 (2007).

318. Irons, T. D., Kelly, P. E., Hunter, D. L., MacPhail, R. C. & Padilla, S. Acute administration of dopaminergic drugs has differential effects on locomotion in larval zebrafish. *Pharmacol. Biochem. Behav.* **103**, 792–813 (2013).

319. Anichtchik, O. V., Kaslin, J., Peitsaro, N., Scheinin, M. & Panula, P. Neurochemical and behavioural changes in zebrafish Danio rerio after systemic administration of 6-hydroxydopamine and 1-methyl-4-phenyl-1,2,3,6-tetrahydropyridine. *J. Neurochem.* **88**, 443–53 (2004).

320. Bretaud, S., Lee, S. & Guo, S. Sensitivity of zebrafish to environmental toxins implicated in Parkinson's disease. *Neurotoxicol .Teratol.* **26**, 857–864 (2004).

321. Gaasch, J. A., Geldenhuys, W. J., Lockman, P. R., Allen, D. D. & Van der Schyf, C. J. Voltage-gated Calcium Channels Provide an Alternate Route for Iron Uptake in Neuronal

Cell Cultures. *Neurochem. Res.* **32**, 1686–1693 (2007).

322. Calabrese, V., Scapagnini, G., Ravagna, A., Fariello, R. G., Stella, A. M. G. & Abraham, N.G. Regional distribution of heme oxygenase, HSP70, and glutathione in brain: Relevance for endogenous oxidant/antioxidant balance and stress tolerance. *J. Neurosci. Res.* **68**, 65–75 (2002).

323. Catoni, C., Calì, T. & Brini, M. Calcium, Dopamine and Neuronal Calcium Sensor 1: Their Contribution to Parkinson's Disease. *Front. Mol. Neurosci.* **12**, 55 (2019).

324. Lan, J. & Jiang, D. H. Excessive iron accumulation in the brain: a possible potential risk of neurodegeneration in Parkinson's disease. *J Neural Transm* **104**, 649–660 (1997).

325. Pelizzoni, I., Marco, R., Morini, M. F., Zacchetti, D., Grohovaz, F. & Codazzi, F. Iron handling in hippocampal neurons: Activity-dependent iron entry and mitochondria-mediated neurotoxicity. *Aging Cell* **10**, 172–183 (2011).

326. Ma, Z. G., Zhou, Y. & Xie, J. X. Nifedipine prevents iron accumulation and reverses iron-overload-induced dopamine neuron degeneration in the substantia nigra of rats. *Neurotox. Res.* **22**, 274–279 (2012).

327. Fredriksson, A. & Archer, T. Postnatal iron overload destroys NA-DA functional interactions. *J. Neural Transm.* **114**, 195–203 (2007).

328. Mata, A. M. Plasma membrane Ca^{2+}-ATPases in the nervous system during development and ageing. *World J. Biol. Chem.* **1**, 229 (2010).

329. Moreau, V. H. Oxidative damage to sarcoplasmic reticulum Ca2+-ATPase at submicromolar iron concentrations: Evidence for metal-catalyzed oxidation. *Free Radic. Biol. Med.* **25**, 554–560 (1998).

330. Jones, D. C. & Miller, G. W. The effects of environmental neurotoxicants on the dopaminergic system: A possible role in drug addiction. *Biochem. Pharmacol.* **76**, 569–581 (2008).

331. Perry, S. F., Ekker, M., Farrell, A. P. & Brauner, C. J. *Zebrafish*. *Academic Press* **Fish Phys**, (Elsevier Inc., 2010).

332. Naderi, M., Salahinejad, A., Ferrari, M. C. O., Niyogi, S. & Chivers, D. P. Dopaminergic dysregulation and impaired associative learning behavior in zebrafish during chronic dietary exposure to selenium. *Environ. Pollut.* **237**, 174–185 (2018).

333. Naderi, M., Salahinejad, A., Jamwal, A., Chivers, D. P. & Niyogi, S. Chronic Dietary Selenomethionine Exposure Induces Oxidative Stress, Dopaminergic Dysfunction, and Cognitive Impairment in Adult Zebrafish (Danio rerio). *Environ. Sci. Technol.* **51**, 12879–12888 (2017).

334. Spulber, S., Killian, P., Ibrahim, W. N. W., Onishchenko, N., Ulhaq, M., Norrgren, L., Negri, S., Di Tuccio, M. & Ceccatelli, S. PFOS induces behavioral alterations, including spontaneous hyperactivity that is corrected by dexamfetamine in zebrafish larvae. *PLoS One* **9**, e94227 (2014).

335. Colwill, R. M. & Creton, R. Imaging escape and avoidance behavior in zebrafish larvae. *Rev. Neurosci* **22**, 63–73 (2011).

336. Carmean, V. & Ribera, A. B. Genetic Analysis of the Touch Response in Zebrafish (Danio

rerio). *Int. J. Comp. Psychol. Neuhauss al* **23**, 91–102 (2010).

337. Pietri, T., Manalo, E., Ryan, J., Saint-Amant, L. & Washbourne, P. Glutamate drives the touch response through a rostral loop in the spinal cord of zebrafish embryos. *Dev. Neurobiol.* **69**, 780–795 (2009).

338. Richendrfer, H., Creton, R. & Colwill, R. The Embryonic Zebrafish As a Model System to Study the Effects of Environmental Toxicants on Behavior. in *Zebrafish* 245–264 (2014).

339. O'Malley, D. M., Kao, Y. H. & Fetcho, J. R. Imaging the functional organization of zebrafish hindbrain segments during escape behaviors. *Neuron* **17**, 1145–1155 (1996).

340. Budick, S. A. & OMalley, D. M. Locomotion of larval zebrafish. *J. Exp. Biol.* **203**, 2565–2579 (2000).

341. Nakano, Y., Fujita, M., Ogino, K., Saint-Armant, L., Kinoshita, T., Oda, Y. & Hirata, H. Biogenesis of GPI-anchored proteins is essential for surface expression of sodium channels in zebrafish Rohon-Beard neurons to respond to mechanosensory stimulation. *Development* **137**, 1689–1698 (2010).

342. Metcalfe, W. K., Myers, P. Z., Trevarrow, B., Bass, M. B. & Kimmel, C. B. Primary neurons that express the L2/HNK-1 carbohydrate during early development in the zebrafish. *Development* **110**, 491–504 (1990).

343. Won, Y. J., Ono, F. & Ikeda, S. R. Characterization of Na+ and Ca2+ channels in zebrafish dorsal root ganglion neurons. *PLoS One* **7**, e42602 (2012).

344. Reyes, R., Haendel, M., Grant, D., Melancon, E. & Eisen, J. S. Slow Degeneration of Zebrafish Rohon-Beard Neurons during Programmed Cell Death. *Dev. Dyn.* **229**, 30–41 (2004).

345. Gleason, M. R., Higashijima, S.-I., Dallman, J., Liu, K., Mandel, G. & Fetcho, J. R. Translocation of CaM kinase II to synaptic sites in vivo. *Nat. Neurosci.* **6**, 217–218 (2003).

346. Low, S. E., Woods, I. G., Lachance, M., Ryan, J., Schier, A. F. & Saint-Amant, L. Touch responsiveness in zebrafish requires voltage-gated calcium channel 2.1b. *J. Neurophysiol.* **108**, 148–159 (2012).

347. Umeda, K., Ishizuka, T., Yawo, H. & Shoji, W. Position- and quantity-dependent responses in zebrafish turning behavior. *Sci. Rep.* **6**, 27888 (2016).

348. Gahtan, E., Sankrithi, N., Campos, J. B. & O'Malley, D. M. Evidence for a Widespread Brain Stem Escape Network in Larval Zebrafish. *J. Neurophysiol.* **87**, 608–614 (2017).

349. Chong, M. & Drapeau, P. Interaction between hindbrain and spinal networks during the development of locomotion in zebrafish. *Dev. Neurobiol.* **67**, 933–947 (2007).

350. Umeda, K., Ishizuka, T., Yawo, H. & Shoji, W. Position- and quantity-dependent responses in zebrafish turning behavior. *Sci. Rep.* **6**, 27888 (2016).

351. Hen Chow, E. S. & Cheng, S. H. Cadmium affects muscle type development and axon growth in zebrafish embryonic somitogenesis. *Toxicol .Sci.* **73**, 149–159 (2003).

352. Asharani, P. V, Lianwu, Y., Gong, Z. & Valiyaveettil, S. Comparison of the toxicity of silver, gold and platinum nanoparticles in developing zebrafish embryos. *Nanotoxicology* **5**, 43–54 (2011).

353. Chen, J., Huang, C., Zheng, L., Simonich, M., Bai, C., Tanguay, R. & Dong, Q. Trimethyltin chloride (TMT) neurobehavioral toxicity in embryonic zebrafish. *Neurotoxicol. Teratol.* **33**, 721–726 (2011).

354. Sonnack, L., Kampe, S., Muth-Kohne, E., Erdinger, L., Henny, N., Hollert, H., Schafers, C. & Fenske, M. Effects of metal exposure on motor neuron development, neuromasts and the escape response of zebrafish embryos. *Neurotoxicol. Teratol.* **50**, 33–42 (2015).

355. Rice, C., Ghorai, J. K., Zalewski, K. & Weber, D. N. Developmental lead exposure causes startle response deficits in zebrafish. *Aquat. Toxicol.* **105**, 600–608 (2011).

356. Bostanci, M. Ö. & Bagirici, F. Blocking of L-type calcium channels protects hippocampal and nigral neurons against iron neurotoxicity: The role of L-type calcium channels in iron-induced neurotoxicity. *Int. J. Neurosci.* **123**, 876–882 (2013).

357. Lockman, J. A., Geldenhuys, W. J., Bohn, K. A., DeSilva, S. F., Allen, D. D. & Van der Schyf, C. J. Differential effect of nimodipine in attenuating iron-induced toxicity in brain- and blood-brain barrier-associated cell types. *Neurochem. Res.* **37**, 134–142 (2012).

358. Sztal, T. E., Ruparelia, A. A., Williams, C. & Bryson-Richardson, R. J. Using Touch-evoked Response and Locomotion Assays to Assess Muscle Performance and Function in Zebrafish. *J. Vis. Exp.* (2016). doi:10.3791/54431

359. Burgess, H. A. & Granato, M. Modulation of locomotor activity in larval zebrafish during light adaptation. *J. Exp. Biol.* **210**, 2526–2539 (2007).

360. Velki, M., Di Paolo, C., Nelles, J., Seiler, T. B. & Hollert, H. Diuron and diazinon alter the behavior of zebrafish embryos and larvae in the absence of acute toxicity. *Chemosphere* **180**, 65–76 (2017).

361. Liu, X., Lin, J., Zhang, Y., Peng, X., Guo, N. & Li, Q. Effects of diphenylhydantoin on locomotion and thigmotaxis of larval zebrafish. *Neurotoxicol. Teratol.* **53**, 41–47 (2016).

362. Bouwknecht, J. A. & Paylor, R. Pitfalls in the interpretation of genetic and pharmacological effects on anxiety-like behaviour in rodents. *Behav. Pharmacol.* **19**, 385–402 (2008).

363. Velki, M., Paolo, C. Di, Nelles, J., Seiler, T.-B. & Hollert, H. Diuron and diazinon alter the behavior of zebrafish embryos and larvae in the absence of acute toxicity. *Chemosphere* **180**, 65–76 (2017).

364. Fuse, Y., Nguyen, V. T. & Kobayashi, M. Nrf2-dependent protection against acute sodium arsenite toxicity in zebrafish. *Toxicol. Appl. Pharmacol.* **305**, 136–142 (2016).

365. Wang, L. & Gallagher, E. P. Role of Nrf2 antioxidant defense in mitigating cadmium-induced oxidative stress in the olfactory system of zebrafish. *Toxicol. Appl. Pharmacol.* **266**, 177–186 (2013).

366. Nishizawa, H., Matsumoto, M., Shindo, T., Saigusa, D., Kato, H., Suzuki, K., Sato, M., Ishii, Y., Shimokawa, H. & Igarashi, K. Ferroptosis is programmed by the coordinated regulation of glutathione and iron metabolism by BACH1. *bioRxiv* 644898 (2019). doi:10.1101/644898

367. Watanabe, Y., Ishimori, K. & Uchida, T. Dual role of the active-center cysteine in human peroxiredoxin 1: Peroxidase activity and heme binding. *Biochem. Biophys. Res. Commun.* **483**, 930–935 (2017).

368. Kerins, M. J. & Ooi, A. The Roles of NRF2 in Modulating Cellular Iron Homeostasis. *Antioxid. Redox Signal.* **29**, 1756–1773 (2018).

369. Chen, X., Dong, Q., chen, Y., Zhang, Z., Huang, C., Zhu, Y. & Zhang, Y. Effects of Dechlorane Plus exposure on axonal growth, musculature and motor behavior in embryo-larval zebrafish. *Environ. Pollut.* **224**, 7–15 (2017).

370. Zeddies, D. G. Development of the acoustically evoked behavioral response in zebrafish to pure tones. *J. Exp. Biol.* **208**, 1363–1372 (2005).

371. Archer, T. & Fredriksson, A. Functional consequences of iron overload in catecholaminergic interactions: The Youdim factor. *Neurochem. Res.* **32**, 1625–1639 (2007).

372. Herculano, A. M. & Maximino, C. Serotonergic modulation of zebrafish behavior: Towards a paradox. *Prog. Neuro-Psychopharmacology Biol. Psychiatry* **55**, 50–66 (2014).

373. Ghosh, S. & Hui, S. P. Regeneration of zebrafish CNS: Adult neurogenesis. *Neural. Plast.* **2016**, 1–21 (2016).

8 Supplementary Material

Two Way Analysis of Variance Saturday, August 17, 2019, 4:06:56 PM

Data source: Data 2 in Notebook1
General Linear Model
Dependent Variable: Col 3

Normality Test (Shapiro-Wilk): Passed (P = 0.209)

Equal Variance Test (Brown-Forsythe): Passed (P = 0.332)

Source of Variation	DF	SS	MS	F	P
Col 1	1	0.00269	0.00269	0.000179	0.990
Col 2	1	17.885	17.885	1.189	0.304
Col 1 x Col 2	1	14.190	14.190	0.943	0.357
Residual	9	135.388	15.043		
Total	12	170.011	14.168		

The difference in the mean values among the different levels of Col 1 is not great enough to exclude the possibility that the difference is just due to random sampling variability after allowing for the effects of differences in Col 2. There is not a statistically significant difference (P = 0.990).

The difference in the mean values among the different levels of Col 2 is not great enough to exclude the possibility that the difference is just due to random sampling variability after allowing for the effects of differences in Col 1. There is not a statistically significant difference (P = 0.304).

The effect of different levels of Col 1 does not depend on what level of Col 2 is present. There is not a statistically significant interaction between Col 1 and Col 2. (P = 0.357)

Power of performed test with alpha = 0.0500: for Col 1 : 0.0500
Power of performed test with alpha = 0.0500: for Col 2 : 0.0676
Power of performed test with alpha = 0.0500: for Col 1 x Col 2 : 0.0500

Least square means for Col 1 :

Group	Mean	SEM
3.000	7 .989	1.583
5.000	8.018	1.481

Least square means for Col 2 :

Group	Mean	SEM
CTR	6.821	1.481
FAC	9.185	1.583

Least square means for Col 1 x Col 2 :

Group	Mean	SEM
3.000 x CTR	7.860	2.239
3.000 x FAC	8.118	2.239
5.000 x CTR	5.783	1.939
5.000 x FAC	10.253	2.239

Figure S1. Two-way ANOVA for *ef1a*

Two-way analysis to determine stability of *ef1a* under control and treatment (FAC) conditions, as well as developmental age. Col1 represents developmental age (3 dpf or 5 dpf) and Col2 represents treatment (control or FAC). Data collected from ddPCR, represented as copies of sample per μL. Results show that there is no significant difference in *ef1a* levels between treatments and developmental ages.

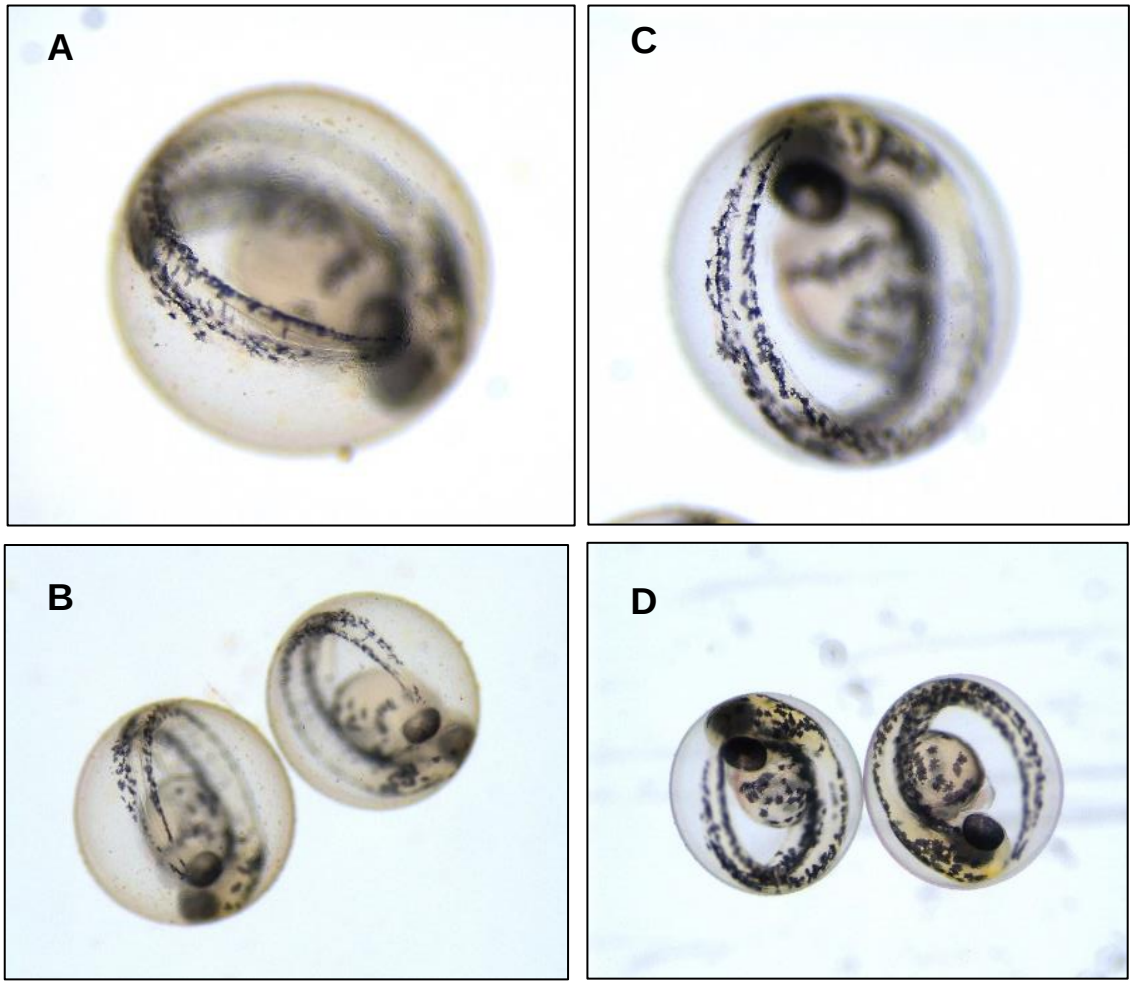

Figure S2. Ferric Iron Precipitates.
(A, B) Colloidal iron precipitates (the brownish colouration with specs of orange) can be seen coating the chorion of 2 dpf FAC-exposed embryonic zebrafish. On the other hand, chorions from 2 dpf control embryonic zebrafish possess a normal appearance **(C, D).** It should be noted that these precipitates remained on the embryos following daily renewal of exposure water and Petri dish.

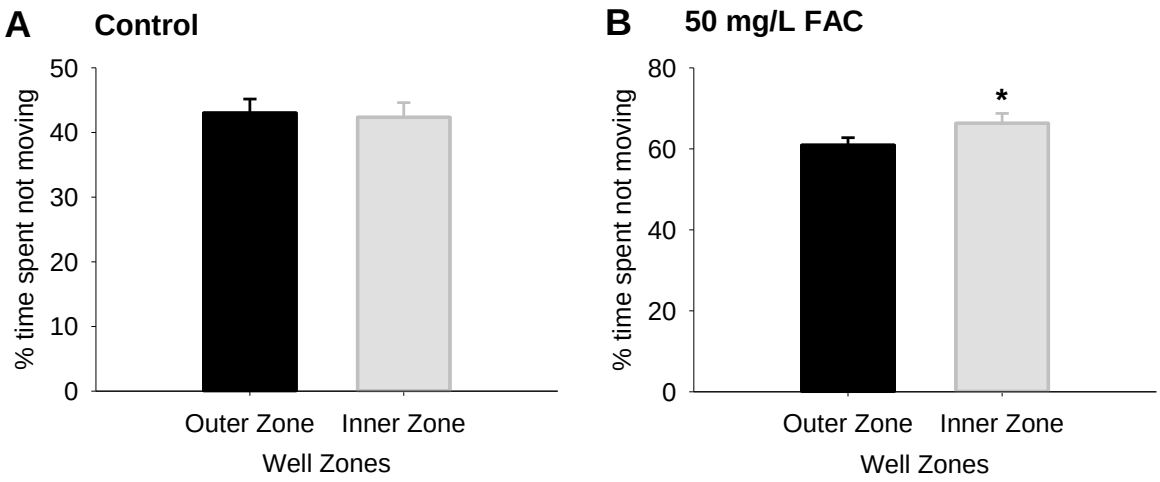

Figure S3. % Time Spent Not Moving Per Zone
% time spent not moving per zone by **(A)** control and **(B)** FAC-exposed larvae during the thigmotactic response (i.e., 5 mins of darkness). While control larvae spent the same time actively swimming in either zone, FAC-exposed larvae spent more time immobile while in the inner zone, compared to control (control: 42% vs FAC: 66%; *$p<0.01$, student's t-test). Increased time spent in inner zone by the FAC-exposed larvae can therefore be accounted by the higher incidence of time spent not moving in that zone.

Table S1. Total Protein Content in Larval Zebrafish. Total protein content (μg/fish) of control and iron-exposed larvae, at 3 dpf and 5 dpf, quantified using a BCA Protein Assay Kit. N=5-6 per treatment, 20 pooled larvae per replicate. Results from two-way ANOVA propose that there is a significant difference with developmental age, but there is no statistical difference between control and FAC treatments.

	3 dpf	5 dpf
Control	14.14 ± 0.17	12.78 ± 0.33
FAC	13.74 ± 0.65	10.80 ± 0.91

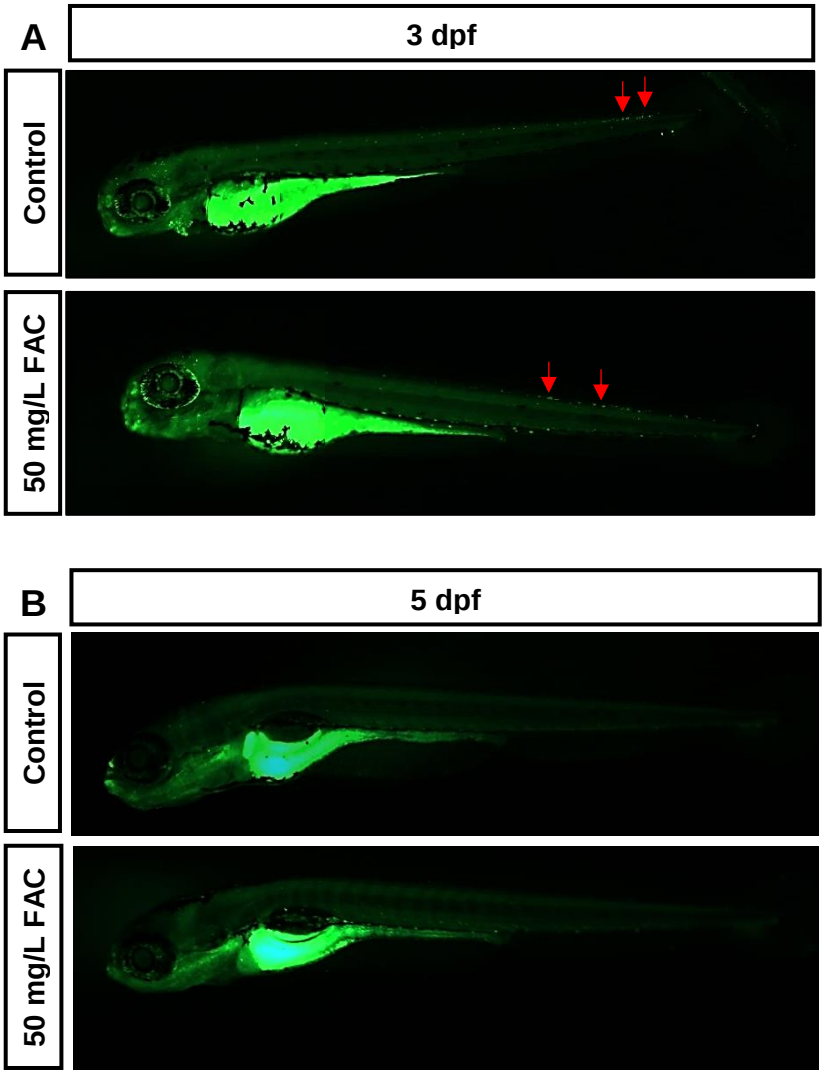

Figure S4. Apoptosis Assay Using AO.
(A) 3 and **(B)** 5 dpf control and iron-exposed larval zebrafish were incubated for 1.5 hours in 1 μg/ml acridine orange (AO) to detect apoptotic cells. Larvae were washed 3X with AF before fluorescence imaging. Preliminary results show no evident difference between iron-exposed and control larvae, suggesting that the concentration of iron used does not result in apoptosis, despite seeing increased ROS. 3 dpf larvae in general possessed relatively higher apoptotic cells when compared to 5 dpf, since they are still undergoing development and regulated apoptotic cell death (e.g. RB cells along tail; red arrows).

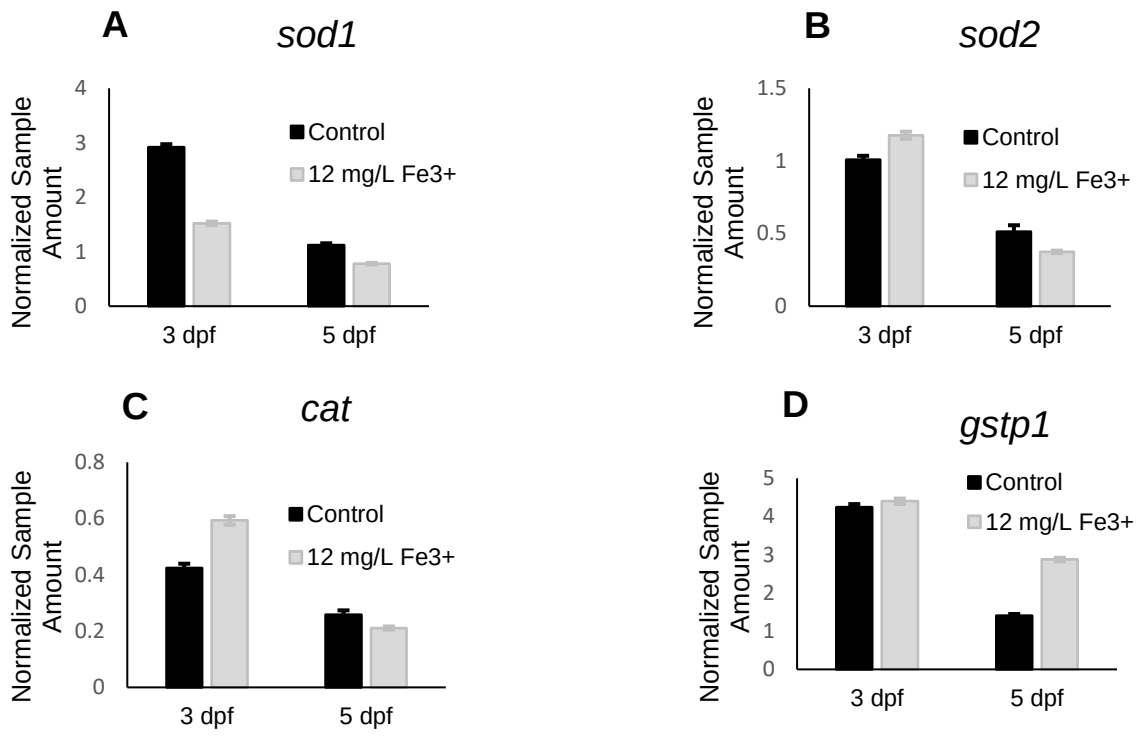

Figure S5. Normalized Sample Amount of oxidative stress-response genes in control and FAC-exposed 3 and 5 dpf larvae.

mRNA expression levels of **(A)** *sod1*, **(B)** *sod2*, **(C)** *cat*, and **(D)** *gstp1* normalized to *ef1a* and presented as normalize sample amounts. These datasets were used to calculate fold change difference in expression levels between control and treatment. Note the general trend for the mRNA expression of oxidative stress response genes to decrease through developmental age. Furthermore, low basal *cat* expression is seen when compared to other genes (which may render the larval zebrafish vulnerable to Fe-mediate OH· production), whereas *gstp1* transcript abundance is comparatively the highest amongst these four genes.

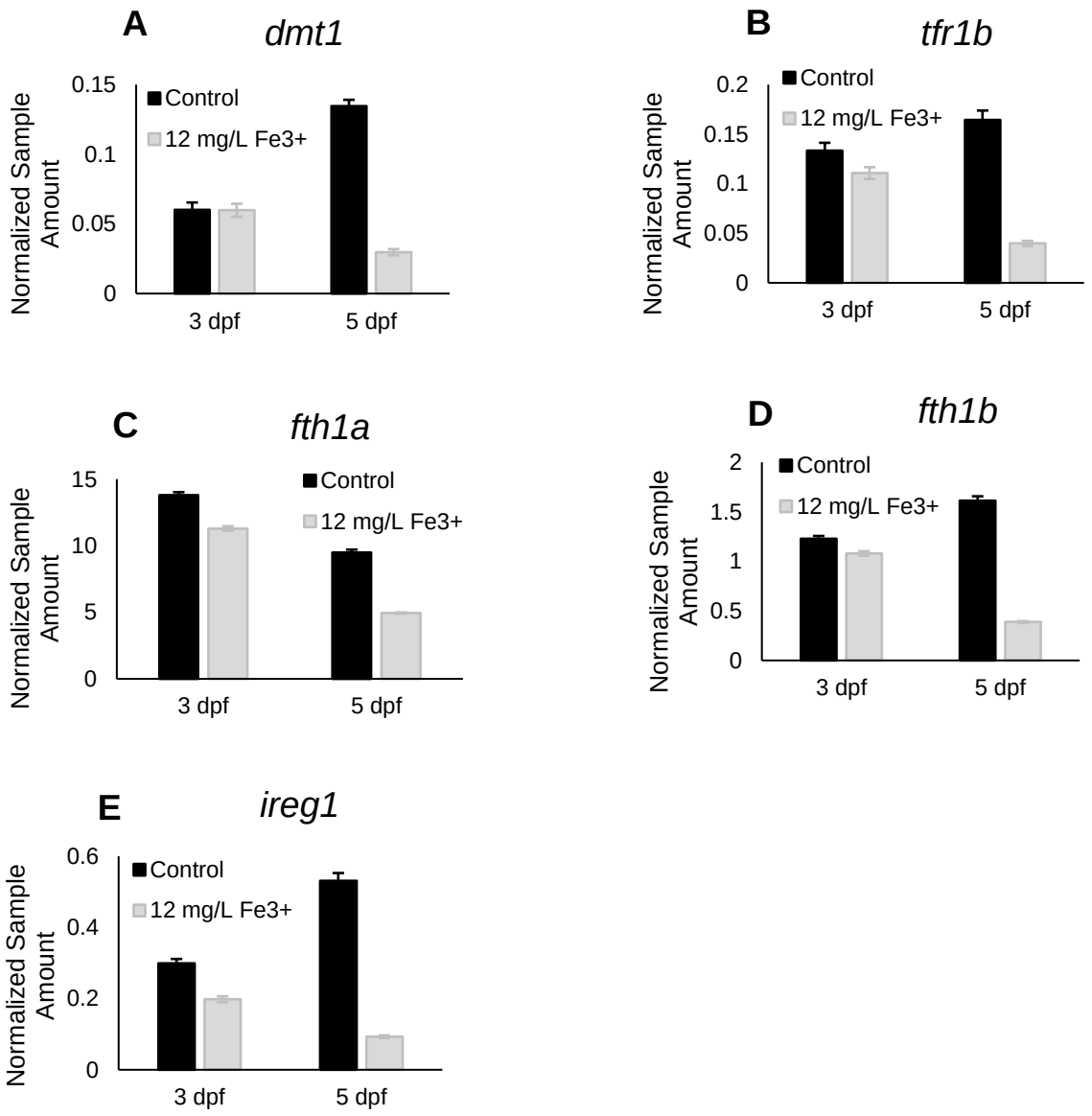

Figure S6. Normalized Sample Amount of iron transport and storage genes in control and FAC-exposed 3 and 5 dpf larvae.

mRNA expression levels of **(A)** *dmt1*, **(B)** *tfr1b*, **(C)** *fth1a*, **(D)** *fth1b,* and **(E)** *ireg1* normalized to *ef1a* and presented as normalize sample amounts. These datasets were used to calculate fold change difference in expression levels between control and treatment. Note the general trend for the mRNA expression of oxidative stress response genes to increase through developmental age, except for *fth1a*. Especially low basal expression of *dmt1* is detected at 3 dpf, however it undergoes almost a 3-fold increase in transcript abundance by 5 dpf. On the other hand, the highest mRNA expression levels come from *fth1a* and fth1b, indicating the importance of iron storage in early development.